Università degli Studi di Napoli Federico II

Tesi di Dottorato di Ricerca in Ingegneria Chimica
XVIII ciclo

Morphology of complex fluids: "Viscoelastic effects on drop deformation of polymeric blends under shear flow between parallel plates"

Candidate:
Vincenzo Sibillo

Promoter:
Prof. G. Marrucci

Advisor:
Prof. S. Guido

Scientifc Committee:
Ing. V. Guida
Prof. F. Greco
Ing. M. Simeone

Nov/2005

Abstract

A complete three-dimensional shape of an isolated drop in an immiscible liquid phase undergoing simple shear flow with non Newtonian fluids was investigated by contrast-enhanced optical microscopy. Drop was observed either along the vorticity direction or along the velocity gradient direction of the shear flow. The effects on drop deformation and break up of the viscoelastic content of the liquid phases were investigated. Two situation of a viscoelastic matrix with a Newtonian drop and of viscoelastic drop in a Newtonian matrix are considered. When possible my data are compared with theoretical or phenomenological predictions. Finally I investigated also the influence of confinement on the steady state of the drop in a regime where drop diameter is comparable to gap width between the shearing parallel plates.

Summary

The objective of this PhD thesis is to investigate the flow-induced microstructure of viscoelastic liquid-liquid dispersions, to better understand the influence of viscous and elastic properties on droplets shape during the shear flow, using a single drop model system. The main objective is to well understand the relationship between the flow, phases rheological properties and droplet shape, in order to provide basic guidelines on how to control flow-induced microstructure of synthetic “real” polymer blends during blending industrial processes.

The stated objective passes through the selection of a single drop model system with non Newtonian highly elastic matrix or drop phase, with appropriate rheological properties, in order to separate elastic and viscous non Newtonian effects on drop shape. In addition the hydrodynamic problem of drop subjected to flow becomes more complex in the case in which one or both the component fluids are viscoelastic. The choice of non Newtonian fluids with an appropriate constitutive equation is necessary, that allows to get results of general validity. A theoretical or phenomenological drop shape characterization is also necessary to well interpret the experimental results.

For a fully Newtonian system the influence of confinement on drop shape is also investigated to present a complete analysis of flow induced droplet morphology.

To this porpoise, constant viscosity, elastic polymer solutions (Boger fluids) were used as viscoelastic phase. These fluids have a constant viscosity with a second order rheological behaviour, so that it has been possible to isolate the contribution due to the only elasticity on the drop deformation and to get results valid for all viscoelastic

"Second order fluids". For the first time, two properly chosen "inverse" non Newtonian systems are considered, namely, a Newtonian drop immersed in a Boger fluid, and vice versa.

Non dimensional parameter $p = \frac{\Psi_1 \sigma}{2R\eta^2}$, where η and Ψ_1 are the viscosity and the first normal stress coefficient of the viscoelastic fluid respectively, σ is the interfacial tension, R is the undeformed drop radius, has been used to quantify the weight of the elasticity content of the fluids on the flow-induced drop deformation. This parameter introduced for the first time by Leal (2001)[1], and formalized by the theory on the steady state drop shape in slow flow with non Newtonian second order fluid ,Greco (2002)[2], can be interpreted as the ratio between constitutive relaxation time of the viscoelastic phase $\tau_R = \frac{\Psi_1}{2\eta}$ and emulsion time $\tau_{em} = \frac{\eta R}{\sigma}$. Drop flow-induced deformation has been also studied as a function of the Capillary number, $Ca = \frac{\eta_C \dot{\gamma}}{\sigma / R}$, where η_C is the matrix phase viscosity, $\dot{\gamma}$ the shear rate and the drop to matrix viscosity ratio $\lambda = \frac{\eta_D}{\eta_C}$.

In the case of Newtonian single drop immersed into a viscoelastic matrix, drop dynamics at start-up and after flow cessation of shear flow is investigated at a fixed viscosity ratio, comparing the data with predictions from two recently proposed phenomenological models. A very precise characterization of drop shape is achieved during transients, to catch fine details of the transient dynamic. Briefly, drop evolutions at start-up and after flow cessation are quite different with respect to the fully Newtonian case.

[1]Tretheway D. C., Leal L. G., "Deformation and relaxation of Newtonian drops in planar extensional flows of a Boger fluid", J. Non-Newtonian Fluid Mech. 99 (2001) 81–108.

[2] Greco F.. "Second-order theory for the deformation of a Newtonian drop in a stationary flow field". Phys. Fluids, 14, (2002) 946-954.

Moreover the effect of matrix elasticity on the break-up of a sheared Newtonian drop will be presented. In this case three drop to matrix viscosity ratio were explored, in order to well understand the role of the elasticity and viscosity on drop dynamic. An accurate determination of the shear stress at break-up (Critical capillary number) as a function of the matrix elasticity content (p parameter) is here presented.

When one or both the component fluids are non Newtonian, the fluid-dynamics of the drop become complex. Authors who studied viscoelastic systems generally used polymeric melts, which are also shear thinning. As a consequence a clear identification of separate elastic and viscous non Newtonian effects on drop break-up was in fact non achieved. By using Boger fluids, conversely, this difficult can be overcome, also because of the absence of any sear thinning. Even though I have used model fluids in this work to reproduce non Newtonian polymeric blends, I think that my analysis can be also relevant for “real” blend under shear flow.

For what concerns the system of non Newtonian drop immersed into a Newtonian matrix, a complete drop shape 3D analysis was achieved, focusing the attention on the drop behaviour for high hydrodynamic shear stresses; drop elastic content changes the break-up mechanism and hinders drop break-up, when compared with the equivalent fully Newtonian system. Single drop dynamics was also investigated during start up and after cessation of the shear flow. Moreover, a new method to obtain a non Newtonian polymer blend with constant viscosity Boger dispersed phase will be illustrated.

Finally I investigated the influence of confinement on the steady state drop shape sheared between parallel plates in a regime where drop diameter is comparable with gap width using a fully Newtonian drop-matrix system. It was observed that the closeness to the walls exacerbates the deformation of the drop. Moreover the drop pushed by the walls is closer to the velocity direction with respect to the Newtonian case without

confinement.

1 Introduction

Immiscible liquid-liquid suspensions, such as emulsion, polymer blends, are very often encountered in nature and industrial processes, so the understanding and control of their structure and flow properties is of great importance. It is well known that many physical properties of these systems, called “complex fluids”, are strongly influenced by their morphology, exactly by the mean droplets size, inner phase shape and the degree of dispersion. The knowledge about the effects of the flow, to which these systems are submitted during the industrial processes, on their morphology becomes a critical aspect to control the properties of the finished product. This has generated a basic scientific interest in the fluid-dynamics of these liquid-liquid suspensions. It is almost obvious that flow-induced single drop deformation and its breakup, as well as coalescence, are the primary mechanisms responsible of the inner phase shape, droplets size distribution and complex rheological behaviour of a liquid-liquid dispersion submitted to flow. The dynamic of an isolated sheared drop can be regarded as a sort of elementary event, which can provide some interesting knowledge to better understand the complex rheological behaviour of flowing dispersion of drops. So a rather literature is dedicated to the single drop system, which is summarized in several reviews (J.M Rallison, (1984)[3]; H.W. Stone, (1994)[4]; S. Guido and F. Greco, (2004)[5]). The majority of the research papers has been focused mainly on purely viscous Newtonian systems (i.e. dispersed and continuous phase liquids are Newtonian and do not exhibit any measurable degree of elasticity). On the other hand only few investigations can be found

[3] Rallison, J. M., “The deformation of small viscous drops and bubbles in shear flows”, Annual Review of Fluid Mechanics, 16, 45-66, (1984).

[4] Stone H A (1994) Dynamics of drop deformation and breakup in viscous fluids. Ann. Rev. Fluid Mech., 26, 65-102.

[5] S. Guido and F. Greco, “Rheology Review 2004”, BSR Aberystwyth, UK 2004.

in the literature, which are devoted to the non Newtonian case, in spite of its practical relevance. In many experiments, moreover, the fluids investigated include both viscosity and normal stress "thinning" with the flow rate (Mighri F, (1998)[6]; Elmendorp J. J: (1985)[7]; Flumerfelt R W, (1972)[8]). So a clear identification of separate elastic and viscous non Newtonian effects had not been obtained and a full 3D characterization of drop shape for a viscoelastic system is still lacking. There are only a few predictions of non Newtonian effect on drop morphology. By using constant viscosity Boger fluids I overcame this difficulty. Moreover, recently some progresses have been made both on the experimental and theoretical side (Guido et al.(2003)[9]; Greco F. (2002)[10]. So it has been possible to estimate viscoelastic effects on dynamic of the drop submitted to a well defined flow. A perturbative calculation of drop shape submitted to a "slow" flow has been developed for second order non Newtonian fluids with constant viscosity by F. Greco (2003). Drop shape in shear flow with viscoelastic fluids is governed by the non dimensional Capillary number $Ca = \frac{\eta_C \dot{\gamma}}{\sigma / R}$, where η_C is the continuous phase viscosity, $\dot{\gamma}$ the shear rate, σ the interfacial tension of the couple of fluids and R is the spherical drop radius and by the drop to matrix viscosity ratio $\lambda = \frac{\eta_D}{\eta_C}$, as for the fully Newtonian case, and by another non dimensional parameter $p = \frac{\Psi_1 \sigma}{2R\eta^2}$, where η is the viscosity of

[6] Mighri F, Carreau P J and Ajji A (1998) Influence of elastic properties on drop deformation and breakup in shear flow. J. Rheol., 42, 1477-1490.

[7] Elmendorp J. J. and R. J. Maalcke, "A study on polymer blending microrheology. 1" Polym. Eng. Sci. 25, 1041-1047 (1985).

[8] Flumerfelt R W, (1972) Drop breakup in simple shear fields of viscoelastic fluids. Ind. Eng. Chem. Fundam., 11, 312-318.

[9] Guido S, Simeone M and Greco F, "Deformation of a Newtonian drop in a viscoelastic matrix under steady shear flow. Experimental validation of slow flow theory", J. Non-Newtonian Fluid Mech., 114 (2003) 65-82.

[10] Greco F.. "Second-order theory for the deformation of a Newtonian drop in a stationary flow field". Phys. Fluids, 14, (2002) 946-954.

the second order fluid and Ψ_1 is the first normal stress coefficient. This parameter p introduced for the first time by Leal, can be easily interpreted as the ratio between constitutive relaxation time of the viscoelastic phase $\tau_R = \frac{\Psi_1}{2\eta}$ and emulsion time $\tau_{em} = \frac{\eta_C R}{\sigma}$. With a few words theoretical analysis predicts that viscoelastic effects come to play a significant role when p>1. When necessary, during this thesis I will recall theoretical predictions for a rapid comparison with the experimental results.

This thesis is organized as follows. First I will speak briefly about the materials and the experimental apparatus used.

I will illustrate drop dynamics at start-up and after cessation of shear flows, comparing the data with some phenomenological models predictions. Drop break-up phenomenon will be also investigated. In both cases a model system with a non Newtonian highly elastic continuous phase and a Newtonian drop phase was considered.

Then a complete 3D analysis of the shape evolution of a single viscoelastic drop (Boger fluid) immersed in a Newtonian matrix and subjected to shear flow was performed as a function of the drop elastic content. Drop break-up mechanism will be also illustrated.

Another important aspect to be analysed, to understand and control the flow-induced microstructure of a liquid-liquid dispersions, is the effect of the confinement on the drop shape in the regime where drop diameter is comparable with gap width. This is a first step to better understand the shape evolution of a single drop flowing into a dispersion of droplets, where drop is submitted to the confinement of many other droplets. In this case a single drop model system with Newtonian phases was considered. This problem was treated in the last section.

2 Experimental

2.1 Materials

Boger fluids were used as matrix and drop phase, in order to obtain a viscoelastic fluid with second order rheological behaviour and constant viscosity ($N_1 = \Psi_1 \dot{\gamma}^2$, where N_1 is the of the first normal stresses difference and Ψ_1 the coefficient). Viscoelastic fluid was carefully prepared in order to explore a wide range of the p parameter and of the viscosity ratio. Boger fluid was prepared by mixing a Newtonian polyisobutilene (PIB) sample (Napvis 10 and Napvis 30) with small amount of a high molecular weight grade of the same polymer, preliminarily dissolved in kerosene at the concentration of 4% wt. The fluids used as viscoelastic dispersed phase and viscoelastic matrix phase in this work will be listed in the results sections with their rheological properties. Their preparation protocol will be also illustrated in detail. Newtonian phase is a simple silicone oil mixture (PDMS, polydimetisiloxane).

Rheological data were obtained by using a constant stress rheometer equipped with a normal stress transducer (Bolin, CVO 120), in the cone and plate configuration. It was verified that viscosity of the Boger fluids were essentially constant in the range of the shear rate investigated (up to 20 s^{-1}), and rather large values of the first normal stress difference were found. As an example, the rheological data of the Boger fluids used in the section 4 are show in Figure 12. The solid line is a fit to the first normal stress difference data in log scale. The slope of the fitting lines is equal to 2, in agreement with the assumption of second order fluids. The first normal stress difference coefficient Ψ_1 was calculated by fitting the data to a line f slope 2 in log scale. On the other hand, silicon oils mixtures were purely Newtonian fluids with a constant viscosity and no normal stress.

The fully Newtonian system used to explore the wall effects on the drop shape is constituted by a silicon oil drop immersed in a Newtonian PIB sample with low molecular weight.

The interfacial tension of all the fluid pairs used in the experimental campaign was evaluated by applying the theory of Greco (2003) to data at steady state drop shape in shear flow. The method used every time will be briefly illustrated in the single section.

2.2 Experimental apparatus

The shear device used in his work is well described by Guido and Villone (1998). Simple shear flow was generated by a parallel plate apparatus. Two interchangeable set-ups designed to observe drop deformation either along the velocity gradient direction or along the vorticity axis were used. Flow direction is parallel to the x-axis, the velocity gradient is along the y-axis, and the vorticity axis coincides with the z-axis. In the set-up used to look along the vorticity gradient (z-set-up or side view experiment) each plate is an optical glass bar of square section (100 mm x 5 mm x 5 mm) and is glued on a glass slide, which fits in a window cut on a rigid mount, as shown in Figure 1. In the other set-up, used to look along the velocity gradient direction (y-set-up), each plate, made of optical glass (100 mm x 50 mm x 6 mm), is glued in a window cut on a rigid mount, as shown Figure 1. In either set-up, one of the mounts is screwed on a set of two micrometric stages (Newport), for rotary and tilting motion.

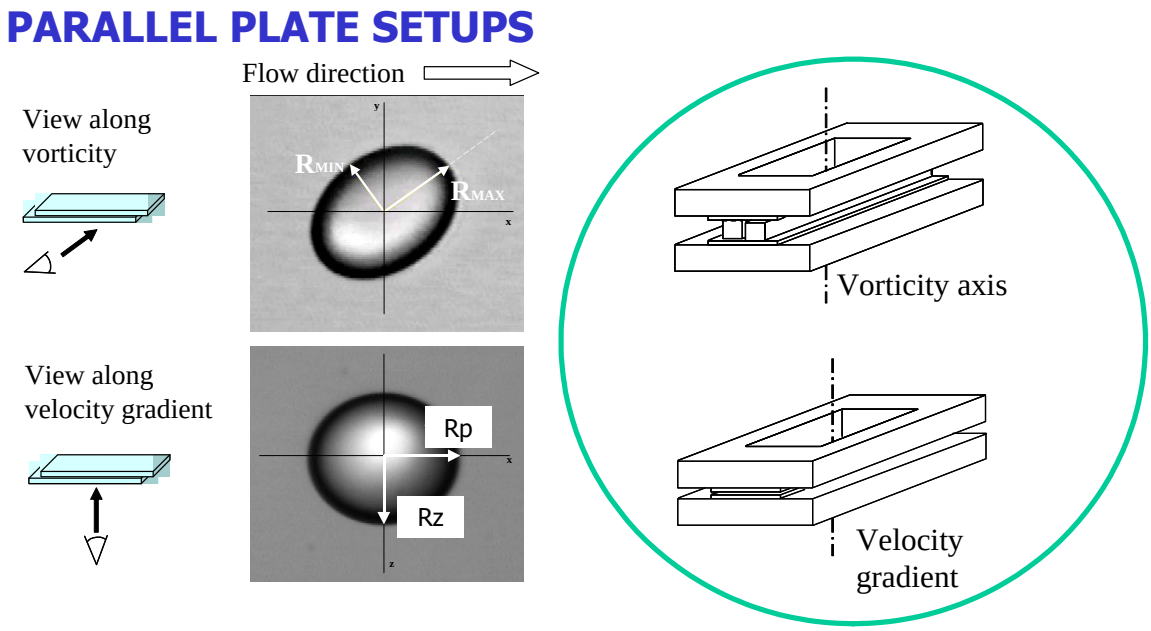

Figure 1:The two arrangements of the parallel plates used in the experiments. (a) Set-up to look along the vorticity direction (z-set-up); (b) set-up to look along the velocity gradient direction (y-set-up).

The whole assembly (mount and micrometric stages) is mounted on a 2-axes translating stage, equipped with two computer-controlled stepper motors (LEP). Minimum and maximum motor speeds are 0.0084 mm/s and 30 mm/s, respectively. The full travel in either direction is 100 mm, with a positioning accuracy of 5 μm. By using the 2-axes motorised stage one plate can be displaced along two perpendicular directions in the horizontal plane. Adjustment of either the tilting stage (z set-up) or the rotary stage (y set-up), with the aid of a stage micrometer, guarantees that the moving plate translates in its own plane. The mount supporting the fixed plate is screwed on an assembly of micrometric stages, including one rotary, two tilting and one vertical stage (Newport). The latter is used to set the gap between the plates. The rotary and tilting stages are used to make the fixed plate parallel with respect to the moving one by exploiting the reflections of a laser beam from the glass surfaces confining the sample. Parallelism was checked and further refined by focussing the glass surfaces with a microscope. In either set-up, the parallelism accuracy was estimated to about 10 μm

over the whole plate length of 100 mm, i.e. less than 0.01%.

The sample was observed through a transmitted light microscope (Axioscop FS, Zeiss), equipped with a B/W CCD video camera (KP-ME1, Hitachi) and a motorised focus system (LEP). The microscope itself was mounted on a motorised translating stage (Newport), which was used to keep the deformed drop within the field of view during shear flow. In all the experiments, observations were performed in bright field, using long working distance optics (2.5x, 10x, 20x and 40x objectives, Zeiss). The total magnification was varied by using an additional lens holder (Optovar slider, Zeiss), with factors of 1.25x and 1.6x, and a zoom lens with a continuously adjustable zoom factor in the range 0.5 - 2.0x. The whole apparatus, which is shown schematically in the z-set-up in Figure 2, was placed on a vibration-isolated workstation (Newport).

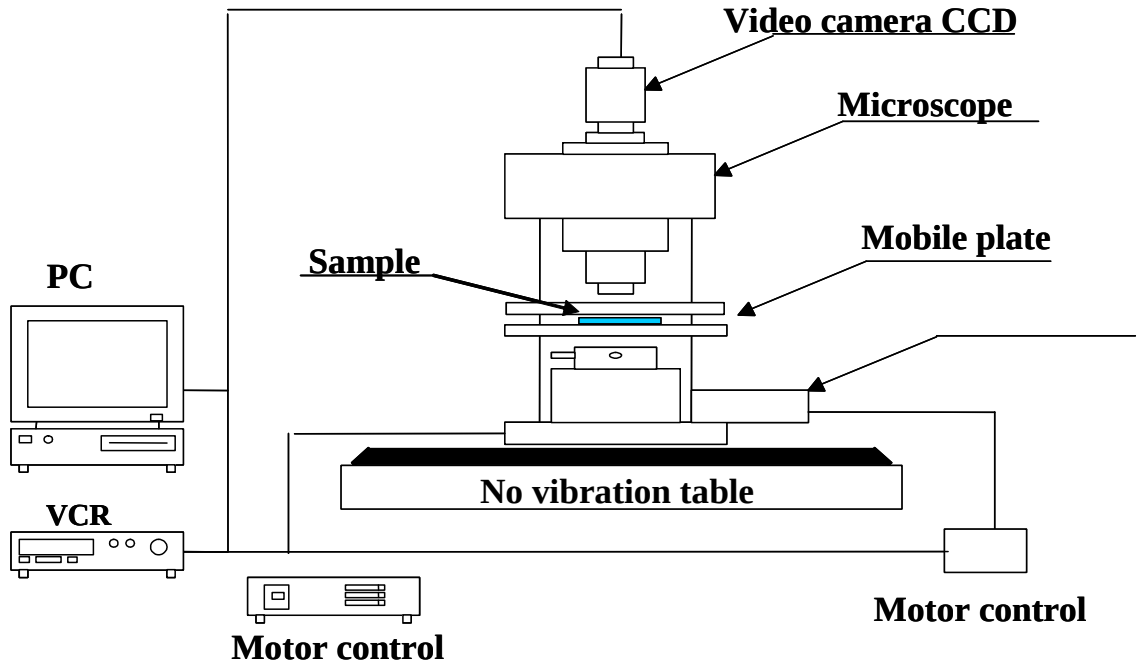

Figure 2: Schematic view of the video microscopy workstation with the shearing device in the z-set-up.

2.2.1 Sample loading and experimental protocol

In either z or y set-up, once alignment of the glass surfaces was completed, the moving plate was driven apart from the fixed one by means of the motorised stage. The moving plate was then accessible to load the continuous phase, by carefully pouring it on the moving plate from a glass syringe. Care was taken to avoid air bubble formation. The moving plate was then approached again to the fixed one, until the desired gap was reached. Parallelism was checked again by using the microscope to measure the gap thickness at several positions, to see if some misalignment was introduced by squeezing a viscous fluid between the two plates. The small deviations possibly found, if any, were then corrected by using the micrometric stages.

In the z-set-up, some edge effects coming from the confining surfaces of the two glass slides are expected. Such effects become negligible within a distance along z of

the order of the size of the gap between the two plates, as shown by de Bruijn for a Couette geometry (1989). To minimise edge effects, in all the experiments the gap between the plates was set at ~ 0.5 mm. Besides, an experimental test of apparatus performance in the z-set-up was carried out by measuring velocity profiles in the x-y plane at several values of z. Such measurements were performed by tracking the motion of dust particles inside the sample. Velocity profiles were linear and independent of z, as expected for simple shear flow.

After loading the continuous phase between the glass plates, a few drops of the dispersed phase were injected in the sample by using a tiny glass capillary (tip size: O.D. ~ 0.3 mm, I.D. ~ 0.1 mm), which had been obtained by pulling one end of a glass tube. Prior to use, the glass tube was filled with the dispersed phase and the end opposite to the capillary was connected either to a compressed air line or to a vacuum pump. By a judicious alternate operation of "push and pull" drops with diameters variable in the range 30-200 μm were generated. The glass tube was attached to a home-made micromanipulator for a precise positioning of the capillary inside the gap. In the z-set-up, care was taken to generate isolated drops at about half-way distance between the two glass slides along the z-axis in order to avoid edge effects, as discussed above. After drop injection, the capillary was gently extracted from the gap.

Drop diameter was always at least 5-10 times smaller than the gap, in order to minimise wall effects. As we will see next, I observed that, for an isolated drop, the effect of a wall is to generate an increase in drop deformation. Such effects decrease with increasing ratio d/R, where d is the gap width. The effects become negligible for d/2R above 5, a condition which was well satisfied in all the experiments presented in this work.

Buoyancy effects were estimated by evaluating the non-dimensional quantity

$\frac{\Delta\rho gR}{\eta_c\dot{\gamma}}$, representative of the ratio between sedimentation and shear velocity, where R is the radius of the drop at rest, η_c is the viscosity of the continuous phase and $\dot{\gamma}$ is the shear rate. According to Phillips et al. (1980), buoyancy effects are negligible when $\frac{\Delta\rho gR}{\eta_c\dot{\gamma}}$ is less than 0.3. In this work, such quantity was at most 0.01, thus ensuring that drop deformation was not affected by sedimentation.

After drop injection in the continuous phase between the parallel plates, the speed of the moving plate was set at the lowest value selected for the experiment (which was usually 0.01 mm/s). Motion was then started and the sample was sheared for a time long enough to reach a stationary drop shape. At this point, the flow was stopped and the drop allowed to relax back to the spherical shape. The whole sequence, including start-up and retraction upon cessation of flow, was recorded on videotape for later analysis. Speed and travel of the moving plate were then progressively increased for each of the subsequent runs, until a stationary drop shape could not be attained anymore (a condition of incipient break-up). Due to the limited travel of the moving plate, flow direction was reversed from time to time. The overall magnification was decreased in the course of the experiment by changing zoom and objectives, to make it easier to follow drop motion at higher speeds. Reproducibility was assessed by repeating the experiment *ex novo,* i.e. starting from the preparation of fresh solutions of the biopolymers. Furthermore, drop phase and continuous phase were also inverted.

Non Newtonian fluids and drop diameter were varied during the experimental campaign in order also to explore a wide range of p, that is a function of drop radius and first normal stress difference of the viscoelastic phase.

2.2.2 Quantitative analysis of drop shape

Quantitative parameters representative of drop shape were obtained by an automated procedure based on image analysis techniques. Images of the deformed drop, captured by the CCD video camera and recorded on videotape, were digitised by an 8-bit frame grabber (Spectrum, Imagraph) installed on a Pentium III host computer. Contrast was enhanced by adjusting gain and offset of the incoming video signal prior to digitisation. The images were analysed by a Visual Basic macro, exploiting standard image analysis routines provided by a commercial software package (Image-Pro Plus 4.0, Media Cybernetics). The macro implemented an automated procedure of edge detection, based on maximisation of the contrast of the drop with respect to the background while preserving a closed contour. In the z set-up , the two axes a and b of the deformed drop (as observed in the plane of shear) and the angle θ between the major axis a and the velocity gradient direction (see the schematic drawing in Figure 3) were calculated for an equivalent ellipse (i.e., having the same area and first and second moments of area of the actual drop).

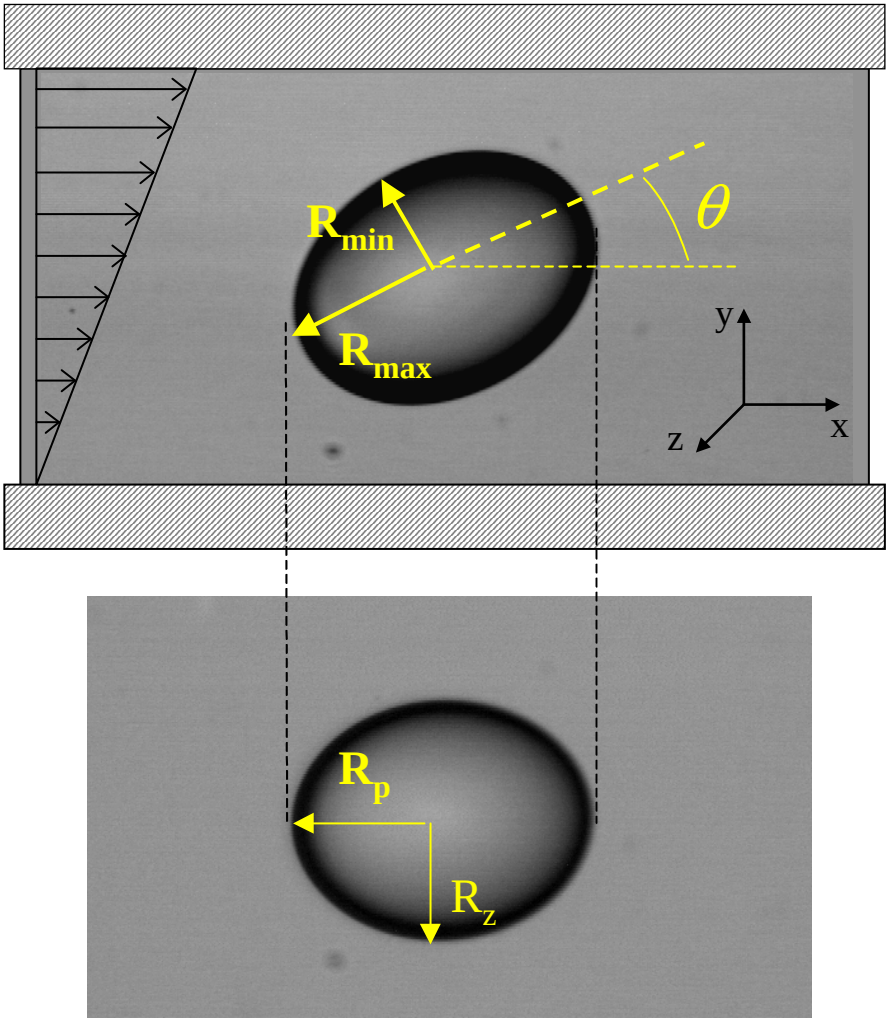

Figure 3: Drop as observed along vorticity axis and velocity gradient direction. Deformation parameters are also reported.

Morphology evolution of a Newtonian drop immersed into a viscoelastic phase under shear flow.

First chapter of this section illustrates drop dynamics at start-up and after cessation of shear flows, comparing the data with some phenomenological models predictions, while second part is concerned about drop high deformations and break-up. In both cases a model system with a non Newtonian highly elastic continuous phase and a Newtonian drop phase was considered.

3 Start-up and retraction dynamics

Acknowledgements

I wish to thank Prof. Pier Luca Maffettone and Doctor Francesco Greco for their theoretical support. Some comments of this part are taken from the paper presented at the Annual European Rheology Conference 2005 in Grenoble and approved for publication: Sibillo, Vincenzo; Simeone, Marino; Guido, Stefano; Greco, Francesco; Maffettone, Pier Luca. "*Start up and retraction dynamics of a Newtonian drop in a viscoelastic matrix under simple shear flow*". Journal of Non-Newtonian Fluid Mechanics.

Keywords: Drop dynamics, viscoelastic matrix, Boger fluid, start-up, overshoot, retraction, shear flow.

3.1 Introduction

In this part, I will focus on transient dynamics. Specifically, I will describe the Newtonian drop dynamics at start-up and after cessation of shear flows in the case of a non-Newtonian external fluid. Experimental data are taken with the rheo-optical computer-assisted shearing device, allowing for drop observation under microscopy only from the vorticity direction of the shear flow, showed in the chapter "materials and methods". A very precise characterization of drop shape along the vorticity direction is achieved, even at small deformations during transients. At a fixed viscosity ratio (drop to matrix viscosity is unity), I will show the effects of varying the flow rate (Capillary number), and of varying the "elasticity content" of the system.

Transient behaviour of drop deformation at low shear rates will be illustrated in the first part of this section, and a comparison of these data with the predictions gotten

from two recently proposed phenomenological models of drop dynamics will also be illustrated and briefly discussed (Maffettone-Greco model - MG (Maffettone and Greco, 2004)[11] and the Yu-Bousmina-Zhou-Tucker model - YBZT (Yu et al., 2004)[12]). In spite of the fact that the phenomenological models were designed for the non-Newtonian case at low-to intermediate drop deformations, which is the case examined in the first part, fine details of the transient dynamics are not caught by the models. Rather, systematic discrepancies between data and predictions are found, as it will be discussed in the following.

Finally, the start-up transient of drop deformation at high capillary numbers and with a fixed value of matrix elasticity will be briefly showed, focusing the attention on the new "overshoot phenomenon" of the deformation parameters, R_{MAX}/R, R_{MIN}/R and D, during which the drop enhanced its orientation toward the flow direction. Data will be compare with only MG predictions. It will be showed that the model performs adequately, giving quantitative predictions of the overshoot phenomenon up to a moderate drop deformation.

3.2 Materials and methods

Materials and experimental methods used to investigate drop dynamics upon start-up and cessation of shear flow are the same used by Guido et al. (2003)[13], and have been illustrated in the experimental section. Briefly, in all the experiments the matrix was a constant-viscosity elastic polymer solution (Boger fluid), and the dispersed Newtonian phase was a mixture of silicone oils (Dow Corning). The Boger fluids were prepared by mixing a Newtonian polyisobutylene (PIB) sample (Napvis 5, BP

[11] Maffettone P. L. and Greco F., "An ellipsoidal drop model for single drop dynamics with non-Newtonian fluids", J. Rheol. (2004), 48, 83-100.

[12] Yu W, Bousmina M, Zhou CX, Tucker CL, "Theory for drop deformation in viscoelastic systems", J. Rheol. (2004) 48, 417-438.

[13] Guido S, Simeone M and Greco F, "Deformation of a Newtonian drop in a viscoelastic matrix under steady shear flow. Experimental validation of slow flow theory", J. Non-Newtonian Fluid Mech., 114 (2003) 65-82.

Chemicals) with a small amount of a high molecular weight grade of the same polymer (Aldrich), preliminary dissolved in kerosene at the concentration of 4% wt, as discussed in the previous section.

The Boger fluids viscosity η_C was essentially constant in the range of shear rate investigated ($\dot{\gamma}$ up to 20 s^{-1}), and rather large values of the first normal stresses difference N_1 were found. Furthermore, the slope of N_1 vs. shear rate $\dot{\gamma}$ in log scale was equal to 2 within experimental error, showing that the Boger fluid used as external phase is in fact a "second-order fluid" at steady state. Rheological data for the viscoelastic matrix are: η_C = 6.6 Pa s and $\Psi_1 = N_1/\dot{\gamma}^2$ = 3.5 Pa s^2 at the temperature of the experiments (25°C). Concerning the drop fluid (i.e., the PDMS silicone oils), silicone oils were properly mixed to have a drop-to-matrix viscosity ratio of 1 at 25°C. For the so obtained mixture, the viscosity η_D was constant and no normal stresses could be measured within the instrumental sensitivity (Bohlin CVO 120) in the range investigated, thus confirming its Newtonian behaviour. The interfacial tension of the fluid pairs was measured by applying the theory by Greco (2002)[14] to data of steady state drop shape in shear flow. The so obtained values were around 1.3 mN/m (more details can be found in Guido et al. (2003)). The "elasticity content" of the single drop system was quantified with the parameter $p = \frac{\Psi_1 \sigma}{R\eta^2}$, that can be interpreted, as explained in the introduction, as the ratio between the constitutive relaxation time of the matrix fluid $\tau = \frac{\Psi_1}{2\eta_C}$ and the emulsion time $\tau_{em} = \frac{\eta_C R}{\sigma}$.

The parallel plate apparatus used to generate simple shear flow has been also

[14] Greco F., "Drop deformation for non-Newtonian fluids in slow flows", J. non-Newtonian Fluid Mech., 107 (2002) 111-131.

described in detail elsewhere by Guido et al. (2003). One plate was displaced with respect to the other by a 2-axis motorized translating stage. Observations along the vorticity axis of shear flow were performed by optical microscopy through a standard monochromatic CCD video camera. The deformed drop under shear flow was kept in the field of view by translating the microscope itself through a motorized stage.

Drop diameter was at least ten times smaller than the gap (~1 mm), so that wall effects were negligible. Images from the experimental runs were both recorded on a videotape and stored on an hard disk after digitization by a frame grabber installed on a personal computer. At steady state, images were digitized during the experiment with a time step of a few seconds. To improve the temporal resolution during start-up and retraction and to compare with the good possible way experimental data with the phenomenological predictions, images were acquired offline from the videotape at 25 frames per second. The maximum (R_{MAX}) and minimun (R_{MIN}) drop axis in the shear plane (i.e., as seen from the vorticity direction) and the orientation angle θ were measured in each image by an automated image analysis procedure, based on an edge-detection algorithm to identify the side-view drop contour. Transient behaviour of drop submitted to low shear rates, its steady shape and the comparison of these data with the two phenomenological models predictions were characterized only by the "deformation parameter" introduced by Taylor $D=(R_{MAX}-R_{MIN})/(R_{MAX}+R_{MIN})$. The start-up transient of drop submitted to high capillary numbers was characterized by all the deformation parameters R_{MAX}/R, R_{MIN}/R, D and θ. Only the time evolution of D will be compare with MG-model predictions.

Calibrated reticules were used to calculate the scale factors (micron/pixel) for the optics used in the experiments, and to correct for the small image distortions introduced by the CCD camera. But residual errors, which are also due to image digitalization, can

be estimated by the value of the deformation parameter D that is measured when the drop is in the spherical configuration at rest. In fact, due to image digitalization, the deviations from the theoretical value D = 0 depend on drop size in the image window (the larger is the size, i.e., the number of pixels delineating drop contour, the smaller the deviation). In the same experiment, the optical magnification and thus the apparent drop size in the image window was lowered with increasing the flow rate, to allow one of us to keep the drop in the field of view at higher speeds, translating the microscope by the joystick. The actual drop size was also changed from one experiment to the other in order to adjust the "elasticity content" of the system (as measured by the parameter p), which is very sensitive to drop radius. In particular, smaller drops had to be used to investigate higher elasticity. In the experiments presented in this work, the deformation parameter D at rest was around $5x10^{-3}$. Though small, such a deviation from 0 is quite evident in the analysis of drop retraction upon cessation of flow, especially when the data are plotted in a log-scale. Hence, a cut-off of 0.01 was used to remove data in the final part of drop retraction analysis.

3.3 Drop dynamics models

To compare our data with theoretical predictions, in the lack of the exact fluid-dynamic solution for the single-drop non-Newtonian problem, two models of drop dynamics have been chosen, namely, the Maffettone-Greco (MG) (Maffettone and Greco, 2004) and the Yu-Bousmina-Zhou-Tucker (YBZT) model (Yu et al., 2004). A brief description, derived from Vincenzo Sibillo et. al. work (2005)[15], of the phenomenological models will be illustrated to better understand the comparison between my experimental data with the selected models predictions. Both these models

[15] V. Sibillo, M. Simeone, S. Guido, F. Greco, P. "Start-up and retraction dynamics of a viscoelastic drop in a Newtonian matrix under simple shear flow." Paper approved for publication on the J. non-Newtonian Fluid Mech., special issue dedicated to AERC2005.

start from the assumption that the drop always maintains an ellipsoidal shape when subjected to an imposed flow field "at infinity". Thus, the "geometric" equation $S(t):\overline{rr}=R^2$ always holds, with r a point of the drop surface, R the drop radius at rest, and **S**(t) a second-order, positive definite, symmetric, time-dependent tensor, the evolution of which fully describes drop dynamics. For the reader's convenience, we report in this Section the time dependent equations of tensor **S**(t), in non dimensional form, derived from the work of Maffettone P.L. and Greco F. (2004) and from Yu W. Bousmina et. al (2004).

For the MG model, it is:

$$\frac{\mathrm{d}\mathbf{S}}{\mathrm{dt}}+\mathrm{Ca}\left[-\left(\mathbf{\Omega}\cdot\mathbf{S}-\mathbf{S}\cdot\mathbf{\Omega}\right)+\mathrm{a}\left(\mathbf{D}\cdot\mathbf{S}+\mathbf{S}\cdot\mathbf{D}\right)+\mathrm{cTr}\left(\mathbf{S}\right)\mathbf{D}\right]=-\mathrm{f}\left(\mathbf{S}-\mathrm{g}(\mathbf{S})\,\mathbf{I}\right) \quad (1)$$

In eq.(1), **D** and **Ω** are the (non dimensional) deformation rate tensor and vorticity tensor, respectively, at infinity, time has been made non dimensional through the so-called emulsion time $\tau_{em}=\eta_C/(\sigma/R)$ (with σ the surface tension of the fluid pair), and Ca is the "capillary number". The three constants a, c, and f, and the **S**-dependent scalar-valued function g in eq.(1) (**I** is the unit tensor) depend on all the constitutive parameters of the fluid pair. For the case of interest here, with a Newtonian drop in a non-Newtonian matrix, these are in fact the inner/outer viscosity ratio $\lambda=\eta_D/\eta_C$ (η_D is the drop viscosity) and the time ratio $p=\tau/\tau_{em}$, with $\tau=\frac{\Psi_1}{2\eta_C}$ the dominant characteristic time of the non-Newtonian matrix and τ_{em} the emulsion time. (Another parameter, which controls the normal stress differences in the non-Newtonian matrix, is not effective in the situations considered here.) The specific formulae for a, c, f, and g

are given in the original MG paper.

For the YBZT model, the needed dynamical equations are (with the notations adopted in Sibillo et al., 2005):

$$\frac{d\mathbf{S}}{dt} = -\mathbf{S}\cdot\mathbf{L} - \mathbf{L}^{T}\cdot\mathbf{S} \tag{2}$$

$$\mathbf{L} = Ca\left(\mathbf{\Omega} + m\mathbf{D}\right) + n\frac{3\mathbf{S}}{Tr\left(\mathbf{S}\right)} + \left(1-\tilde{\lambda}\right)\frac{1}{p}\left[Ca\,\alpha\mathbf{D}\,e^{-\frac{c_1}{p}t}F\left(t\right) + \beta_1\mathbf{g}_1 + \beta_2\mathbf{g}_2\right] \tag{3}$$

$$\frac{d\mathbf{g}_i}{dt} = \frac{3\mathbf{S}}{Tr\left(\mathbf{S}\right)} - \mathbf{I} - \frac{c_i}{p}\mathbf{g}_i\ , \qquad i = 1,2 \tag{4}$$

where, in eq.(3), $F\left(t\right) = p/c_1\,(e^{\frac{c_1}{p}t} - 1)$ during flow, and $F\left(t\right) = p/c_1\,(e^{\frac{c_1}{p}t_{FIN}} - 1)$=const after cessation of flow, i.e., for $t > t_{FIN}$. In eqs.(2)-(4), the seven constants $m, n, \alpha, \beta_1, \beta_2, c_1$ and c_2 all depend on λ and $\tilde{\lambda}$ (their explicit forms are given in the original papers).

To understand the meaning of the new parameter $\tilde{\lambda}$, one should recall that, in the derivation of eqs.(2)-(4), the non-Newtonian matrix was assumed to consist in a Newtonian part (the "solvent") plus a Maxwell fluid, with viscosities η_S and η_M, respectively. The parameter $\tilde{\lambda}$ is then defined as the ratio of the "pure solvent" to the "total" matrix viscosity, namely, $\tilde{\lambda} = \eta_S/(\eta_S + \eta_M) = \eta_S/\eta_C$.

3.4 Results

In the first part of this paragraph, I present single drop deformation data during the start-up and after cessation of shear flow, and compare these data to predictions from the MG and YBZT models. All data presented here are derived from the new work of Sibillo et al. (2005). The viscosity ratio $\lambda = \eta_D/\eta_C$ is always unity, while the p parameter is varied up to 1.4, which stands for a robust elasticity.

As reported later, upon shear start, overshoots of drop deformation may occur. At higher values of the elasticity parameter p, the overshoots are seen at lower Ca-values. These trends are qualitatively reproduced with the MG model, as we will see. However, in this first part I do not want to investigate on the overshoot phenomenon. For this reason, the Ca's investigated now are rather low.

Finally, concerning the extra parameter $\tilde{\lambda}$ of the YBZT model, it should be mentioned that, because of the protocol used to prepare our Boger fluids, I cannot determine a value for $\tilde{\lambda}$. Indeed, kerosene evaporation up to phase equilibrium (see the Materials and Methods Section) forbids a separate evaluation of η_S and η_M, the only measurable quantity being directly η_C. Thus, $\tilde{\lambda}$ will be used in the calculations as an adjustable parameter, see below.

Figure 4 shows the transients for the start-up with Ca = 0.07, and the corresponding relaxation, of a system with p = 0.5. Symbols are experimental data. Dotted lines are Newtonian predictions, whereas solid and dot-dashed lines are viscoelastic predictions from the MG and the YBZT models, respectively. For the YBZT model, $\tilde{\lambda} = 0.5$ has been chosen. (Larger values of $\tilde{\lambda}$ give start-up predictions too close to the Newtonian curve; lower values of $\tilde{\lambda}$ give a "hump" in early time relaxation.) At this low level of both capillary number and elasticity, the viscoelastic predictions are in good quantitative agreement with the experiments. The start-up data

are correctly described up to steady state, while the relaxation data are very well described up to t~2, then the predictions slightly underestimate the observed trend. The comparison with the Newtonian case show that the effect of matrix elasticity is to slow down the dynamics.

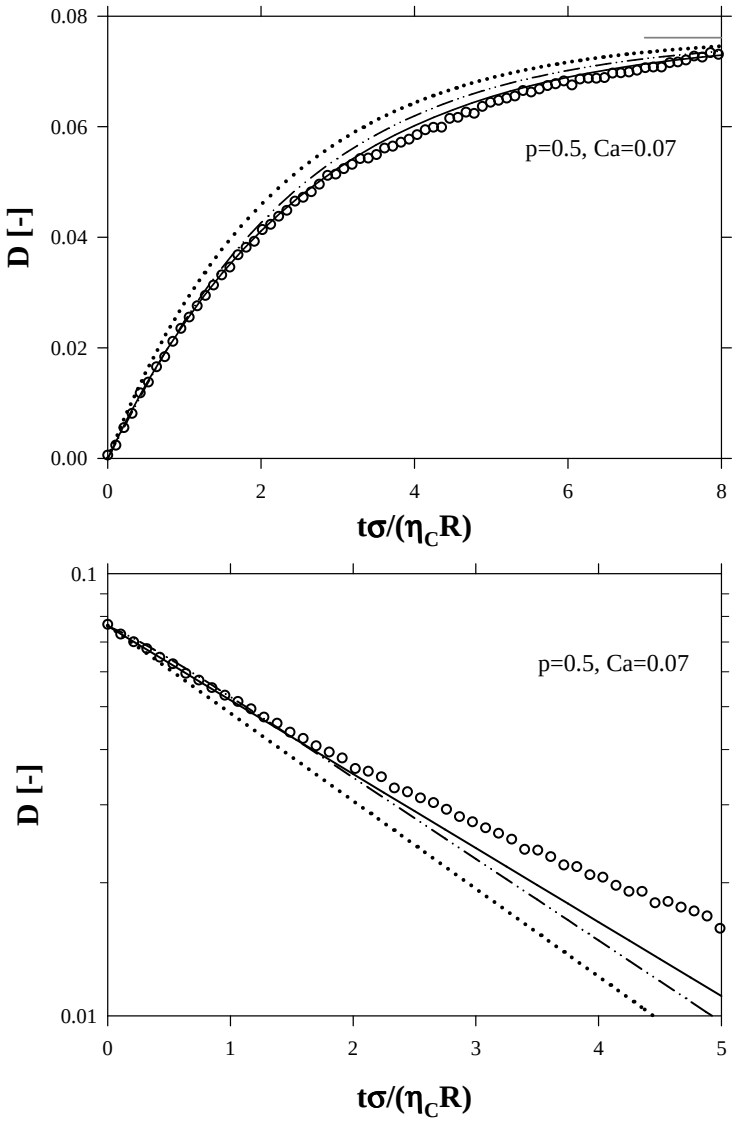

Figure 4: The deformation parameter D as a function of time during start-up (upper plot) and retraction upon cessation of flow (lower plot) for Ca = 0.07 and p = 0.5. Lines are predictions of the Newtonian theory (dotted), MG model (solid) and the YBZT model (dot-dashed).

The effect of the increase of the capillary number is shown in Figure 5, with Ca = 0.14, the elasticity parameter p being kept fixed at the same value of Figure 4 (p = 0.5).

Again, the agreement between both theories and experiments is quite good. Consequently the value of $\tilde{\lambda}$ will be kept constant from now on.

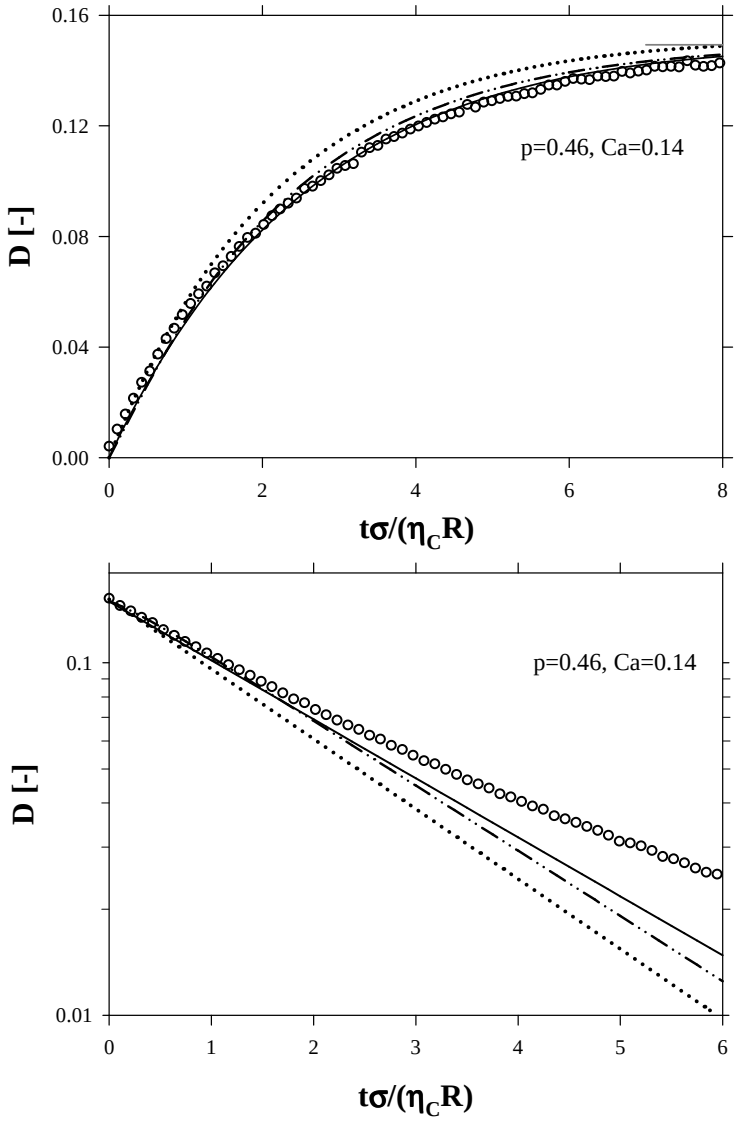

Figure 5: The deformation parameter D as a function of time during start-up (upper plot) and retraction upon cessation of flow (lower plot) for Ca = 0.14 and p = 0.46. Lines are predictions of the Newtonian theory (dotted), MG model (solid) and the YBZT model (dot-dashed).

The effect of the increase of the elasticity parameter is shown in Figure 6, where p = 1.4 and Ca = 0.075. In this case the comparison with the viscoelastic predictions is much less satisfactory than it was obtained at low p. The initial trend is now faster than the predictions, for both start-up and relaxation. It is interesting to note that the

Newtonian predictions are very close to the data for t<2. Above this value of time, data slow down with respect to Newtonian predictions. In this regard, note that the slowing down of the data can be well described by the viscoelastic predictions, and this is particularly evident with relaxation data as reported in Figure 7. In the semilog scale, a negative time shift of the viscoelastic predictions shows that the experimental data line up on this curve in a quite large time window (2<t<4).

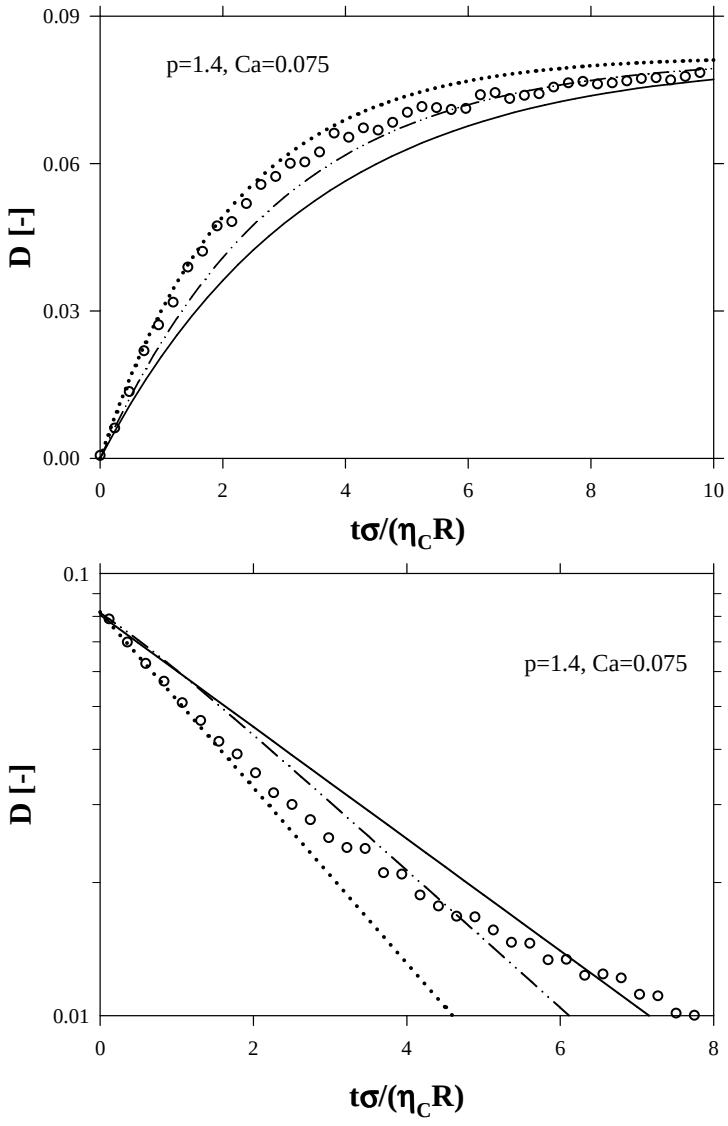

Figure 6: The deformation parameter as a function of time during start-up (upper plot) and retraction upon cessation of flow (lower plot) for Ca = 0.075 and p = 1.4. Lines as model predictions as in the previous figures.

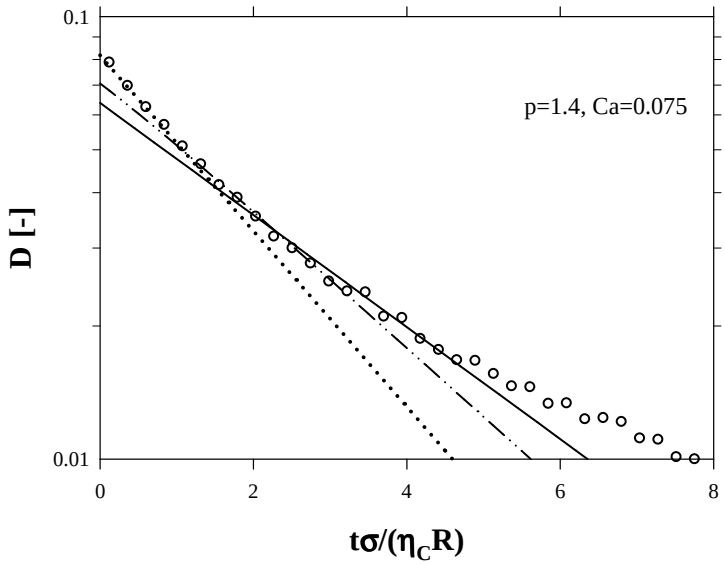

Figure 7: Same results as in the lower diagram of Figure 6 plotted in semi-log scale.

A very similar situation is found at "intermediate" p-values, as illustrated in Figure 8 ($p = 1$, $Ca = 0.073$), for relaxation only. Again, at short times ($t<1.5$) the drop dynamics essentially follows the Newtonian evolution, then it is adequately described ($1.5<t<4$) by the time-shifted MG viscoelastic curve. Here, as in Figure 7, the relaxation data at very large times ($t>4$) show an upturn. It should be mentioned that such an upturn, though corresponding to very low values of the deformation parameter ($D<0.02$) where image digitalization errors are higher (see Materials and Methods), has not been observed in the Newtonian case for drops of similar size (see Guido and Villone, 1999).

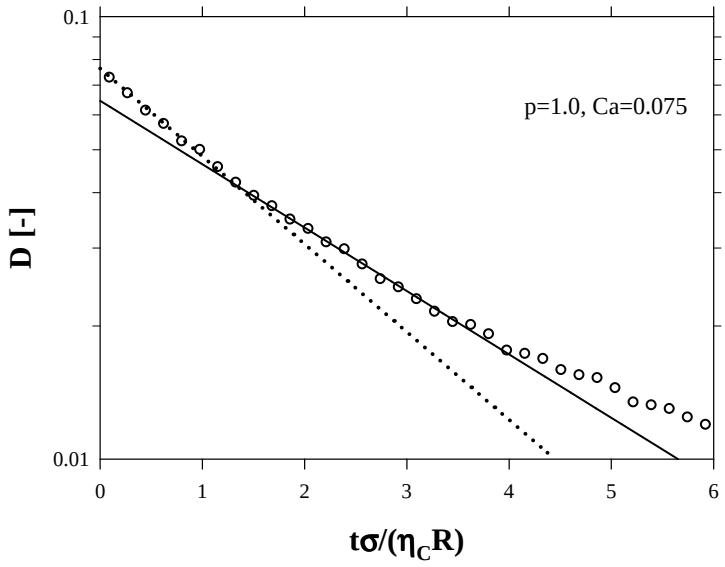

Figure 8: The deformation parameter D as a function of time during retraction upon cessation of flow for Ca = 0.075 and p = 1 Lines as model predictions as in the previous figures.

Finally, in Figure 9 we report data and predictions for p = 1, at a "high" Ca = 0.12. (For Ca>0.12, overshoots would appear in the data for this system, as illustrated in the next section). In the very initial response to shear start-up, data sit in between the Newtonian and YBZT predictions, whereas the MG model behaves better at long times (t>4). (The steady state is almost equal for all the predicted curves.) In relaxation, again, drop deformation starts as Newtonian, to slow down later, towards the non-Newtonian predictions.

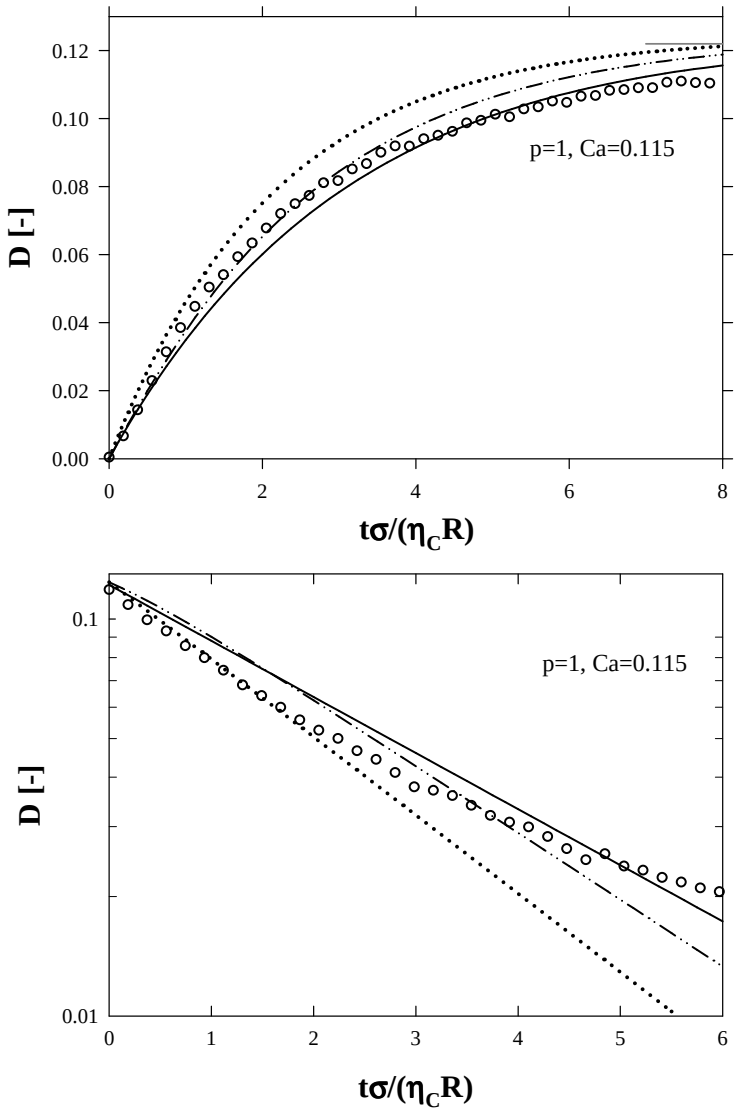

Figure 9: The deformation parameter D as a function of time during start-up (upper plot) and retraction upon cessation of flow (lower plot) for Ca = 0.115 and p = 1 Lines as model predictions as in the previous figures.

Transient behaviour of R_{MAX}, R_{MIN} and the orientation angle θ after the start up of the shear flow are reported in Figure 10 at p = 1, varying the Capillary number. At low capillary number all the parameters, as previously discussed, monotonically change to reach the steady state. As the Ca value increases, the drop initial evolution shows an evident overshoot of R_{MAX} and an undershoot of R_{MIN}, that are more pronounced at Ca = 0.25, during which drop also enhances its orientation toward the flow direction. This feature is qualitatively captured by the MG model as sown in Figure 11, derived from

Sibillo et al. (*Macromol. Symp.* 2005)[16], where is only reported D evolution in time t/τ_{em}. This phenomenon will be also illustrated in the next part of this section. The evolution of D and θ during the start-up of the flow as a function of the p parameter, at high but sub critical Capillary numbers (see next part), will be illustrated and discussed.

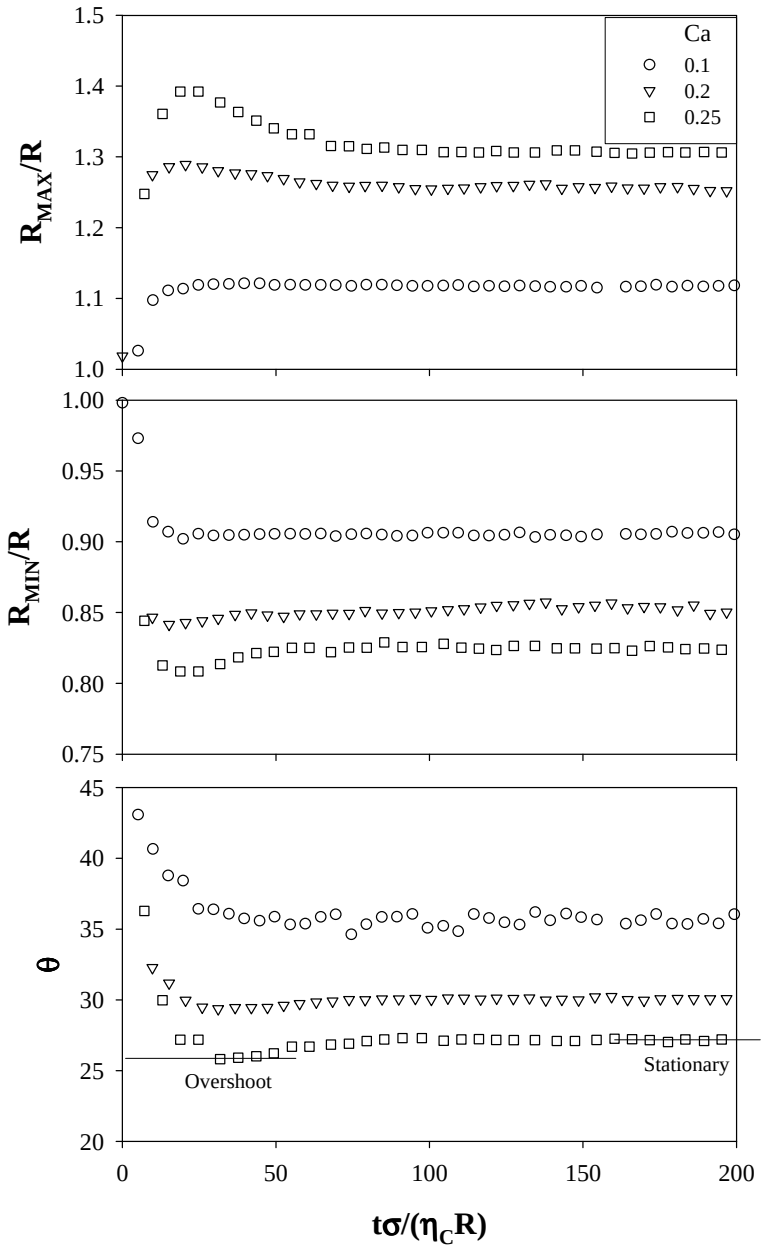

Figure 10: Deformation parameters during start-up flow at λ = 1, p = 1 and different Capillary numbers.

[16] V. Sibillo, S. Guido, F. Greco, P.L. Maffettone. "Single drop dynamics under shearing flow in systems with a viscoelastic phase". Macromolecular Symposium, (2005), 228, 31-39.

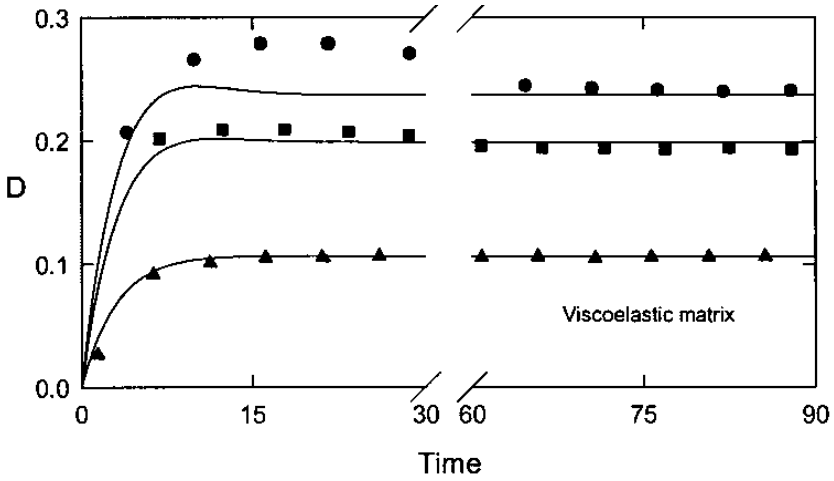

Figure 11: Transient behaviour of the deformation parameter D vs. non dimensional time, at various Capillary numbers: triangle 0.1, squares 0.2 and circles 0.25, for λ = 1, p = 1. Lines are the corresponding MG model predictions.

3.5 Final remarks

In this Section, I illustrated fine details of drop dynamics in shear start-up and relaxation, the external matrix being a constant-viscosity, elastic liquid. First part was about drop small deformations, corresponding to low imposed capillary numbers. Comparison between data and predictions from two available drop dynamics models revealed an unexpected feature, namely, an "elasticity-controlled transition" from Newtonian to non-Newtonian dynamics throughout a single experiment.

Indeed, at a sufficiently "intense" elasticity, early stages of drop dynamics are well described by the fully Newtonian predictions, while non-Newtonian effects become evident (and are well predicted) at later times only. In other words, a "time lag" sets in during transients, in which non-Newtonianness seems to be inactive.

Since such effects are not observed for "weakly" elastic systems, one would be tempted to infer that the range of validity of the (initial) Newtonian dynamics increase as the elasticity increases. Our data, however, are too limited to support such a conclusion.

A sort of "transition" in drop dynamics had already been observed by Leal and

coworkers (Threteway and Leal, 2001)[17] in relaxation after planar elongational flow, and had in fact partly motivated the recent ellipsoidal model by Yu et al. (2004). It should be remarked, however, that the YBZT model, under our experimental conditions, is unable to predict the observed transition, and the same is true for the simple MG model (Maffettone and Greco, 2004). It so appears that some significant ingredient is still absent in the existing theoretical analyses.

Finally, I would like to stress that, in relaxation and at long times, all data invariably show a further upturn beyond the "non-Newtonian" time interval (see Figure 7 and Figure 8). The origin of this upturn is unclear. In this respect, it should be recalled that, in all of these experiments, the selected non-Newtonian fluids are Boger fluids, the properties of which, in transient situations, are always difficult to consider (Solomon and Muller, 1996)[18]. Investigations of drop dynamics with "realistic" non-Newtonian fluids will certainly be needed in the future.

Besides it has been found that the presence of a viscoelastic matrix, during the start-up of flow, induces a transient characterized by an overshoot of the deformation parameters, during which drop enhances its orientation towards the shear direction before reaching the steady state. It has been shown that the MG model is capable of describing this phenomenon, giving quantitative predictions up to moderate drop deformation.

[17] Tretheway D. C., Leal L. G., "Deformation and relaxation of Newtonian drops in planar extensional flows of a Boger fluid", J. Non-Newtonian Fluid Mech. 99 (2001) 81–108.

[18] M. Solomon, S. Muller, "The transient extensional behavior of polystyrene-based Boger fluids of varying solvent quality and molecular weight", J. Rheol. 40 (1996) 837-856.

4 High deformations and Break-up

Keywords: Drop break up, Boger fluid, viscoelasticity, shear flow, optical microscopy

4.1 Introduction

The effect of matrix elasticity on the break-up of an isolated Newtonian drop under step shear flow is herein presented.

It was observed in the introduction that many physical and rheological properties of the liquid – liquid suspensions, as the polymeric blends, are strongly dependent on the morphology, i.e., size and shape of the dispersed phase inclusions. Morphology control of these systems can often be achieved by proper setting of the flow conditions experienced during processing. The interplay between the applied flow and the morphology of the system is quite complex, and is often further complicated by non-Newtonian behaviour of the fluid components. Nevertheless, in general terms, we can say that the mean size of the inclusions decreases as a consequence of drop break-up, caused by an "high-speed flow". This part is concerned with the influence of the viscous and elastic properties of the outer phase on the break up phenomenon of a single Newtonian drop under simple shear flow conditions.

Investigation of drop deformation and break-up under shear flow, when both liquids are Newtonian, as discussed in the introduction, was pioneered by Taylor (1932, 1934)[19][20], and much phenomenological evidence and approximate theoretical analyses have been collected through the years (Stone, 1994)[21]. In extreme synthesis, we know

[19] Taylor G I (1932) "The viscosity of a fluid containing small drops of another fluid". Proc. R. Soc. London A, 138, 41-48.

[20] Taylor G I, (1934) "The formation of emulsions in definable fields of flow". Proc. R. Soc. London A, 146, 501-523.

[21] Stone H A (1994) "Dynamics of drop deformation and breakup in viscous fluids". Ann. Rev.

that the dynamics of isolated drops in shear flow is determined by the two non-dimensional parameters, i.e., the capillary number Ca and the viscosity ratio λ (drop to matrix viscosity) and it is experimentally well known (Grace, 1982[22]; de Bruijn, 1989[23]) that stationary drop shapes (starting from the spherical configuration) are only reached up to a certain critical value Ca_{cr} of the capillary number, which only depends for pure Newtonian systems, on the viscosity ratio λ. Beyond Ca_{cr} a drop keeps deforming, until rupture occurs.

Briefly, when one or both the component fluids are viscoelastic, the fluidodynamics of the drop becomes more complex, as the constitutive time scales of the two fluids also come into play, together with the intrinsic time scale related to the very existence of an interface. As early as in 1972, Flumerfelt[24] reported for the first time experimental results on break-up of Newtonian drops in shear flows of viscoelastic fluids. He found that i) the non-Newtonian critical capillary number is always larger than the corresponding Newtonian one (with same viscosity ratio) and ii) there exists a minimum drop size below which break-up can not be achieved. Point i) was later confirmed in the reverse case (non-Newtonian drop in a Newtonian matrix) by Varanasi et al. (1994)[25], while the existence of a minimum radius for break-up (point ii)) is better seen as a result limited to the range of shear rates investigated by those authors.

In the drop break-up experiments described so far, the non-Newtonian behaviour of the fluids investigated included both viscosity shear-thinning and less than quadratic normal stresses. In other words, it so happened in these experiments that “high” non-

Fluid Mech., 26, 65-102.

[22] Grace H P (1982) “Dispersion phenomena in high viscosity immiscible fluid systems and application of static mixers as dispersion devices in such systems”. Chem. Eng. Commun., 14, 225-277.

[23] de Bruijn R A (1989) “Deformation and breakup of drops in simple shear flows”. PhD thesis, Technische Universiteit Eindhoven.

[24] Flumerfelt R W, (1972) Drop breakup in simple shear fields of viscoelastic fluids. Ind. Eng. Chem. Fundam., 11, 312-318.

[25] Varanasi P, Ryan M E and Stroeve P (1994) “Experimental study on the breakup of model viscoelastic drops in uniform shear flow”. Ind. Eng. Chem. Res., 33, 1858-66.

dimensional shear rates were at play. Hence, a clear identification of separate elastic and viscous non-Newtonian effects was in fact not achieved. By using Boger fluids, conversely, it is expected that this difficulty can be overcome, also because of the absence of any shear-thinning. Mighri et al. (1998)[26] used several pairs of Boger fluids to study break-up conditions with different drop to matrix elasticity ratios. They report the variation of the critical capillary number Ca_{cr} with the elasticity ratio, though limited to viscosity ratios λ ranging between 0.3 and 1.1. Even if the general assertion that drop break-up is somewhat inhibited by elastic effects is present in the literature, a clear understanding of non-Newtonian effects has not yet been achieved.

In this section the effect of matrix elasticity on the break-up of an isolated Newtonian drop is showed. Boger fluids were used as continuous phase and the weight of matrix elasticity is quantified with the parameter $p = \frac{\Psi_1 \sigma}{R\eta^2}$, that can be interpreted, as explained in the introduction, as the ratio between the constitutive relaxation time of the matrix fluid $\tau = \frac{\Psi_1}{2\eta_C}$ and the emulsion time $\tau_{em} = \frac{\eta_C R}{\sigma}$. The matrix rheological properties and drop dimension were properly varied, in order to have p ranging from 0.1 to 10. Extrapolating Greco's conclusions to large drop deformation, $p \geq 1$ is the condition to be fulfilled to make non-Newtonian effects observable. Three viscosity ratios were explored (drop/matrix), i.e. 2, 0.6 and 0.04.

At all the viscosity ratios explored, break-up was hindered by matrix elasticity. The start-up transient of drop deformation, at high, but sub-critical capillary numbers, showed an overshoot, during which the drop enhanced its orientation toward the flow direction. Both phenomena increase if the p parameter increases. Finally, the non-

[26] Mighri F, Carreau P J and Ajji A (1998) Influence of elastic properties on drop deformation and breakup in shear flow. J. Rheol., 42, 1477-1490.

dimensional pinch-off length and break-up time were also found to increase with p.

In the following, the experimental section will be devoted to list the Boger fluids used as continuous phase and to explain briefly the experimental protocol. In the next section, the results will be presented and discussed. Finally, some concluding remarks will be presented.

4.2 Experimental

4.2.1 Experimental apparatus

The rheo-optical apparatus used in this work and the experimental protocol were described in detail in the experimental section and elsewhere (Guido and Simeone, 1997[27]; Guido and Villone, 1998[28]) The apparatus essentially consists of a parallel-plate device coupled with an optical microscope. It has been used with two different, interchangeable setups to observe drop deformation and break-up either along the velocity gradient direction and along the vorticity axis. The drop was injected into the continuous matrix using a tiny glass capillary, which had been preliminarily loaded between the parallel plates. Simple shear flow is generated by displacing the motorised plate with respect to the other. The experiments were all carried out in a room kept at constant temperature (23 ± 0.5°C). During a typical run, flow was impulsively started by driving the moving plate at a given speed. The deforming drop was kept within the field of view during motion by translating the microscope, which is itself mounted on a motorized stage. When the drop was observed along the vorticity direction, the two axes R_{MAX} and R_{MIN} of the deformed drop (as observed in the plane of shear) and the angle θ between the major axis R_{MAX} and the velocity gradient direction (see the schematic drawing in the Materials and methods section) were calculated. On the other hand, when

[27] Guido, S. and Simeone, M. "Binary collisions of drops in simple shear flow by computer-assisted video optical microscopy". Journal of Fluid Mechanics, 357, (1998) 1-20.

[28] Guido, S. and Villone, M. "Three dimensional shape of a drop under simple shear flow". Journal of Rheology, 42, (1998) 395-415.

the drop was observed along the velocity gradient direction, R_p and R_z were measured, where R_p is the projection of R_{MAX} on the plane of shear and R_z is drop axis along the vorticity direction. The data were displayed in real time on the computer monitor and stored. The break-up critical capillary number was determined by performing a set of runs at increasing shear rate until break-up occurred. If steady state deformation was reached, the flow was stopped and the drop was allowed to relax back to the spherical shape before starting the next run. Drop break-up always occurred during the flow. With this protocol, I identified an interval in which the critical capillary number is contained. The extremes of this interval are referred to as inferior critical capillary number (Ca_{cr} inf) and superior critical capillary number (Ca_{cr} sup).

4.2.2 Materials

Newtonian silicone oils (PDMS, Dow Corning 1000, 12500, 60000, 100000) were selected as the dispersed phase. In order to achieve the desired viscosity ratio, silicon oils with different molecular weights were mixed together in proper amounts. The experiments were performed at three viscosity ratios, i.e. 2, 0.6 and 0.04. Viscoelastic Boger fluids were used as the continuous phase. As described, they were carefully formulated in order to: i) have a constant viscosity; ii) exhibit first normal stresses difference proportional to $\dot{\gamma}^2$ and iii) provide a value of the p parameter in the range 0.1 ÷ 10, with a drop radius within the experimental window, i.e. 10 ÷ 100 μm.

Table 1, referred to this section, summarises the properties of the viscoelastic fluids used in this experimental campaign as continuous phase. In particular, column 1 reports a code name, Ci; column 2 reports the mass ratio of high-to-low molecular weight polymer, (the values are multiplied by 10^3); column 3 reports the viscosity at 0.05 and 1.5 s^{-1}, which is roughly the range of shear rate at infinity imposed during the experiments (as shown, shear thinning is limited to 10-15%); column 4 reports the first

normal stress coefficient, Ψ_1 and column 5 reports the viscosity ratio of the experiments performed with that fluid.

Boger fluids	**PIB/Napvis 30 (x10^3)**	**Viscosity at 0.05 – 1.5 s^{-1} (Pa s)**	**Ψ_1 (Pa s^2)**	**Experiment at λ**
C1	3.2	55 – 47.5	210	0.04
C2	0.5	80.1 - 79.7	65	0.6
C3	4.4	35.4 – 31.5	36	0.6
C4	*4.4*	43.1 – 34.8	93	2
C5	0.5	81 – 80.6	63	2
C6	4.4	55 – 48	200	2

Table 1: Fluids used in the experiments.

As example, the rheological data of the Boger fluids C1, C2 and C4 are shown in Figure 12. The solid line in Figure 12 is a fit to the first normal stress difference data in log scale. The slope of the fitting lines is equal to 2 ± 0.1, in agreement with the assumption of second order fluids. The first normal stress difference coefficient $\Psi_1 = \frac{N_1}{\dot{\gamma}^2}$ was calculated by fitting the data of Figure 12 to a line of slope 2 in log scale. On the other hand, no normal stresses could be measured for the silicone oils within the instrumental sensitivity.

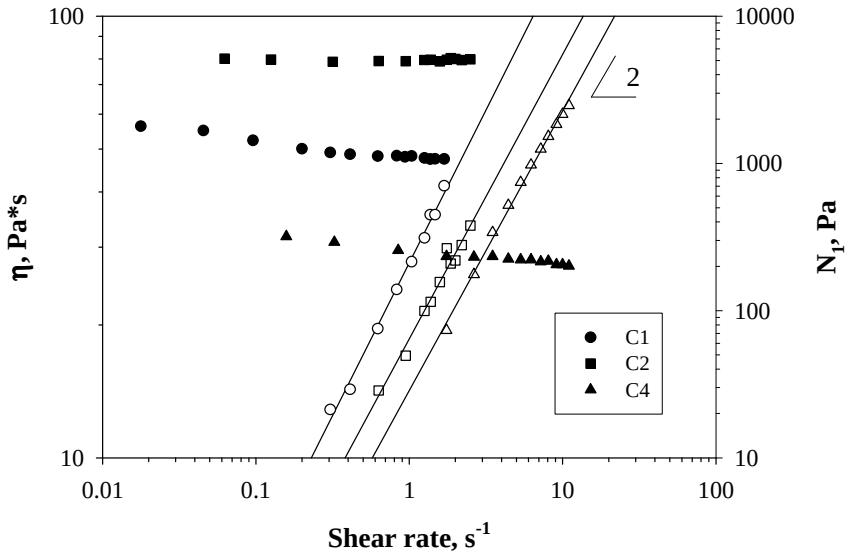

Figure 12: Viscosity and first normal stress difference vs shear rate for the Boger fluids C1, C2 and C4 (see Table I) at 23°C.

The interfacial tension of all the fluid pairs used in the experimental campaign was measured by applying the theory by Greco (2002)[29] to data of steady state drop shape in shear flow, as described elsewhere. Depending on the type of observation of the drop, two different relations were applied. When the drop was observed along the vorticity direction, the deformation parameter $D = \frac{R_{MAX} - R_{MIN}}{R_{MAX} + R_{MIN}}$ was measured and within the limits of the small deformation theory, no contribution of the matrix elasticity is predicted on D at the steady state. The relation for D reduces to the one valid for Newtonian fluids (Taylor 1932, 1934), so interfacial tension was evaluated as described by (Guido et al. 2003)[30] with eq. 5.

$$\mathrm{D} = \frac{19\lambda + 16}{16\lambda + 16}\mathrm{Ca} \qquad (5)$$

On the other hand, when the drop was observed along the velocity gradient

[29] Greco F, "Second-order theory for the deformation of a Newtonian drop in a stationary flow field". Phys. Fluids, 14, (2002) 946-954.

[30] Guido S, Simeone M and Greco F, "Deformation of a Newtonian drop in a viscoelastic matrix under steady shear flow. Experimental validation of slow flow theory", J. Non-Newtonian Fluid Mech., 114 (2003) 65-82.

direction, the interfacial tension was obtained by measuring the ratio R_p/R at steady state within the limit of small deformation and by using the equation 6 introduced for the first time by F. Greco.

$$\frac{R_P}{R} = 1 + Ca^2\left[\frac{1}{2}T^2 + \frac{1}{4}(s_2 + pg_2) + \frac{1}{2}(s_3 + pg_3)\right] \qquad (6)$$

where T, s_2, s_3, g_2 and g_3 are coefficients depending on the fluid properties (Greco, 2002) and p is the already defined parameter introduced by Greco to measure the "weight" of constitutive elasticity for the drop problem.

To assess the consistency of the two methods, the interfacial tension of one pair of fluids was measured both according to eqs. 5 and 6. The data are reported in Figure 13 and Figure 14, respectively. Of course, the two measurements required two different experiments, performed by observing the drop one time along the vorticity and the other time along the velocity gradient direction.

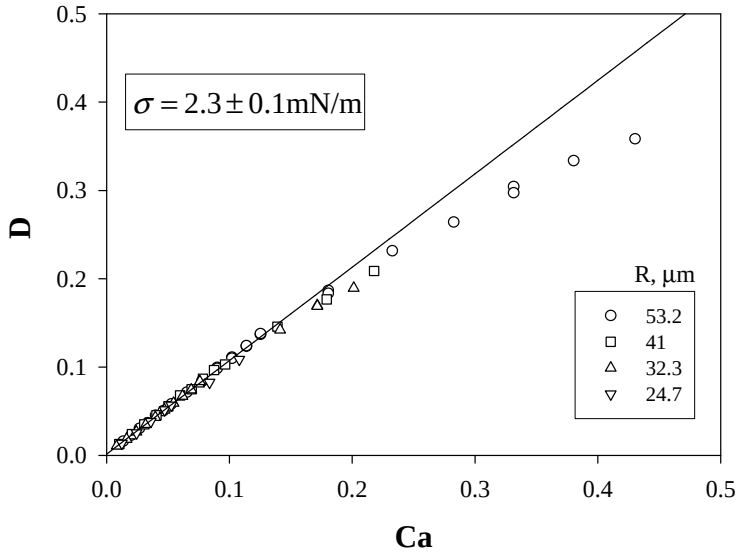

Figure 13: Interfacial tension of the pair silicon oil (drop phase) fluid C4 (matrix phase). λ = 2 a) D vs. non-dimensional time. The line is a fit of eq. 5 to the data. p = 1.5 to 3.5

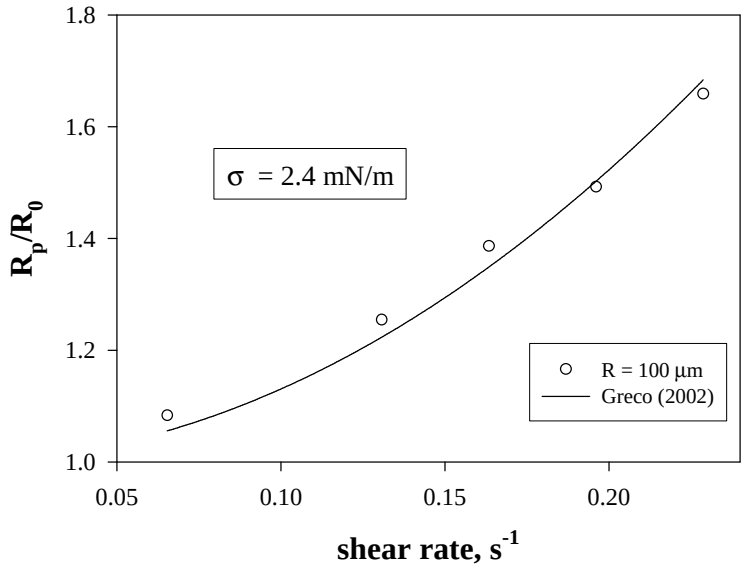

Figure 14: Rp/R vs. non-dimensional time. The line is a fit of eq. 6 to the data. p = 0.75.

4.3 Results

Figure 15 and Figure 16 show the deformation parameter D and the orientation angle θ as a function of the non-dimensional time t/τ_{em} for the case of $\lambda = 2$ and p = 1.5. Micrographs of the deforming drop are reported in Figure 17 at Ca = 0.43 (left side) and at Ca = 0.47 (right side). The symbols refer to three different Ca numbers. The open circles of Figure 15 and Figure 16 refer to Ca = 0.06, well within the small deformation limit. In this case, after an initial transient, steady state shape is reached. In the runs at much higher Ca, e.g. Ca = 0.43 (filled squares), the deformation parameter D goes through a maximum as a consequence of shear rate start up. After the maximum (micrograph 2), the deformation parameter goes through an initial „rapid“ relaxation (up to micrograph 3) and steady state shape is reached only afterwards, at time 140 ca. (micrograph 4). While the deformation parameter goes through an overshoot, the drop temporarily enhances its orientation toward the flow direction, and this reflects into an undershoot in the plot of the orientation angle vs. non-dimensional time (Figure 16). This behaviour is due to matrix elasticity, as described in the previous part of this

section, and no overshoot is present in the Newtonian case. Finally, the open squares of Figure 15 and Figure 16 refer to the deformation parameter and to the orientation angle, when the critical capillary number is slightly exceeded. Micrographs of the drop during this run, including drop break-up, are reported in Figure 17. Similarly to the case of Newtonian matrix, drop deformation progressively increases, a neck forms in the middle (micrograph 2) and break-up leads to two daughter drops and one tiny satellite (micrograph 3 and 4).

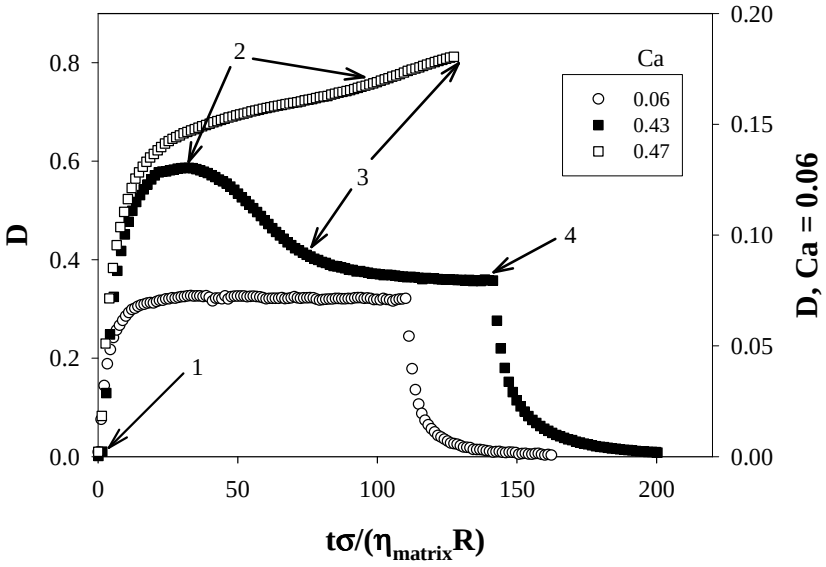

Figure 15: D vs. non dimensional time. λ = 2 and p = 1.5. Matrix phase: fluid C4.

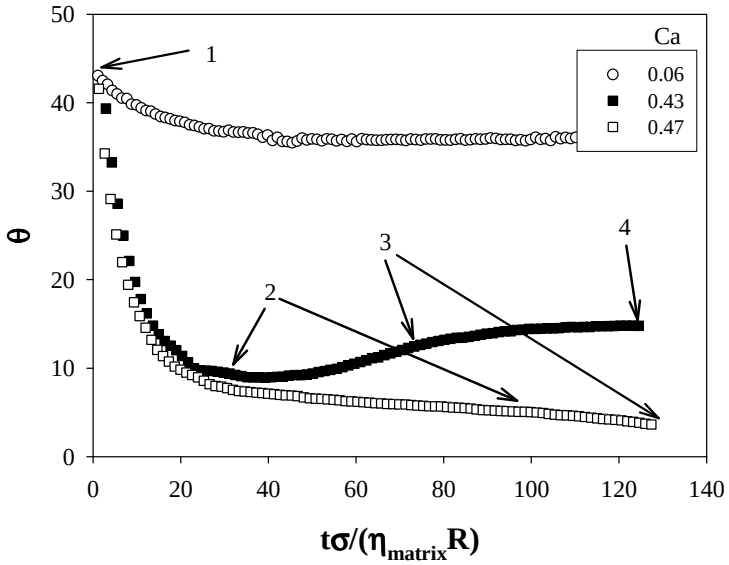

Figure 16: θ vs. non dimensional time. λ = 2 and p = 1.5. Matrix phase: fluid C4.

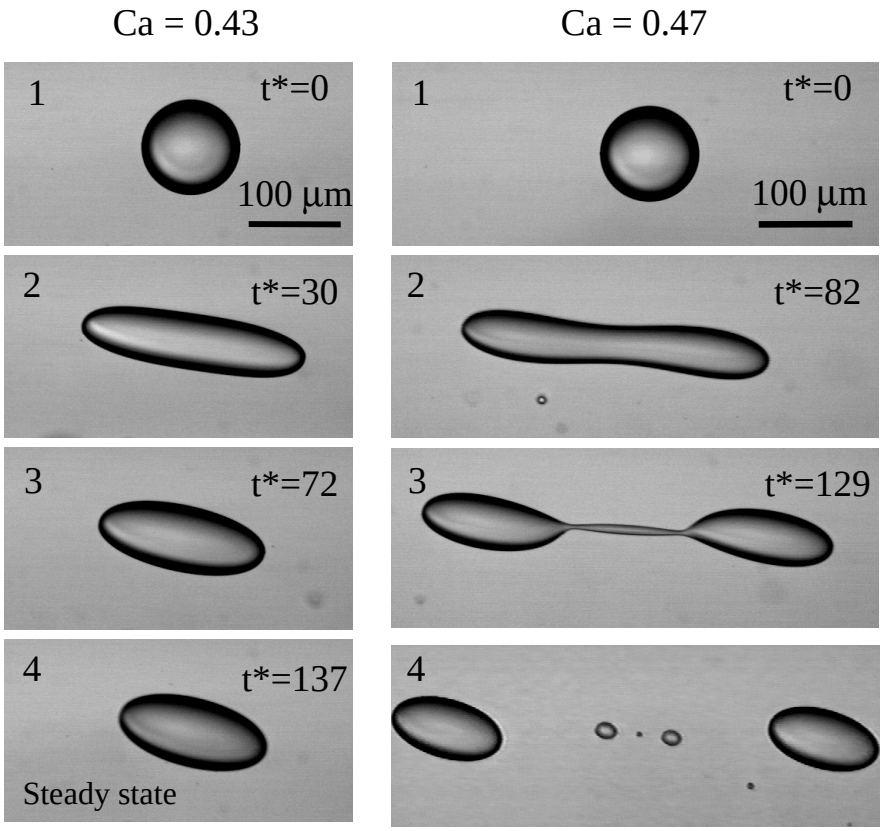

Figure 17: Micrographs of the drop of Figure 16 and Figure 17. The non-dimensional time t^* is reported on the micrograph.

Figure 18 shows, at increasing values of p, the deformation parameter measured

along the velocity gradient direction, $D' = (R_P-R_Z)/(R_P+R_Z)$, as a function of the non-dimensional time. The viscosity ratio is 2 and the values are normalised with respect to the steady state value of the deformation parameter. The runs refer to the highest subcritical condition explored at the corresponding value of p. As shown in Figure 18, the overshoot increases with the p parameter up to the point that, for p = 1.2, the maximum deformation reached by the drop is five times higher than the steady state value. A similar behaviour was observed for viscosity ratio 0.6, as illustrated in Figure 20, and 0.04. Some data are omitted for the sake of brevity. Micrographs of the three drops, captured at the maximum deformation and at steady state, are reported in Figure 19.

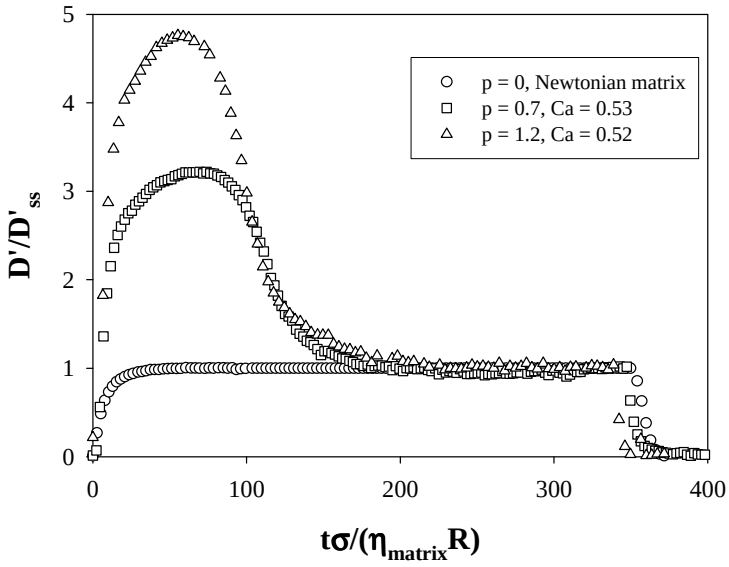

Figure 18: D′ vs. non dimensional time. λ = 2. Matrix phase: p = 0 fluid Napvis 30; p = 0.7 fluid C5; p = 1.22 fluid C5.

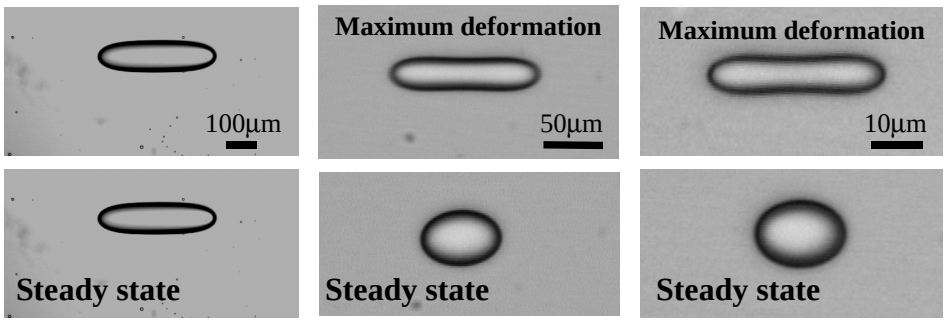

Figure 19: Micrographs of the drops of Figure 18.

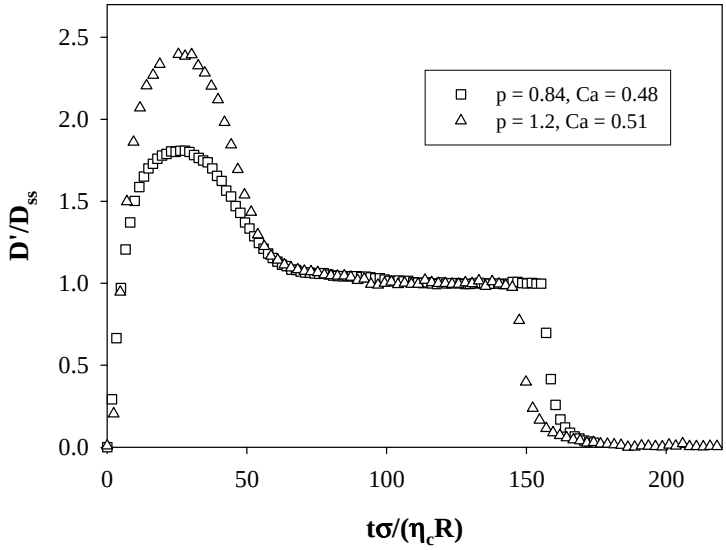

Figure 20: D′ vs. non dimensional time. λ = 0.6; p = 0.8, p = 1.2 fluid C3

In the micrographs of Figure 21 the 3D drop shape time evolution is qualitatively illustrated at p almost 1 and at fixed high Ca. The overshoot phenomena caused by matrix elasticity content at high Ca is so clear. Drop shape and its orientation pass across a “summit”, after which they drastically change, to reach the steady state value.

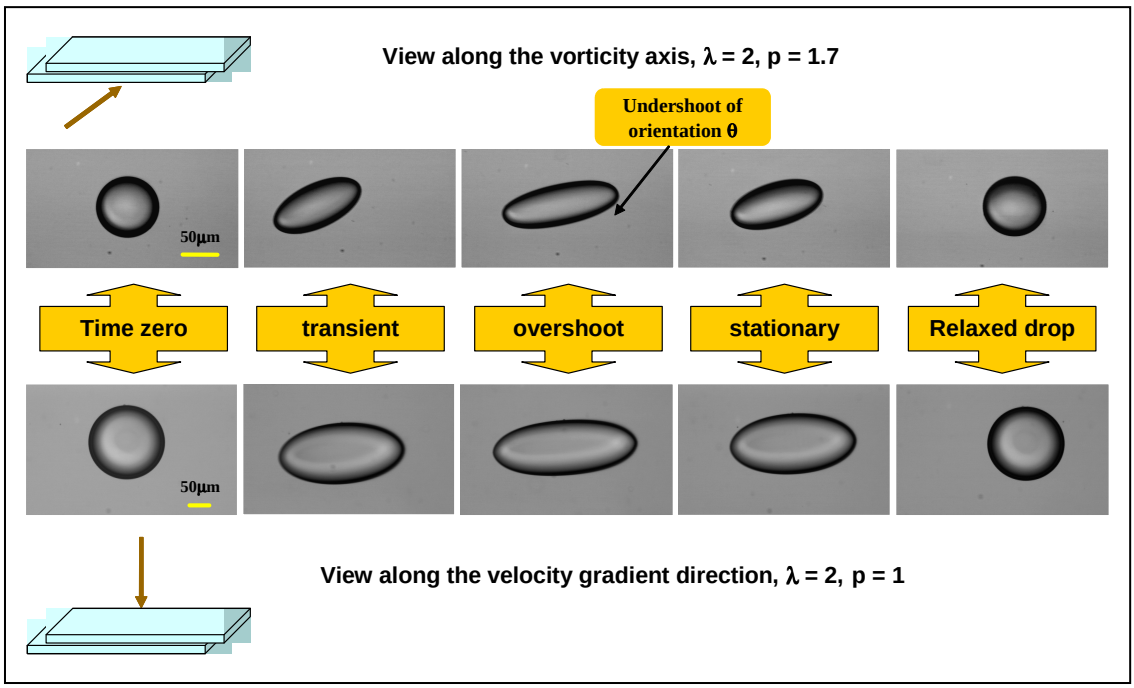

Figure 21: 3D time evolution of the drop.

Figure 22, Figure 23 and Figure 24 report the critical capillary number as a function of the p parameter for the case of viscosity ratio 2, 0.6 and 0.04, respectively. The open symbols represent the maximum capillary number at which steady state deformation was achieved (Ca_{cr} inf), while the filled symbols represent the minimum capillary number at which steady state deformation was not reached anymore (Ca_{cr} sup). The different shapes of the symbols refer to different experiments. Indeed, for each viscosity ratio, several pairs of fluids were used, in order to vary the value of the p parameter. It is worth noting how the rheological properties of the fluids used to perform the experiments at the same viscosity ratio are quire different (see Table 1). Nevertheless, as expected, the data relative to different fluid pairs superimpose nicely, when plotted vs the p parameter. On the y-axis of Figure 22, Figure 23 and Figure 24, the critical capillary number for Newtonian drops is pointed out. It was experimentally measured during this work for the case of viscosity ratio 2, by using the low molecular weight PIB (Napvis 30) as matrix and silicon oil as drop phase. For the case of viscosity ratio 0.6 and 0.04 it was gained from literature data (Cristini et al., 2001, de Bruijn, 1989)[31].

The increase of critical capillary number with the p parameter is a common trend for the three viscosity ratios explored, allowing to conclude that matrix elasticity hinders drop break-up. It is also confirmed that matrix elasticity becomes important when the p parameter assumes values higher than one.

[31] Cristini V, Blawzdziewicz J and Loewenberg M, (2001). An Adaptive Mesh Algorithm for Evolving Surfaces: Simulations of Drop Breakup and Coalescence. J. Comput. Phys., 168, 445-463.

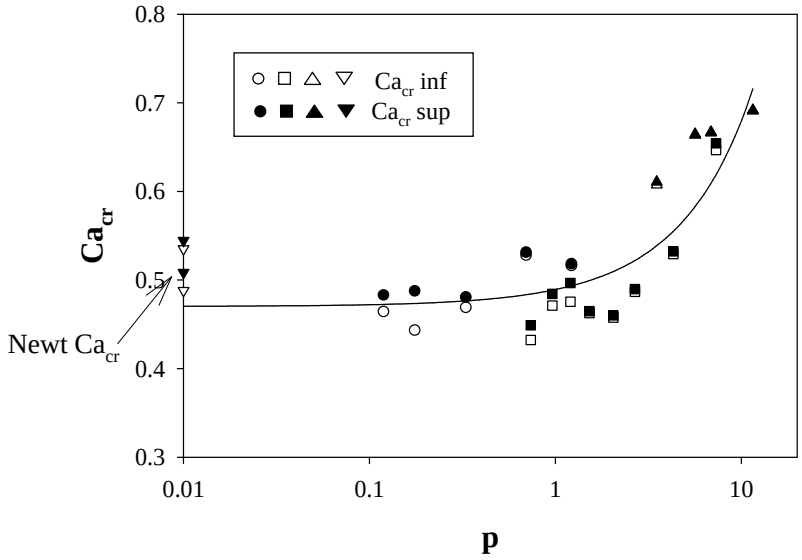

Figure 22: Critical capillary number as a function of p. λ = 2. Open symbols: Ca_{cr} inf. Filled symbols: Ca_{cr} sup. The fluids used as matrix phase are: circle C5, square C4, triangle up C6, triangle down Napvis 30.

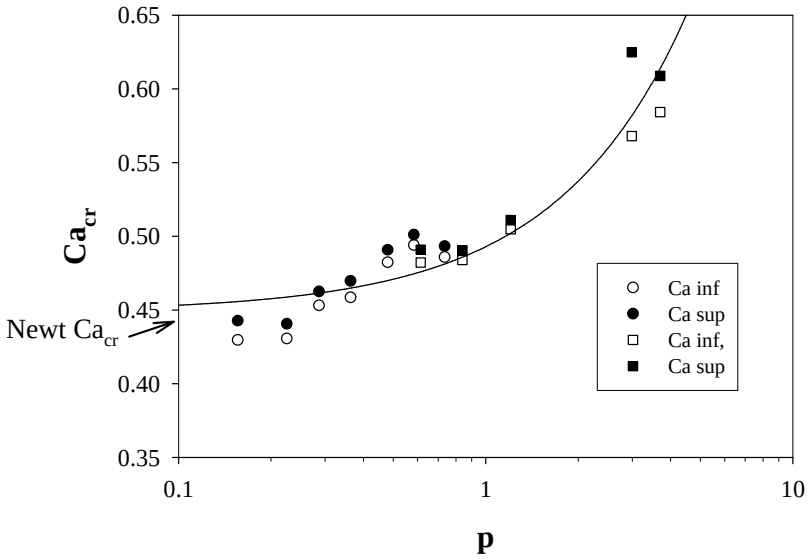

Figure 23: Critical capillary number as a function of p. λ = 0.6. Open symbols: Ca_{cr} inf. Filled symbols: Ca_{cr} sup. The fluids used as matrix phase are: circle C2, square C3.

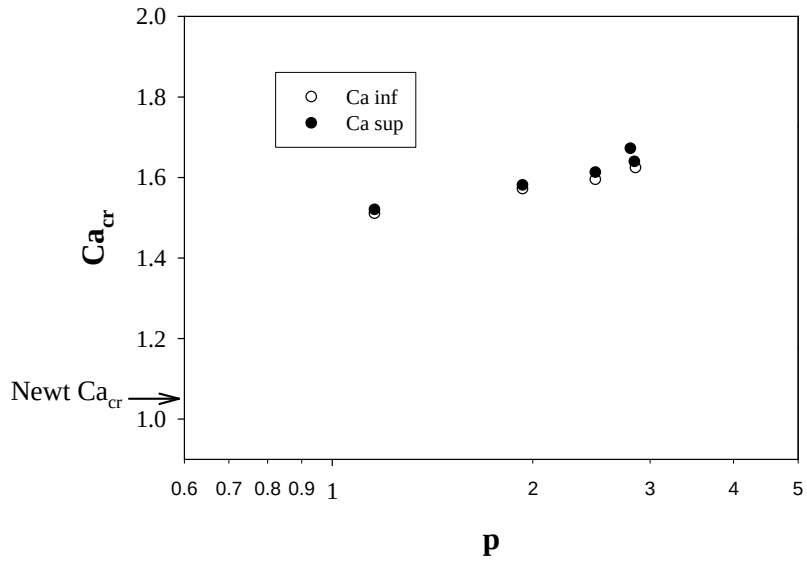

Figure 24: Critical capillary number as a function of p. λ = 0.04. Open symbols: Ca_{cr} inf. Filled symbols: Ca_{cr} sup. The fluids used as matrix phase are: circle C1.

It is worth commenting, at this point, that the effect of matrix elasticity on the critical capillary number may be much larger than what measured in this work. Indeed, the experiments were always performed by turning on the shear flow stepwise. As a consequence of this, at high capillary numbers (but below the critical value), drop deformation went through a maximum and then relaxed to a much lower steady state value, until drop break-up occurred. I believe that, by applying a progressive increase of shear rate with a „slow“ ramp, the drop would break up at a much higher capillary number. Indeed, the drop would progressively increase its deformation by passing through the steady state values that correspond to the instantaneous shear rate, and no overshoot would be present. Considering that the steady state deformation is several folds smaller that the maximum deformation reached during the transient, I argue that a much stronger flow is required to deform and break-up the drop if the start up transient is suppressed. Further work is needed to elucidate this point.

Figure 25 and Figure 26 report the non-dimensional pinch-off length (L^*) and time, respectively, for the case of viscosity ratio 2. For the non-dimensional length,

depending on the direction of observation, R_{MAX}/R_0 or R_p/R_0 was measured; being the drop at break-up highly oriented toward the flow direction, the two data sets were considered as identical. It is worth mentioning, at this point, that the measurement of the pinch-off non-dimensional length is very delicate since it greatly increases as soon as the critical capillary number is exceeded. For this reason, the data reported in Figure 25 and Figure 26 refer only to the cases where break-up leads to two daughter drops and a single tiny satellite. This is typical of near critical break-up. On the other hand, when more than one satellite was formed, break-up was considered to have taken place under super critical conditions and the data were discarded. The data indicate that both the non-dimensional pinch-off length and time increase with p. Furthermore, we observed that the pinch-off non dimensional length is independent of the viscosity ratio, while the pinch-off non dimensional time is strongly influenced by the viscosity ratio. When p was much lower than one, i.e. in the Newtonian limit, the non dimensional pinch-off time were 100, 70 and 20 for viscosity ratio 2, 0.6 and 0.04, respectively (these data are not shown for sake of brevity).

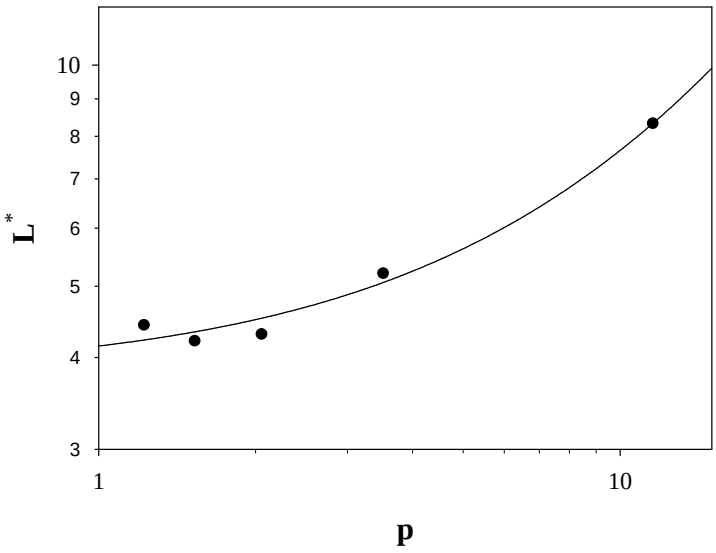

Figure 25: Non-dimensional pinch-off length vs. p. λ=2.

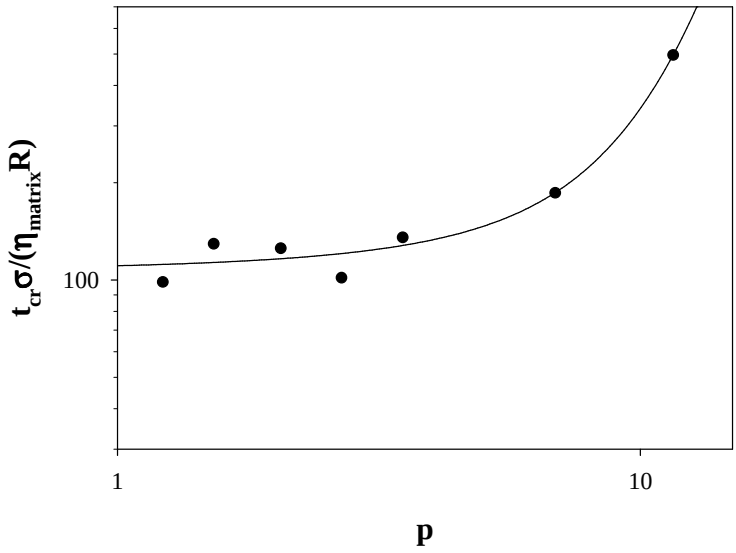

Figure 26: Non-dimensional pinch-off time vs. p at λ=2.

4.4 Final remarks

We explored the effect of matrix elasticity on drop break-up under step shear flow. Three viscosity ratios were considered, i.e. 2, 0.6 and 0.04. The entity of matrix elasticity was quantified through the non-dimensional parameter p, introduced by Greco (2002). The results presented allow to conclude that matrix elasticity hinders drop break-up. This was found at all three viscosity ratios explored and was quantified by measuring the critical capillary number as a function of the p parameter. The maximum increase of critical capillary number measured was 50% ca. when the p was increase to 10 ca (λ=2). At high, but sub-critical capillary numbers, drop deformation goes through an overshoot during which the drop temporarily enhances its orientation toward the flow direction. The entity of this phenomenon increases with p. Finally, the non dimensional pinch-off length and time were measured for the case of viscosity ratio 2. The data indicate that both quantities increase with p.

Section References

1. Cristini V, Blawzdziewicz J and Loewenberg M, (2001). An Adaptive Mesh Algorithm for Evolving Surfaces: Simulations of Drop Breakup and Coalescence. J. Comput. Phys., 168, 445-463.
2. de Bruijn R A (1989) Deformation and breakup of drops in simple shear flows. PhD thesis, Technische Universiteit Eindhoven.
3. Flumerfelt R W, (1972) Drop breakup in simple shear fields of viscoelastic fluids. Ind. Eng. Chem. Fundam., 11, 312-318.
4. Grace H P.. "Dispersion phenomena in high viscosity immiscible fluid systems and application of static mixers as dispersion devices in such systems". Chem. Eng. Commun., 14, (1982) 225-277.
5. Greco F.. "Second-order theory for the deformation of a Newtonian drop in a stationary flow field". Phys. Fluids, 14, (2002) 946-954.
6. Guido S, Simeone M and Greco F, "Deformation of a Newtonian drop in a viscoelastic matrix under steady shear flow. Experimental validation of slow flow theory", J. Non-Newtonian Fluid Mech., 114 (2003) 65-82.
7. Guido, S. and Simeone, M. "Binary collisions of drops in simple shear flow by computer-assisted video optical microscopy". Journal of Fluid Mechanics, 357, (1997) 1-20.
8. Guido, S. and Villone, M. (1998) Three dimensional shape of a drop under simple shear flow. Journal of Rheology, 42, 395-415.
9. Maffettone P. L. and Greco F., "An ellipsoidal drop model for single drop dynamics with non-Newtonian fluids", J. Rheol. (2004), 48, 83-100.
10. Mighri F, Carreau P J and Ajji A (1998) Influence of elastic properties on drop deformation and breakup in shear flow. J. Rheol., 42, 1477-1490.
11. V. Sibillo, S. Guido, F. Greco, P.L. Maffettone. "Single drop dynamics under shearing flow in systems with a viscoelastic phase". Macromolecular Symposium, (2005), 228, 31-39.
12. V. Sibillo, M. Simeone, S. Guido, F. Greco, P. "Start-up and retraction dynamics of a viscoelastic drop in a Newtonian matrix under simple shear flow." Paper approved for publication on the J. non-Newtonian Fluid Mech., special issue dedicated to AERC2005.
13. M. Solomon, S. Muller, "The transient extensional behavior of polystyrene-based Boger fluids of varying solvent quality and molecular weight", J. Rheol. 40 (1996) 837-856.
14. Stone H A (1994) Dynamics of drop deformation and breakup in viscous fluids. Ann. Rev. Fluid Mech., 26, 65-102.
15. Taylor G I (1932) The viscosity of a fluid containing small drops of another fluid. Proc. R. Soc. London A, 138, 41-48.
16. Taylor G I, (1934) The formation of emulsions in definable fields of flow. Proc. R. Soc. London A, 146, 501-523.
17. Tretheway D. C., Leal L. G., "Deformation and relaxation of Newtonian drops in planar extensional flows of a Boger fluid", J. Non-Newtonian Fluid Mech. 99 (2001) 81–108.
18. Varanasi P, Ryan M E and Stroeve P (1994) Experimental study on the breakup of model viscoelastic drops in uniform shear flow. Ind. Eng. Chem. Res., 33, 1858-66.
19. Yu W, Bousmina M, Zhou CX, Tucker CL, "Theory for drop deformation in viscoelastic systems", J.

Rheol. (2004) 48, 417-438.

Morphology evolution of a single drop under shear flow, with non Newtonian dispersed phase.

First part of this section illustrates experimental results concerning drop deformation and orientation during a "slow" shear flow, both at steady state and in time dependent situations (during the start-up and after cessation of the flow), comparing the data with the non Newtonian second order theory, while second part examines the drop high deformations and break-up. In both cases a model system with a non Newtonian, highly elastic drop phase and a Newtonian matrix phase was considered.

5 Single viscoelastic drop under shear flow

Beginning from the fundamental theoretical and experimental contribution of Taylor (1932, 1934)[32], regarding the small deformation and breakup of an isolated drop, most works in literature had as subject the morphological evolution and breakup of an isolated drop subjected to a well defined flow, focusing the attention on Newtonian mixtures only, in which the two phases didn't exhibit any elastic behaviour. Conversely a large part of the liquid-liquid dispersions currently used for the production of new materials are gotten with non Newtonian components. For this reason from some years, the attention of the scientific world is moved on the understanding of the effects of the phases viscoelastic properties on the flow-induced morphology of a dispersion with non

[32] Taylor G I (1932) The viscosity of a fluid containing small drops of another fluid. Proc. R. Soc. London A, 138, 41-48.
Taylor G I, (1934) The formation of emulsions in definable fields of flow. Proc. R. Soc. London A, 146, 501-523.

Newtonian fluids (S. Guido, F. Greco, 2004[33]; Elmendorp, J. J. et al (1985)[34]; Flumerfelt, R. W. (1972)[35]; Mighri, F. et al. (1999)[36]; Varanasi P, Ryan M E and Stroeve P (1994)[37]). In the case in which one or both phases are viscoelastic fluids, the dispersed drops are subjected to both viscous and elastic forces, as well as to interfacial one. Therefore the mechanism of drop deformation and breakup in viscoelastic systems will be quite different in comparison to Newtonian systems as predicted by those authors. Unfortunately a clear picture that illustrates the effects of the only elastic content of the dispersed phase on the morphology of the drop doesn't still exist.

In this section the video enhanced contrast optical microscopy has been used to explore the 3D shape evolution of a single viscoelastic drop (Boger fluid)[38] immersed in a Newtonian matrix and subjected to a well defined shear flow. Fundamental target will be to come to a full knowledge about drop shape at steady state, comparing experimental data with Greco's theory[39] predictions and to have a clear picture about the influence of the viscoelastic properties of the dispersed phase on the drop evolution during the transients of flow, start-up and after cessation of the shear flow. Finally the break-up mechanism of the viscoelastic drop will be illustrated as a function of the drop phase elastic content.

In extreme synthesis, as discussed in the introduction section, for Newtonian systems the dynamics of an isolated drop submitted to a shear flow in absence of inertia

[33] S. Guido and F. Greco, "Rheology Review 2004", BSR Aberystwyth, UK 2004.

[34] Elmendorp J. J. and R. J. Maalcke, "A study on polymer blending microrheology. 1" Polym. Eng. Sci. 25, 1041-1047 (1985).

[35] Flumerfelt R W, (1972) Drop breakup in simple shear fields of viscoelastic fluids. Ind. Eng. Chem. Fundam., 11, 312-318.

[36] Mighri F, Carreau P J and Ajji A (1998) Influence of elastic properties on drop deformation and breakup in shear flow. J. Rheol., 42, 1477-1490.

[37] Varanasi P, Ryan M E and Stroeve P (1994) Experimental study on the breakup of model viscoelastic drops in uniform shear flow. Ind. Eng. Chem. Res., 33, 1858-66.

[38] D.V. Boger, R. Binnington, "Separation of elastic and shear thinning effects in the capillary rheometer", Trans. Soc. Rheol. 21 (1977) 515-34.

[39] Greco F, (2002) Second-order theory for the deformation of a Newtonian drop in a stationary flow field. Phys. Fluids, 14, 946-954.

is function of two only non dimensional parameters: the capillary number $Ca = \frac{\eta_C \dot{\gamma}}{\sigma / R}$, in which η_C is the continuous phase viscosity, $\dot{\gamma}$ the shear rate, σ the interfacial tension of the couple of fluids and R is the spherical drop radius, and the viscosity ratio between the two phases, drop to matrix viscosity, $\lambda = \frac{\eta_D}{\eta_C}$. The capillary number is the ratio between the hydrodynamic stress, that deforms the drop and the interfacial stress, that tends to restore the drop to a spherical shape. The critical capillary number corresponds to the critical shear rate at which the drop in a steady flow is no longer able to assume a steady shape, it becomes unstable and breaks. It depends on the flow type and on the viscosity ratio only (Grace, 1982)[40] (de Bruijn R A, 1989, Ph.D thesis)[41]. The hydrodynamic problem becomes more complex in the case in which one or both the component fluids are viscoelastic. In fact the choice of a non Newtonian dispersed phase with an appropriate constitutive equation is necessary, to get results of general validity. In addition it is experimentally not easy to separate the role of the fluids elasticity and of the viscosity dependence with the shear rate on the drop evolution. The viscoelastic fluids used in this work as dispersed phase were the constant viscosity Boger fluids, with a second order rheological behaviour. So it has been possible to isolate the contribution due to the only elasticity on the drop deformation, getting some results applicable in a large class of non Newtonian fluids, defined Noll's "simple fluids". These so called "Second Order Fluids" (G. Astarita and G. Marrucci, "Principles of Non-Newtonian fluid mechanics, McGraw Hill, Maidenhead, 1974) exhibit a first normal stresses difference, N_1, proportional to the square of the shear rate

[40] Grace H P (1982) Dispersion phenomena in high viscosity immiscible fluid systems and application of static mixers as dispersion devices in such systems. Chem. Eng. Commun., 14, 225-277.

[41] de Bruijn R A (1989) Deformation and breakup of drops in simple shear flows. PhD thesis, Technische Universiteit Eindhoven.

in a wide range ($N_1 = \Psi_1 \dot{\gamma}^2$, where Ψ_1 is the coefficient of the first normal stresses difference). Non dimensional parameter $p = \frac{\Psi_1 \sigma}{2R\eta^2}$, in which η is the viscosity of the second order fluid, has been used to quantify the weight of the dispersed phase elasticity on the dynamic of drop deformation under the shear flow. It changes varying the drop radius or the pair of fluids. This parameter introduced for the first time by Leal (2001)[42], and formalized by the Greco theory on the steady state drop shape in slow flow with non Newtonian second order fluids (F. Greco, 2002), can be interpreted as the ratio between constitutive relaxation time of the dispersed phase $\tau_R = \frac{\Psi_1}{2\eta_D}$ and emulsion time $\tau_{em} = \frac{\eta_C R}{\sigma}$. From the non dimensional analysis of the problem it is possible to establish that the effects of the dispersed phase elasticity on the drop shape are observable when p is around 1. Much more details about the theoretical analysis can be found in the work of S. Guido et al., (2003)[43].

5.1 Materials and methods

The pair of fluids used as viscoelastic dispersed phase and Newtonian continuous phase were selected in order to have a single drop system with a parameter p almost 1, with a drop of radius within the range 10 – 50 μm, and with a viscosity ratio λ (drop to matrix viscosity) equal to 1 and 2.6. In a few words the fluids were prepared as follows. The viscoelastic drop phase was a constant viscosity Boger fluid. It has been prepared by mixing a small fraction of high molecular weight polymer (Polyisobutylene PIB, Sigma Aldrich, Mw = 4.6 x 106) with a Newtonian solvent, Polybutene, PB,

[42] Tretheway D. C., Leal L. G., "Deformation and relaxation of Newtonian drops in planar extensional flows of a Boger fluid", J. Non-Newtonian Fluid Mech. 99 (2001) 81–108.

[43] Guido S, Simeone M and Greco F, "Deformation of a Newtonian drop in a viscoelastic matrix under steady shear flow. Experimental validation of slow flow theory", J. Non-Newtonian Fluid Mech., 114 (2003) 65-82.

commercially known as Napvis (BP Chemicals). The PIB was previously dissolved in Kerosene at 4% weight concentration. Then the high molecular weight PIB-kerosene solution was mixed to the PB in order to have the desired final mass ratio PIB/PB. This solution was slowly stirred at room temperature for a week, to avoid the formation of clots and it was placed in a vacuum oven at 40°C for one month, to remove the whole kerosene. The Newtonian continuous phase was made by mixing Silicon Oil fluids, PDMS (Polydimethylsiloxane, Dow Corning) with different average molecular weight, in order to have the desired experimental viscosity ratio.

After the injection of a pure Polybutene drop in a pure Silicon Oil fluid, a decrease in drop diameter was observed because of a small solubility of the PB in PDMS (Guido *et al.* Rheol. Acta, 1999)[44]. To avoid, during an experiment, every geometrical, rheological and interfacial properties variation of the blend constituted by a single drop of viscoelastic PB immersed into PDMS, it was necessary to realize the thermodynamic phase equilibrium between the pair of fluids previous described. Equal volumes of viscoelastic Boger fluid and PDMS were emulsified. The emulsion so gotten, was left for about a week under static conditions. The two phases at the thermodynamic equilibrium were separated by ultra centrifugation and used for the experiments. The absence of any diffusion phenomenon was verified before every experiment, observing for one day a drop of viscoelastic phase inserted in the Silicon Oil phase. No significant changes in drop size were found.

Two phases rheological properties were obtained using a constant-stress rheometer, equipped with a normal stress sensor (Bohlin, CVO 120), with the cone and plate configuration. As an example, rheological data of two viscoelastic phases, to be exact D4 and D5, used for the experiments at viscosity ratio 1 and 2.6, are presented in

[44] S. Guido, M. Simeone, M. Villone, "Diffusion effects on the interfacial tension of immiscible polymer blends". Rheol. Acta 38 (1999) 287-296.

Figure 27, at the experimental temperature 23°C. It is clear that the dispersed phase viscosity η_D was essentially constant in the range of shear rate investigated during the experiments (up to 5 s-1) and that the first normal stress difference N_1 had a quadratic dependence from the shear rate, in a completely agreement with the assumption of second order fluids made in the theoretical analysis (F. Greco, 2002). The first normal stress difference coefficient Ψ_1 was obtained by fitting the data to a line of slope 2 in log scale. It was also verified that the Silicon Oil phase was a Newtonian fluid with a constant viscosity and with no appreciable normal stress in a wide range of shear rate. All fluids used as dispersed viscoelastic phases in the experimental campaign are shown in Table 2, together with their rheological properties at the experimental temperature, 23°C. In particular, column 1 reports a code name, Di; column 2 reports the mass ratio of high-to-low molecular weight polymer, (the values are multiplied by 10^3); column 3 reports the viscosity at 0.05 and 1.5 s^{-1}, which is roughly the range of shear rate at infinity imposed during the experiments (as shown, shear thinning is limited to 10-20%); column 4 reports the first normal stress coefficient, Ψ_1, column 5 reports the viscosity ratio of the experiments performed with that fluid and columns 6 and 7 report the p parameter and the type of experimental observation. Newtonian silicon fluids used as continuous phases are absent.

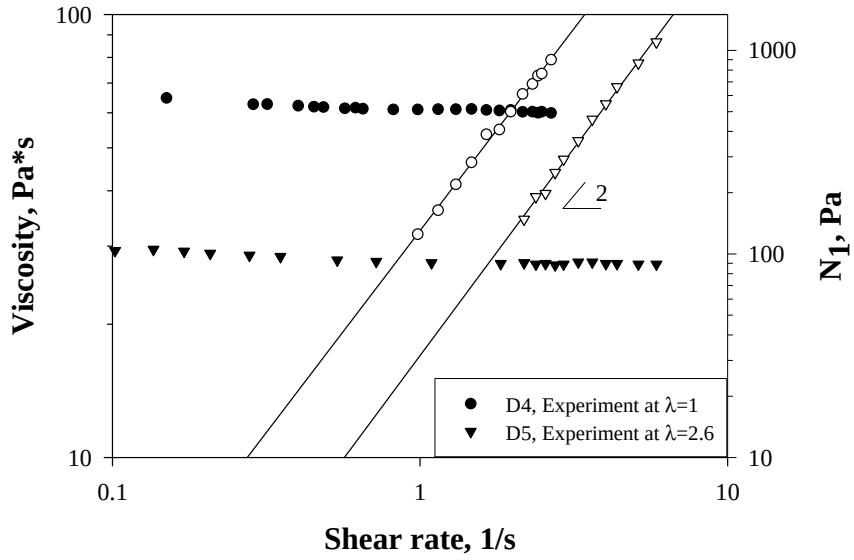

Figure 27 rheological data of the drops D4 and D5 at 23°C.

Dispersed phase	**PIB/Napvis ($x10^{-3}$)**	**Viscosity at 0.05 – 1.5 s^{-1} (Pa s)**	**Ψ_1 (Pa s^2)**	**Experiment at λ**	**p, vorticity view**	**p, gradient direction**
D1	3.0	10.7 - 8.5	11	1	1.6; 2.4	1.3; 1.9; 2.9
D2	3.0	78 – 76.8	145	1	0.7	
D3	3.5	46 – 42.3	67	1	3	
D4	3.0	67 - 61	127	1	1.1	
D5	2.0	28	31	2.6	0.6; 0.85; 1.7	

Table 2: Experimental viscoelastic fluids used as drop phase.

The rheo-optical apparatus and the images analysis techniques used in this work to shear a drop and to monitor the drop shape during the flow were described in detail in the materials and methods section of S. Guido, M. Simeone (1998)[45] and S. Guido, M. Villone (1998)[46]. The experimental apparatus essentially consists of a couple of parallel glass plates mounted on motorized supports and of an optical microscope, Axioscop FS (Zeiss) equipped with an analogical CCD camera. Two different parallel plates devices,

[45] Guido, S. and Simeone, M. (1998) Binary collisions of drops in simple shear flow by computer-assisted video optical microscopy. Journal of Fluid Mechanics, 357, 1-20.

[46] Guido, S. and Villone, M. (1998) Three dimensional shape of a drop under simple shear flow. Journal of Rheology, 42, 395-415.

easily interchangeable, were used for observing the drop along the vorticity axis and along the velocity gradient direction of the shear flow. When the drop was observed along the flow vorticity direction, the two axes R_{MAX} and R_{MIN} of the deformed drop (as observed in the plane of shear) and the angle θ between the major axis R_{MAX} and the velocity direction (see the schematic drawing in the Materials and method section) were calculated. On the other hand, when the drop was observed along the velocity gradient direction, R_P and R_Z were measured, where R_P is the projection of R_{MAX} on the plane of shear and R_Z is drop axis along the vorticity direction. The experiments were carried out at constant temperature, 23°C± 0.5 °C. Briefly, during the experimental campaign drop was submitted to step up shear flows varying the shear rate and starting from spherical shape. Its morphology and orientation were analysed in time during the start up, the steady state, and after flow cessation.

Within the limit of small deformations, as predicted by the theory (Greco, 2002), observing the drop along the vorticity axis of the shear flow, no deviation of the major and minor axes of the deformed drop at the steady state is predicted with respect to the corresponding Newtonian case. In addition the deformation parameter D reduces to one predicted by the Newtonian theory of Taylor, according to which D at steady state is linear with the shear rate, as illustrated in Figure 31.

Therefore the interfacial tension of all couples of fluids has been calculated from the slope of the linear fit of D at steady state versus the shear rate, within the limit of $D<2$.

5.2 Results

I start this paragraph presenting in a few words data that I usually obtain with the rheo-optical apparatus shearing the drop by turning on the shear flow at a given value of shear rate, observing the viscoelastic drop along the vorticity axis, as illustrated in the

"materials and method" section. In Figure 28 the deformation parameter D of the drop D2 during a typical step up shear flow is plotted versus the time, made non dimensional using the emulsion time τ_{em} of the system. The drop has been submitted to a shear rate 0.1. From its spherical shape (D=0), drop deforms monotonously itself, up to a stationary state (D=0.1). After the cessation of the flow the drop relaxes for reaching its initial rested shape, D=0. The corresponding evolution of the orientation angle θ is shown in the Figure 30. Micrographs of the drop evolution are reported in Figure 29. This morphological evolution of the drop under a step up shear flow is quite similar to the pure Newtonian system illustrated by S. Guido and M. Villone (1998).

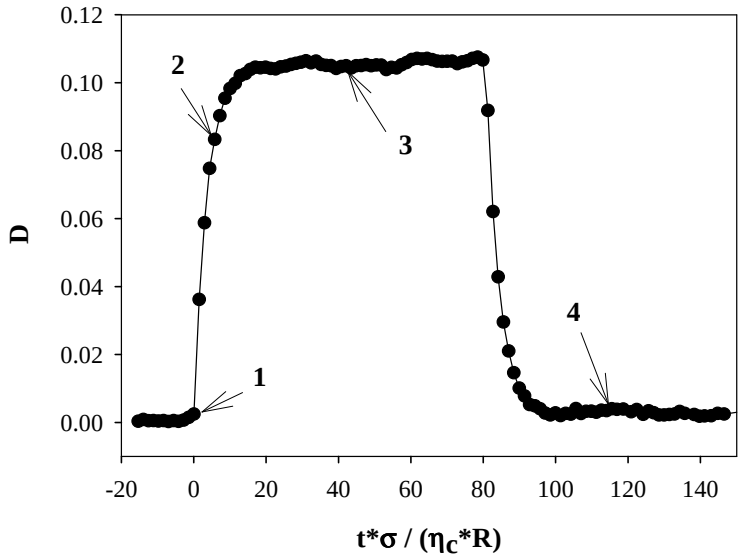

Figure 28: Evolution of the D parameter of drop D2, with p = 0.7, λ=1, Ca=0.1.

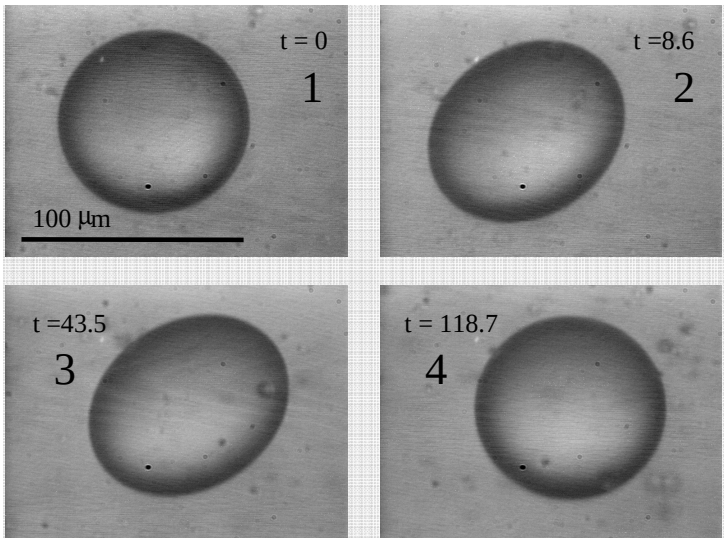

Figure 29: Micrographs associated with Figure 28 and Figure 30

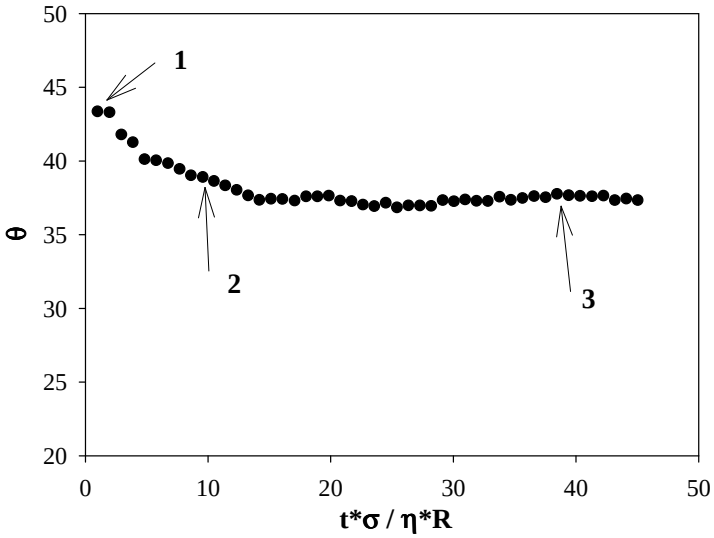

Figure 30: Evolution of the orientation angle θ of drop D2, with p = 0.7, λ=1, Ca=0.1.

First part of this section is devoted to explain all results obtained during my Ph.D. about the 3D shape of the viscoelastic drop at steady state, comparing, *for the first time*, the experimental data with the theoretical predictions obtained by F. Greco (*Drop deformation for non Newtonian fluids in slow flow*). Subsequently I will investigate the drop shape evolution during the transients of start-up and after cessation of the shear flow as a function of the viscous and elastic properties of the drop phase. Finally I will

show to the reader some “nice” drop evolutions, that happen when the shear flow is fast or in other words when the drop is submitted to a Capillary near the critical value, to finish with the evaluation of the critical capillary number as a function of the viscoelastic drop properties.

5.2.1 Three dimensional drop shape at steady state. Comparison with the second order theoretical predictions.

I start the explanation of this first part from the case with viscosity ratio 1. In such a case, three fluids have been selected, namely D1, D2 and D4 (see the table of fluids) to make the single drop blend. It is important to notice that the dispersed phase components of these three blends largely differ in their elasticity, as measured by the first normal stress coefficient Ψ_1. So, different values of the p parameter, that gauges the non Newtonian effects, can be obtained not only by changing the drop radius for a given fluid pair, as illustrated in the introduction, but also by changing the fluid pair itself. So by using different pairs of fluids, a stringent test of the theoretical predictions and a good and complete experimental study will be performed without any doubt.

In Figure 31 the deformation parameter D at steady state is plotted versus the Capillary number Ca, for three values of p: 0.7 obtained using D2 as drop phase, 1.1 obtained using D4 as drop phase and 1.6 and 2.4, obtained using D1 as drop phase with two different drop radii. The continuous line is the prediction from second order theory (Greco, 2002). As discussed in the introduction the prediction for D derived from that theory is independent of the phases elasticity and the relation for D reduces to the one valid for Newtonian fluids (Taylor 1932, 1934). Within the limit of small deformations, all data points fall on the theoretical line up to a certain value of Ca, which should decrease with increasing p, as described by S. Guido and F. Greco (2003). No significant discrepancy between experimental data and the theoretical line was found

with increasing p up to Capillary 0.2, excluding the experimental errors for σ evaluation. In other words, it seems that the range of validity of the theoretical prediction is independent of p when the dispersed phase is a non Newtonian fluid and viscosity ratio is 1.

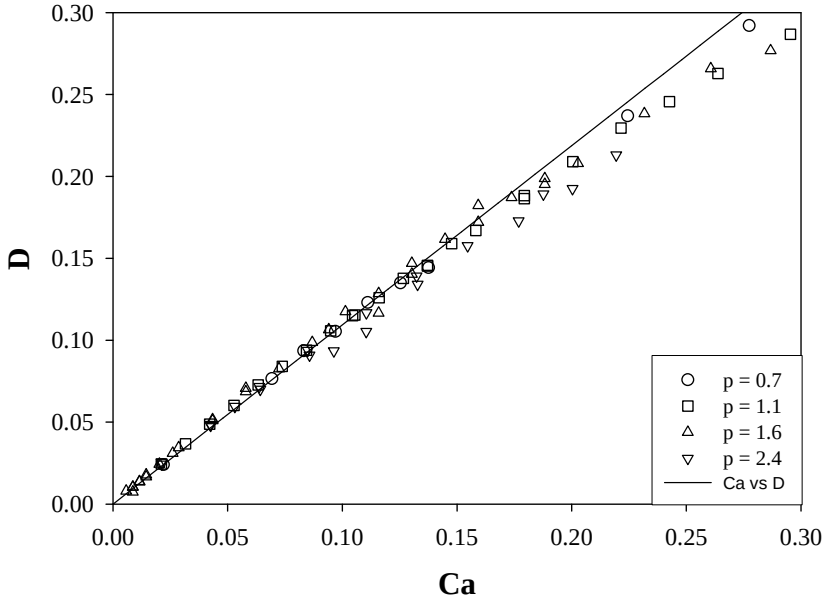

Figure 31: Deformation parameter vs. Ca at steady state, using as dispersed phase the fluids D1, p = 1.6 – 2.4; D2, p = 0.7; and D4, p = 1.1. The solid line is the Taylor theoretical prediction. All data are at λ = 1.

In Figure 32 non dimensional axes R_{MAX}/R and R_{MIN}/R are reported, as measured in the view along the vorticity axis of the shear flow, versus the Capillary number Ca at steady state, using D1 fluid as dispersed phase. P parameter was 1.6. Dashed and continuous lines correspond to the Newtonian and non Newtonian second order predictions, respectively. It is clear, as before illustrated for D, that the two lines are very closed to each other in a wide range of Capillary number. Besides experimental data overlap to the predictions up to Capillary 0.2. Therefore I can assert that the non Newtonianness of the dispersed phase does not produce any effect on the deformation of the drop observed along the vorticity axis, compared with the Newtonian case, at low

Ca values.

In Figure 33 the experimental data of D plotted versus Ca at steady state, for p = 1.1, are compared with the value of D obtained from the predictions of R_{MAX} and R_{MIN} of the second order non Newtonian theory, using the definition of D, $D = (R_{MAX} - R_{MIN})/(R_{MAX} + R_{MIN})$.

It is important to notice that the experimental data fall on the continuous line up to Capillary 0.6. Therefore the "numerical or phenomenological" prediction of the deformation parameter D at the steady state gotten from the theoretical values of R_{MAX} ed R_{MIN} is valid in a wide range of Ca and it is better than the Taylor's formula. Moreover the viscoelastic system displays a less deformed drop with respect to the fully Newtonian case, i.e. $D<D_{Newt}$ for "high" Capillary numbers (V. Sibillo et. al., 2005)[47].

In fact as we will see later, the droplet is "stabilized" by the dispersed phase elasticity and the non Newtonian critical capillary number is always larger than the corresponding Newtonian one.

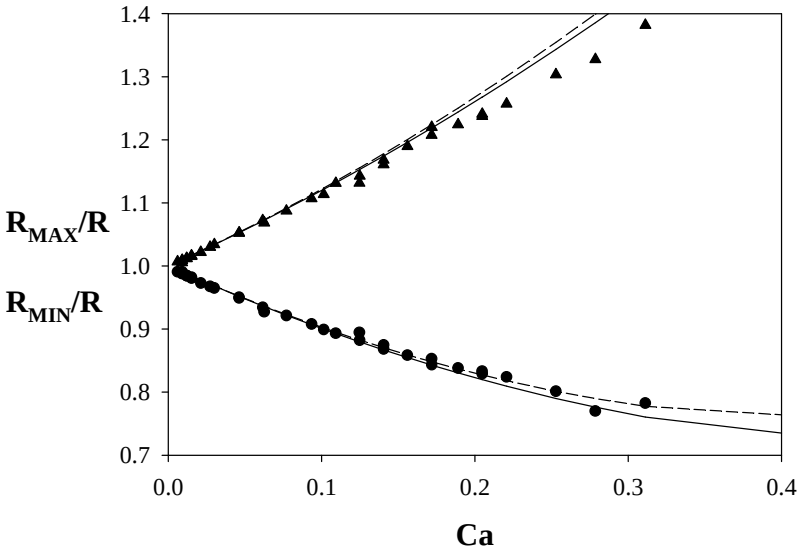

Figure 32: Major and minor non dimensional axes vs. Ca, using D1 with p = 1.6 as dispersed phase, at λ = 1. Dashed lines are second order Newtonian theory.

[47] V. Sibillo, S. Guido, F. Greco, P.L. Maffettone. "Single drop dynamics under shearing flow in systems with a viscoelastic phase". Macromolecular Symposium, (2005), 228, 31-39.

Continuous lines are non Newtonian theory.

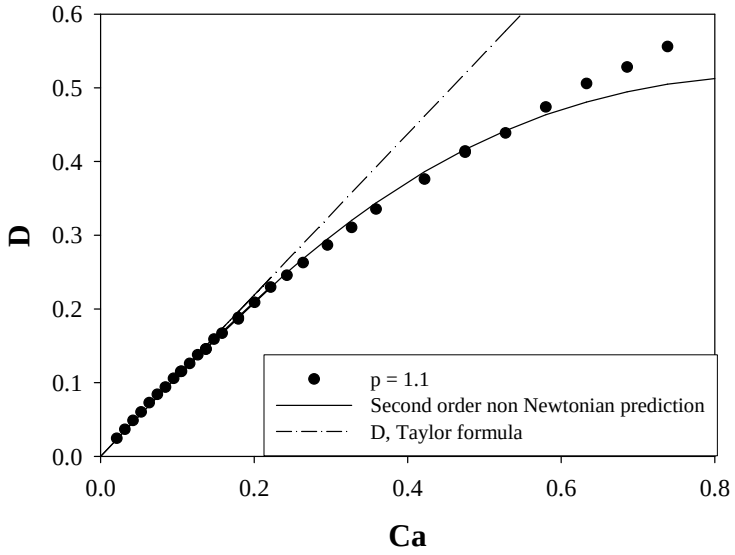

Figure 33: Deformation parameter vs. Ca at steady state, using as dispersed phase the fluids D4, p = 1.1. The continuous line is the numerical prediction of D, gotten by the values of R_{MAX} and R_{MIN} drawn by second order non Newtonian theory. The dashed-dot line represents the Taylor theoretical prediction.

Figure 34 shows the drop orientation angle θ with respect to the velocity direction at steady state, for drop D4, λ = 1. Dashed and continuous lines refer to the Newtonian and non Newtonian theoretical predictions, respectively. As described by S. Guido and F. Greco, (2003), and by Sibillo et al., (2005), the difference between the two curves is now clear. This reveals that the drop orientation depends on p, that is linked to the first normal stresses difference N_1. This theoretical prediction is here confirmed by the experimental data of θ, that is lowered with respect to the Newtonian equivalent system. Unfortunately, in the case of viscoelastic drop in shear flow of a Newtonian matrix, the non Newtonian prediction overestimates experimental data. While as described by S. Guido et al. (2003) in the case of Newtonian drop subjected to a shear flow of a viscoelastic matrix experimental data of the orientation angle θ provide an excellent confirmation of the non Newtonian prediction, obtaining an univocal correlation

between the slope of θ vs. Ca curve with the matrix first normal stresses difference N_1. In Figure 35 the orientation angle of drop D1 at steady state is plotted vs. Ca, with p = 2.4 and λ = 1. It confirms without any doubt, what has previously been illustrated.

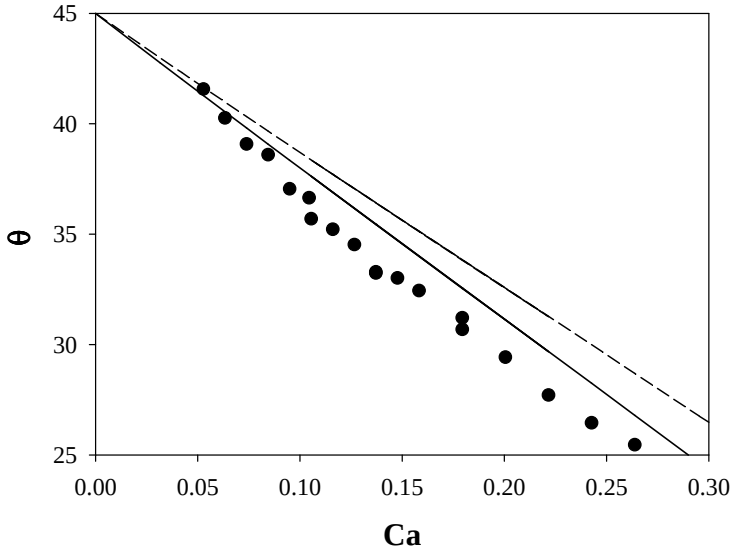

Figure 34: Drop orientation angle θ vs. Ca at steady state, using as drop phase D4, p = 1.1.

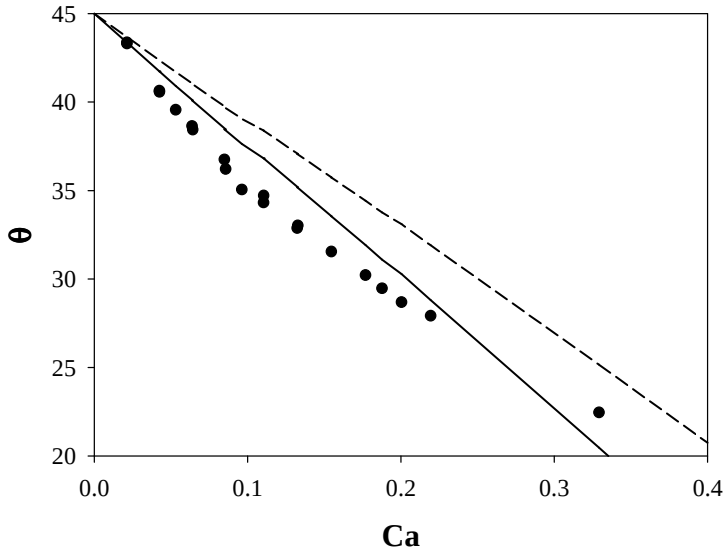

Figure 35: Drop orientation angle θ vs. Ca at steady state, using as drop phase D1 with p = 2.4.

Now we can go to the top view experiments. The deformed drop is now observed

along the velocity gradient direction. In Figure 36 the non dimensional major and minor axes R_P/R and R_Z/R respectively, are plotted as a function of Ca at steady state. The dashed lines are the Newtonian predictions. As exposed by F. Greco, (2003) these two axes depend also on the second normal stresses difference N_2, exactly on the ratio $-N_2/N_1$. The imposed value on that ratio, $-N_2/N_1$, was 0.18<0.25, that represents the condition to reproduce a Weissemberg viscoelastic fluid, as suggested by S. Guido and F. Greco (2003).

Also in this case the two theoretical curves are practically close to each other and the experimental data fall on the two lines for low capillaries.

So if one considers the case when only the drop is a viscoelastic fluid, the optical measurements at steady state of D, θ and R_P/R lead to a good evaluation of the rheological properties of the drop fluid, for a given value of viscosity ratio, i.e. $\lambda = 1$. In other words, the interfacial tension of the couple of fluids can be obtained by the slope of D vs. the shear rate at steady state as illustrated in Figure 31; the slope of θ vs. Ca curve is only determined by the p parameter and it gives us an approximate value for Ψ_1; and finally $-N_2/N_1$ can be evaluated by the quadratic fitting of R_P/R, using the corresponding second order theoretical equation (see the appendix).

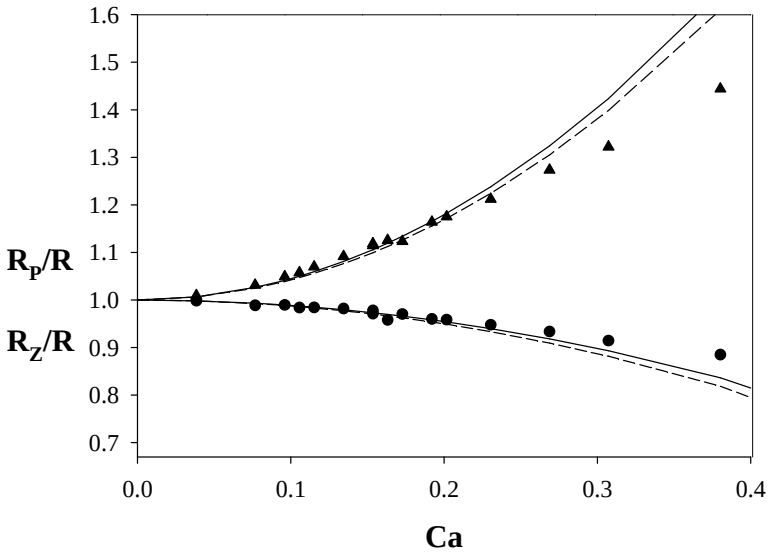

Figure 36: Drop axes of the deformed drop observed along the velocity gradient direction vs. Ca at steady state, using as drop phase D1 with p = 1.9, λ=1. Continuous lines are the non Newtonian prediction when $-N_2/N_1 = 0.18$.

For a full analysis and to illustrate how the theoretical and experimental results depend on the viscosity ratio λ, I show the case at λ = 2.6. The fluid used as drop phase is now D5. Different p parameters were explored, changing the drops radii.

Figure 37 shows the non dimensional axes R_{MAX}/R and R_{MIN}/R vs. Ca. Dashed lines correspond to the Newtonian theory, while continuous lines refer to the non Newtonian predictions. The theoretical assumption about the drop shape under slow flows at steady state is clearly confirmed by the data. Within the limit of small deformations the viscoelastic drop shape does not depend on the p parameter and it is equal to the Newtonian case. Data about D, R_P/R and R_Z/R at λ = 2.6 are omitted for the sake of brevity.

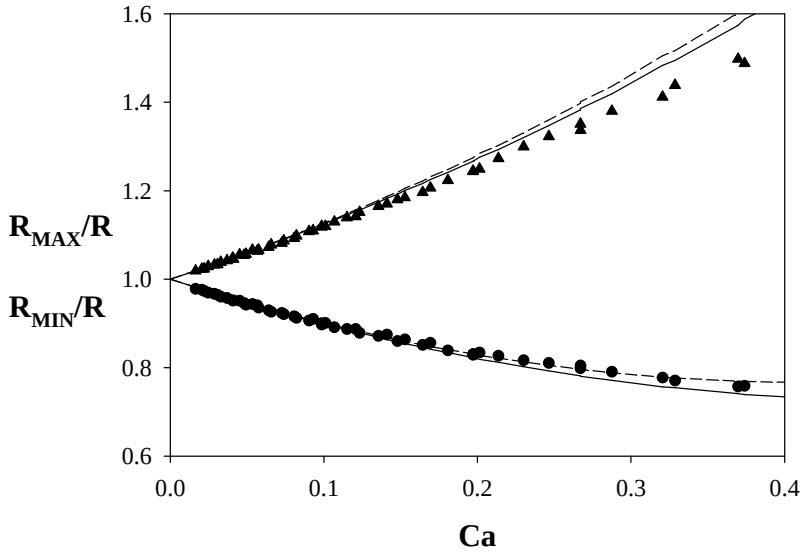

Figure 37: Major and minor axes vs. Ca of drop D5,with p=0.85, at λ=2.6. Continuous lines are non Newtonian theory.

Figure 38 shows the orientation angle θ vs. Ca at steady state for two different p values, with the corresponding non Newtonian predictions, at λ = 2.6. It is clear that the angle do not depend on the drop phase non Newtonianness. At two different p values, 0.85 and 1.7, experimental data fall on the Newtonian line up to Ca = 0.1.

Probably the range of validity of the non Newtonian prediction of θ comes to zero with the increasing of the viscosity ratio, as illustrated by S. Guido et al (2003). In this case every theoretical affirmation becomes impossible to be shown..

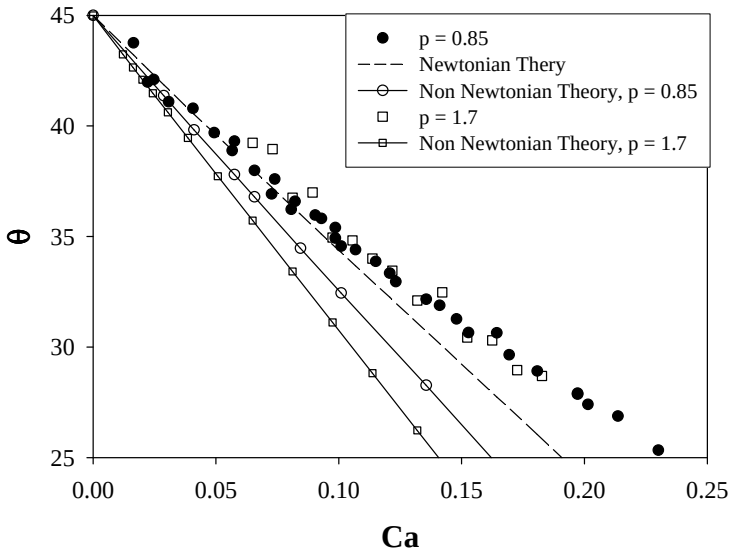

Figure 38: Orientation angle θ vs. Ca at steady state, for the fluid D5, with p = 0.85 and p = 1.7, at λ = 2.6 with the corresponding non Newtonian predictions.

5.2.2 Transient response of the drop deformation at start-up and after flow cessation

Figure 39 shows the transient response of the viscoelastic drop subjected to a step increase in shear rate from rest to the final stable shape. The drop fluid is D5. Viscosity ratio is 2.6. (In all Figures time is made non dimensional using the emulsion time τ_{em}). It is clear that, at low capillary numbers, D increases monotonically up to reach its final steady value. The transient response is quite similar to the Newtonian drop one. As the Ca value increases transient response differs drastically from the Newtonian response, see S. Guido and M. Villone (1998). Non Newtonian drop shape shows an evident overshoot, which depends on Ca. Considering Newtonian drops submitted to a well defined flow of a viscoelastic matrix, this phenomenon has already been illustrated by Sibillo et. al. (2004)[48], and by Tretheway et al. (2001)[49] "*Deformation and relaxation of Newtonian drops in planar flows of a Boger fluid*", and in the previous section. All the

[48] Sibillo V, Simeone M, Guido S, "Break-up of a Newtonian drop in a viscoelastic matrix under simple shear flow", Rheologica Acta, 43, (2004) 449-456.

[49] Tretheway D. C., Leal L. G., "Deformation and relaxation of Newtonian drops in planar extensional flows of a Boger fluid", J. Non-Newtonian Fluid Mech. 99 (2001) 81–108.

authors affirm that, as we increase p or Ψ1 and Ca, the transient response of the viscoelastic drop observed by turning on the shear flow stepwise differs drastically from the Newtonian case. Moreover, as illustrated by Sibillo et al. (2005), the Maffettone - Greco model prediction are very close to the experimental data and it gives a good qualitatively description of the overshoot up to moderate drop deformation D<0.3. This leads to the conclusion that this phenomenon exclusively depends on p and Ca.

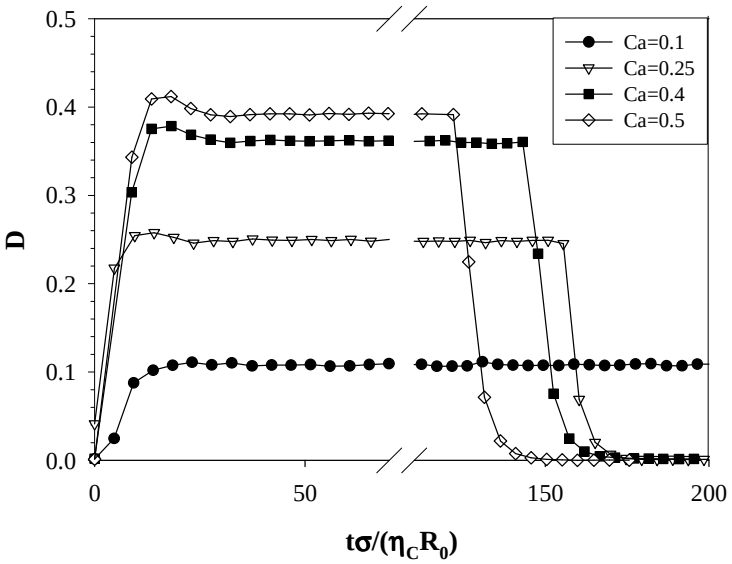

Figure 39: Transient behaviour of the deformation parameter D vs. non dimensional time at various Ca. Drop fluid is D5, with p=0.85 and λ=2.6.

Figure 40 shows transient behaviour for D as a function of the non-dimensional time. Now the viscosity ratio is 1 and the D values are normalised with respect to the steady value of the deformation parameter, D_{SS}. As shown in Figure 39, the overshoot increases with the Ca. Micrographs of the drop evolution in time, submitted to Ca = 1.1 are reported in Figure 41. It is important to notice that for the final capillary number, Ca=1.1, a slight secondary undershoot, after the initial overshoot, is also observed (see micrographs 4 and 5). Moreover it was clear during the experimental tests that the overshoot and the resulting undershoot of deformation were larger for a higher Capillary number. As supposed by Tretheway and Leal, (2001) the overshoot and resulting

undershoot in deformation are the result of a quite subtle interaction between the stretch of non Newtonian long chain polymer, PIB, inside the drop, the drop shape, and the local disturbance velocity field. In absence of exact theoretical predictions I cannot say more than this.

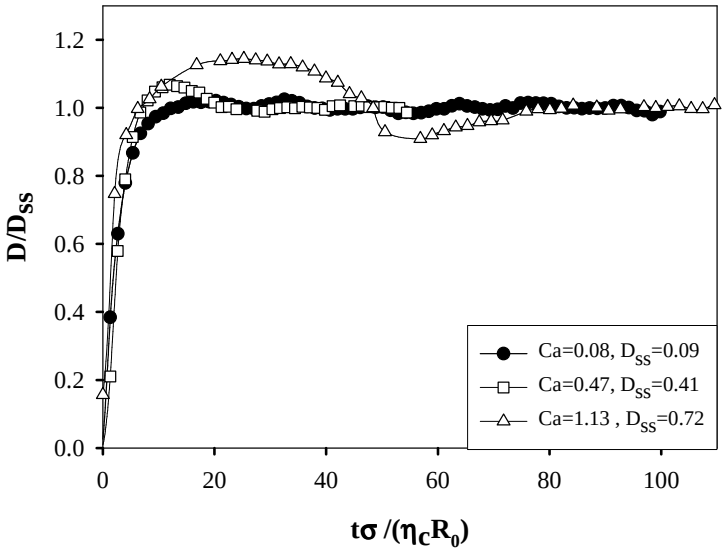

Figure 40: Transient behaviour of the deformation parameter D normalised with respect to the steady value vs. non dimensional time. Drop fluid is D4, with p=1.1, λ=1.

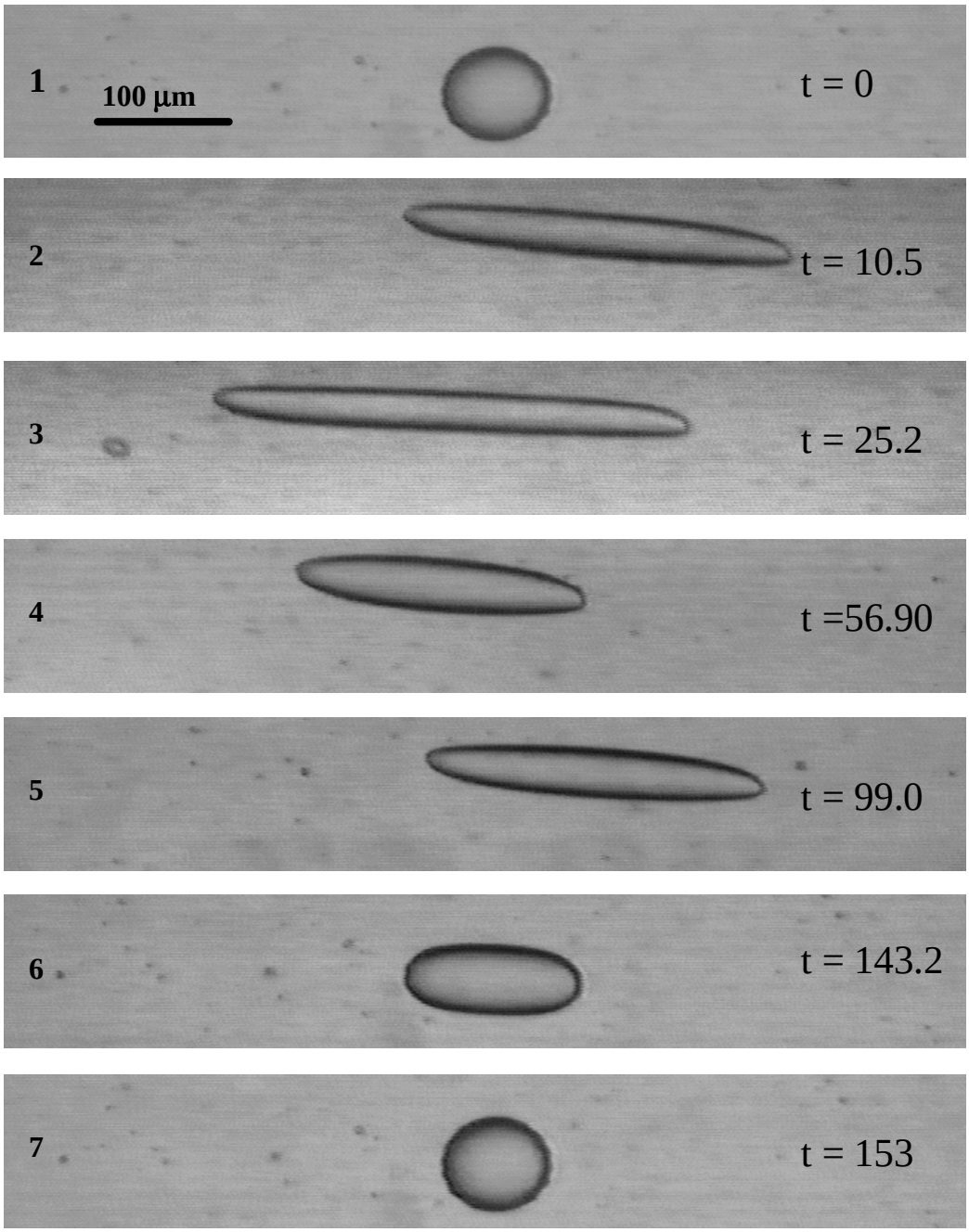

Figure 41: Micrographs of the drop evolution of Figure 40, submitted to Ca=1.1.

The second type of transient phenomenon considered in the experimental section was the relaxation of the drop from a stationary deformed shape after the shear flow cessation. Only the drop relaxation from a little deformed shape (D<0.2) was investigated. The relaxation of drops from the same initial deformation, $Ca = 0.1$ and $D \cong 0.1$, for different p, is reported in Figure 42 by plotting the Taylor deformation parameter normalised with respect to the steady value D_{SS} as a function of the non

dimensional time t/τ_{em}. Figure shows that as the p parameter increases the relaxation time decreases. So the drop elasticity inhibits its relaxation. Unfortunately no models or theoretical predictions are now available to understand the experimental data.

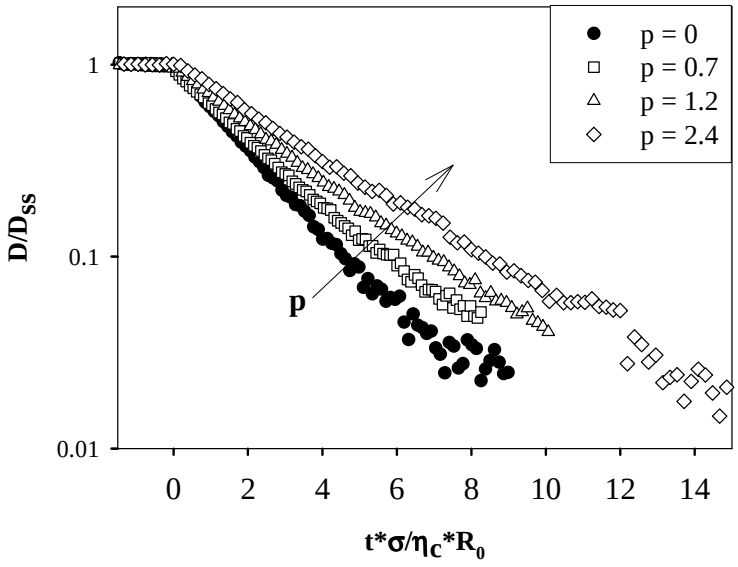

Figure 42: Drop relaxation for different drop systems Di, with the same initial deformation (Ca = 0.1). Newtonian case is also reported (p = 0).

5.2.3 Transient evolution of drop shape for sub critical capillary number and drop break-up.

In Figure 43 non dimensional major and minor axes, R_{MAX}/R and R_{MIN}/R, as well as the deformation parameter D_{SS}, at the steady state, are plotted versus the capillary number and the Weissenberg number, $Wi = \tau_R \cdot \dot{\gamma}$, for the drop D4, comparing the experimental data with the non Newtonian second order theoretical predictions. Viscoelastic drop display a less deformed shape with respect to the Newtonian case for high Deformation parameters. Moreover it needs to underline that the drop reached a stable shape up to capillary around 1, while it is well known in literature that the critical capillary value for Newtonian systems is almost 0.48 at λ=1. The capillary number, at which the drop D4 has been broken, was 1.4 c.a.. It follows that the dispersed phase elasticity hinders drop breakup. It was before illustrated in Figure 41 some micrographs

of the drop D4 evolution at Ca = 1.1, and it was clear that no break-up occurred.

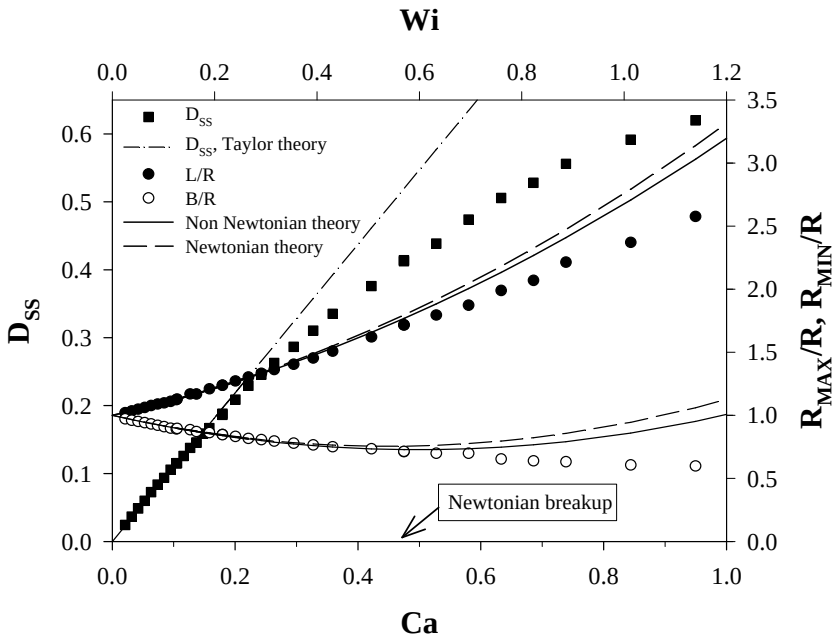

Figure 43: Major (• full symbols), minor axis (o open symbols) and Taylor parameter D_{SS} at steady state of the deformed drop observed along the vorticity-axis of the couple of fluids D4, $\lambda = 1$, $p = 1.1$. Comparison with the theoretical predictions.

In the micrographs of Figure 43 and Figure 45 the shape temporal-evolutions of the drops D4, $\lambda = 1$ and $p = 1.1$, and D5, $\lambda = 2.6$ and $p = 0.85$, are exposed, respectively observed along the vorticity and velocity gradient axis, submitted to an high capillary number, 1.38 and 1.30 respectively. After having started the flow, drops quickly left the ellipsoidal shape (micrographs 2 – b), they were stretched forming a system of two drops joined by a thread, that avoided their separation during the start up of the flow (micrographs 3 – c). The final part of drops extension has been characterized by a thinning of the thread, an increasing of the two extreme drops' dimensions and an inversion of the orientation θ of the drop-thread-drop system with respect to the shear plane (micrographs 2,3,4 - b,c,d). Under these conditions the long thread that links the two drops is like a rigid rod, whose rigidity is due to the extension of the high molecular weight PIB macromolecules dispersed inside the drop and to an elongation component

of viscosity. The inversion of the orientation θ caused a change of the sign of the relative speed between the mass centres of the two system's extremities, with a consequent approach (micrograph 4 - e), collision (micrograph 5 - f) and partial or total coalescence of the two drops (micrograph 6 - g). Because the shear stress induced by the flow on the drop D4 was "high", the two extremity-drops were again moved away from each other (micrograph 7), realizing a second sequence of extension - inversion - collision and partial coalescence (micrograph 7, 8, 9, 10). Also in this case, during the extension time the thread kept the two drops together, avoiding their separation. The drop D4 (Figure 44) was submitted to a capillary 1.38 close to the critical one (1.4) and three big damped oscillations of the maximum length of the drop-thread-drop system occurred. The flow was interrupted because it was reached, in both cases, the maximum run of the parallel plates apparatus, that was almost 15 cm, without any breakup occurred. This phenomenon has been named "Yo-Yo instability". It occurs from a certain capillary number and it always precedes the breakup of the viscoelastic drop, characterized by p>1. The breakup occurs with the disappearance of the thin thread that links the two extremities, during one of the sequences of extension, inversion and collision of the system drop-thread-drop. On the left side of Figure 44 the major length evolution of the drop-thread D4, R_{MAX}/R, is plotted versus the non dimensional time t/τ_{em}, at three different runs with capillary numbers: 0.08, 1.28 and 1.38. In the graph of Figure 44 is shown that for shear flows with high hydrodynamic stresses, Ca=O(1), the shape transient of the drop before the steady state reaching is characterized by a sequence of damped oscillations of the non dimensional major length, that correspond to drop shape oscillations, as discussed before. The amplitude and the number of these damped oscillations increase with the capillary number, as shown in the graph of Figure 40 and Figure 44, up to observe the Yo-Yo phenomenon and they depend on the degree

of elasticity (p) of the drop. The oscillations are absent for Ca <<1 or for p almost zero (Newtonian case). This shows that the dispersed phase elasticity plays an important role on the drop evolution when Weissenberg number is of order 1.

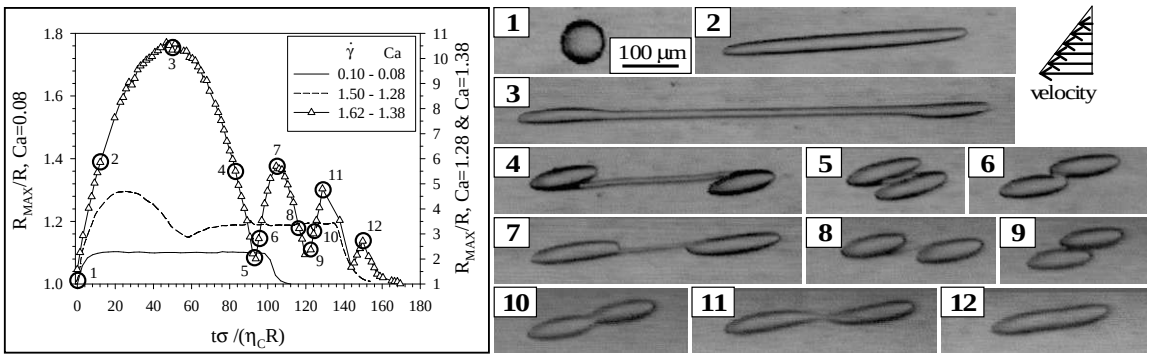

Figure 44: Micrographs of the drop evolution D4, p=1.1, λ=1, submitted to capillary 1.38 and the corresponding measure of the non dimensional major axis. On the graph the evolution of R_{MAX}/R for capillary numbers 0.08 and 1.28 are also reported.

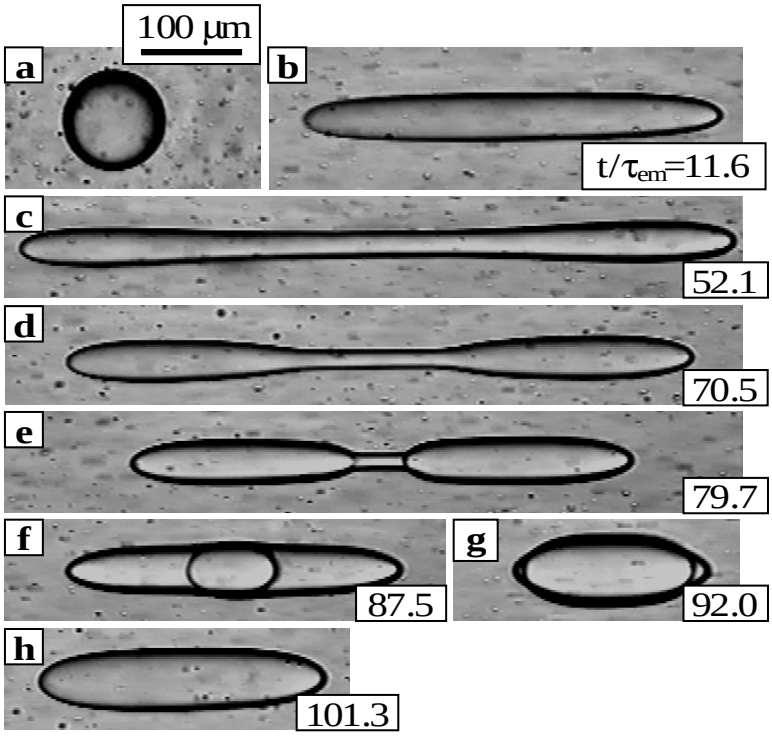

Figure 45: Micrographs of the drop evolution D5, p=0.85, λ=2.6, submitted to capillary 1.30, observed along the velocity gradient direction of the shear flow.

In Figure 46 is showed the disappearance of the thin thread that linked the two

drops-extremities during the Yo-Yo evolution for the system D4 at Ca = 1.4. Our experimental campaign demonstrated that this situation was hard to reproduce perfectly. Indeed the number and the amplitudes of the damped oscillations, before the break-up occurred, might be different.

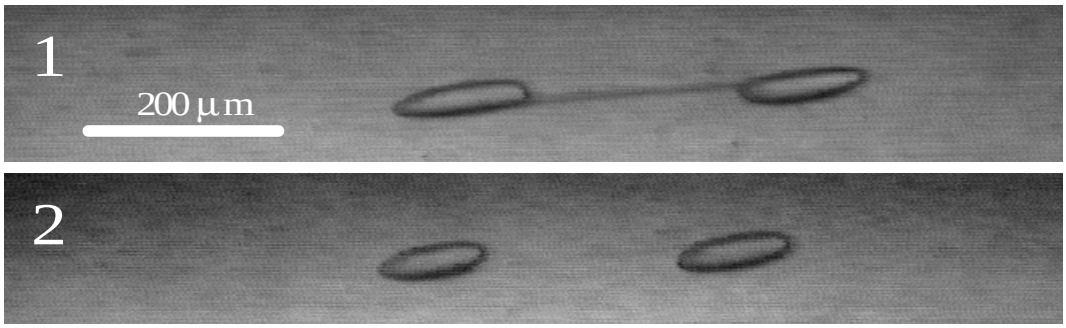

Figure 46: Drop D4 break-up. Ca = 1.4.

It is important to underline that the Capillary at which drop break-up occurred after the Yo-Yo evolution for system D4 was 1.4. Therefore, as illustrated in the previous section for a Newtonian drop under the shear flow of a non Newtonian matrix, phases non Newtonianness hinders drop break-up.

The break-up critical capillary number was determined, as discussed in the previous section, by performing a set of runs at increasing shear rate until break-up occurred. If steady state deformation was reached, after the Yo-Yo, the flow was stopped and the drop was allowed to relax back to the spherical shape before starting the next run. Drop break-up always occurred during the flow. With this protocol, I identified Ca_{cr} inf. and Ca_{cr} sup, or in other words, the interval in which the critical capillary number is contained.

In Table 3 the inferior critical capillary number (Ca_{cr} inf) and the superior critical capillary number (Ca_{cr} sup) are reported for the systems D2 and D4 at two different p parameters, at $\lambda = 1$. The Newtonian critical capillary number is also reported.

It is confirmed that drop elasticity hinders break-up and this effect becomes important when the p parameter assumes values higher than one. We noticed in the

previous section for a Newtonian drop immersed into a viscoelastic matrix that the maximum increase of critical capillary number measured was 50% ca. when the p parameter was increased to 5 at $\lambda = 0.6$ or to 10 ca at $\lambda = 2$. While now, for a viscoelastic drop the maximum increase of critical capillary number with respect to the fully Newtonian case is almost 300% when p parameter is increased to 1.1 at $\lambda = 1$.

p	Ca_{cr} Inferior	Ca_{cr} Superior
0	/	0.48
0.7	0.65	0.66
1.1	1.38	1.40

Table 3: Critical capillary number as function of p.

5.3 Final remarks

The first result of this section was the definition of a protocol to produce a non Newtonian model liquid-liquid dispersion with a constant-viscosity second order drop phase.

For the fist time the experimental validation of the theoretical predictions concerning non Newtonian drop stationary shape submitted to a slow shear flow was achieved. I have presented the first complete viscoelastic drop shape 3D analysis at steady state. Two viscosity ratio were considered, $\lambda=1$ and $\lambda=2.6$. Drop deformation, as observed along the vorticity axis and the velocity gradient direction, for “slow” flows is essentially unaltered with respect to the fully Newtonian case. Moreover the agreement between the experimental results and theory predictions was good in a wide range of Capillary number. This feature confirms that the small deformation limit can be studied to evaluate interfacial tension of viscoelastic liquid-liquid dispersions. I exposed that the interfacial tension can be determined by rheo-optical measurements of the deformation

parameter D as a function of the shear rate in the linear regime, observing the drop along the vorticity axis direction. On the other hand, by looking at the results on the projected axis R_P, the interfacial tension can be measured also using the top view experiment, that is very easier to be realized, if N_1 is known. Finally a complete drop shape 3D analysis can lead to knowledge of the rheological drop phase viscoelastic properties.

Viscoelastic drop dynamics was also investigated during start up and after cessation of the shear flow. At high capillary numbers (Ca>0.3) drop deformation goes through an overshoot and a subsequent slight undershoot during which the drop changes its orientation with respect to the flow direction. The entity of this phenomenon increases with Ca and p up to observe the “Yo-Yo instability” at high, but sub-critical capillary numbers.

The results presented, concerning drop evolution at high capillary number, allow to conclude that drop elastic content changes the break-up mechanism and hinders drop break-up, when compared with the equivalent fully Newtonian system. This was found at viscosity ratio 1 and was quantified by measuring the critical capillary number as a function of the p parameter. The maximum increase of critical capillary number measured was 300% ca. when the p was increase to 1.1 ca.

Finally it was underlined that drop elasticity influences the relaxation time of the drop from a stationary deformed shape after the shear flow cessation.

As described by S. Guido et al. (2003) these results are also useful in evaluating non Newtonian effects for liquid-liquid dispersion processed in industrial application.

Section References

1. D.V. Boger, R. Binnington, “Separation of elastic and shear thinning effects in the capillary rheometer”, Trans. Soc. Rheol. 21 (1977) 515-34.
2. de Bruijn R A (1989) Deformation and breakup of drops in simple shear flows. PhD thesis, Technische Universiteit Eindhoven.
3. Elmendorp J. J. and R. J. Maalcke, “A study on polymer blending microrheology. 1” Polym. Eng. Sci. 25, 1041-1047 (1985).
4. Flumerfelt R W, (1972) Drop breakup in simple shear fields of viscoelastic fluids. Ind. Eng. Chem. Fundam., 11, 312-318.
5. Grace H P.. “Dispersion phenomena in high viscosity immiscible fluid systems and application of static mixers as dispersion devices in such systems”. Chem. Eng. Commun., 14, (1982) 225-277.
6. Greco F.. “Second-order theory for the deformation of a Newtonian drop in a stationary flow field”. Phys. Fluids, 14, (2002) 946-954.
7. S. Guido and F. Greco, “Rheology Review 2004”, BSR Aberystwyth, UK 2004.
8. Guido S, Simeone M and Greco F, “Deformation of a Newtonian drop in a viscoelastic matrix under steady shear flow. Experimental validation of slow flow theory”, J. Non-Newtonian Fluid Mech., 114 (2003) 65-82.
9. S. Guido, M. Simeone, M. Villone, “Diffusion effects on the interfacial tension of immiscible polymer blends”. Rheol. Acta 38 (1999) 287-296.
10. Guido, S. and Simeone, M. “Binary collisions of drops in simple shear flow by computer-assisted video optical microscopy”. Journal of Fluid Mechanics, 357, (1997) 1-20.
11. Guido, S. and Villone, M. (1998) Three dimensional shape of a drop under simple shear flow. Journal of Rheology, 42, 395-415.
12. Mighri F, Carreau P J and Ajji A (1998) Influence of elastic properties on drop deformation and breakup in shear flow. J. Rheol., 42, 1477-1490.
13. V. Sibillo, S. Guido, F. Greco, P.L. Maffettone. “Single drop dynamics under shearing flow in systems with a viscoelastic phase”. Macromolecular Symposium, (2005), 228, 31-39.
14. Sibillo V, Simeone M, Guido S, “Break-up of a Newtonian drop in a viscoelastic matrix under simple shear flow”, Rheologica Acta, 43, (2004) 449-456.
15. Taylor G I (1932) The viscosity of a fluid containing small drops of another fluid. Proc. R. Soc. London A, 138, 41-48.
16. Taylor G I, (1934) The formation of emulsions in definable fields of flow. Proc. R. Soc. London A, 146, 501-523.
17. Tretheway D. C., Leal L. G., “Deformation and relaxation of Newtonian drops in planar extensional flows of a Boger fluid”, J. Non-Newtonian Fluid Mech. 99 (2001) 81–108.
18. Varanasi P, Ryan M E and Stroeve P (1994) Experimental study on the breakup of model viscoelastic drops in uniform shear flow. Ind. Eng. Chem. Res., 33, 1858-66.

Wall effects on drop deformation under simple shear flow

This section illustrates the influence of confinement on the steady state of a single drop sheared between parallel plates, in a regime where the droplet diameter is comparable with the gap width, comparing the experimental data with some theoretical predictions. Drop high deformations were also investigated as a function of the confinement. A single drop model system with Newtonian phases was considered.

6 Wall effects on drop deformation under simple shear flow

Acknowledgements

I wish to thank Eng. Gilberto Pasquariello as co-worker and for his great experimental support during this difficult experimental campaign. Some results of this section are taken from the poster presented at the Annual European Rheology Conference 2005 in Grenoble: Sibillo, Vincenzo; Simeone, Marino; Guido, Stefano; Pasquariello, Gilberto. "*Wall effects on drop deformation under simple shear flow*".

Keywords: Drop dynamic, wall effect, microfluidic, shear flow, microscopy.

6.1 Introduction

In this section I will present briefly, some results obtained during the last year of my Ph. D. on the influence of confinement on the steady state morphology of a single Newtonian drop sheared between parallel plates in a regime where the drop diameter 2R is comparable to the gap width, d.

The regime where drop diameter 2R and gap width d are comparable, where wall effects influence drop dynamic and shape, is not yet well understood. On the other hand many attractive technological applications depend a lot on the fluid-dynamic behaviour of liquid-liquid dispersions flowing through microscopic devices, where chemical reactions or particles interactions can be controlled with a micro metric accuracy.

On the market we can find some miniature devices able to pump, to mix, to check small volumes of liquid-liquid dispersion, i.e. polymer blends, emulsions for food industry, cells suspensions etc., where a knowledge concerning the micro fluidic or the micro-scale processing of emulsion is fundamental.

For example the bioanalyzer illustrated in Figure 47 is a highly successful micro fluidics-based platform for the analysis of DNA, RNA, proteins and cells. It can analyze cells treated with medicines. Cells train is driven through a micro channel by using two converging laminar flows. Optical analyzers can count and characterize fluorescent cells one by one.

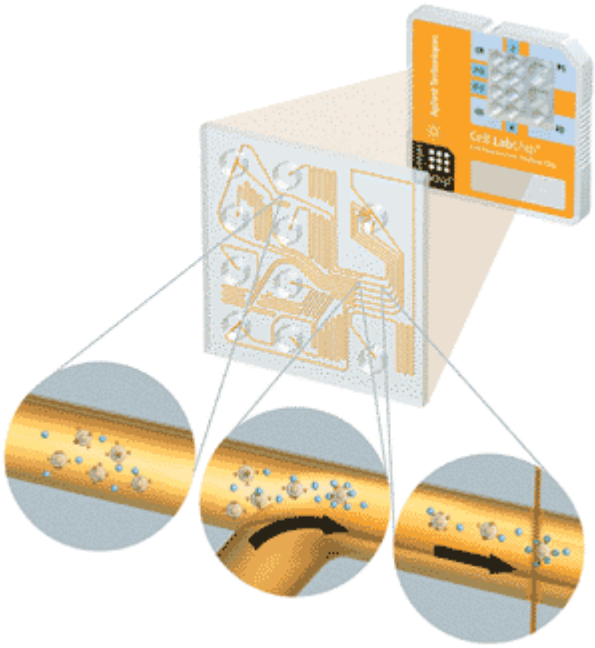

Figure 47: Bioanalyzer.

Diluted polymer blends can be used as model systems to better understand the behaviour of a liquid-liquid dispersion subjected to confined flow. Son [50] has recently reported some important results concerning a polymeric emulsion composed of polyisobutylene (PIB) and poly(dimethylsiloxane) (PDMS), sheared between parallel plates in the regime where droplets diameters are equal to gap width $2R \approx d$. He observed the formation of stable strings, created by the coalescence of the dispersed phase during the shear flow. He found that the transition from the droplet to string morphology is governed by the ratio R/d. He also found that the Rayleigh-Tomotica

[50] Youngoon Son, Nicos S. Martys, John G. Hagerdon, and Kalman B. Migler, "Suppression of Capillary instability of a polymeric thread via parallel plate confinement", Macromolecules, 35, 5825-5833, (2003).

break-up is suppressed by both finite size effect, in the case of wider strings, and by shear confined flow.

The deformation of a drop near a plane wall was considered theoretically by Shapira and Haber[51]. Using the method of reflections they found that the wall confinement exacerbates the deformation of the drop. This was confirmed by numerical results of Kennedy et al. (1994)[52]. They found that the general behaviour of the drop is similar to that of drops in an unbounded shear flow, but with slightly larger deformations and lower angles of orientation as the drop are placed closed to the wall.

Briefly, when a shear field with no confinement is imposed on a Newtonian drop (d>>2R), interfacial tension effects tend to keep the drop spherical, while shear stress tends to deform it. Up to moderate deformation, the steady-state drop shape is well described by an ellipsoid having three different axes. Increasing the shear rate the droplet continues to deform itself until the interfacial tension effects are not able to balance the shear-stress-induced deformation and then the droplet breaks up. Drop deformation, its orientation with respect to the flow direction and break-up phenomenon depend only on the dimensionless Capillary number $Ca = \eta_C \dot{\gamma} R / \sigma$, (where η_C is the matrix viscosity, $\dot{\gamma}$ is the shear rate, R is spherical droplet radius and σ is the interfacial tension of the system) and on drop to matrix viscosity ratio $\frac{\eta_D}{\eta_C}$ (Taylor[53], Grace[54],

[51] M. Shapira and S. Haber, Lew Reynolds number motion of a droplet in shear flow includin wall effect. Int. J. Multiphase Flow 16, 305 (1990).

[52] M. R. Kennedy, C. Pozrikidis and R. Skalak, Motion and deformatio of liquid drops and the rheology of dilute emulsions in simple shear flow. Computer Fluids Vol.23, No.2,pp.251-278, (1994).

[53] Taylor, G. I., "The formation of emulsion in definable fields of flow", Proceedings of the Royal Society of London: A, 138, 41-48, (1934).

[54] Grace, H., "Dispersion phenomena in high viscosity immiscible fluid system and application of static mixers as dispersion devices in such systems", Chemical Engineering Communications, 14, 225-277, (1982).

Guido et al.[55], Rallison J. M.[56], C. Chaffey et al.[57]). Above a certain value of Ca drop becomes unstable and the corresponding Ca is known as the Critical Capillary number Ca_{Cr}, which is a function only of the viscosity ratio λ. Critical Capillary number for viscosity ratio equal to 1 is almost 0.48 (Grace, 1982). Drop deformation can be evaluated using the deformation parameter D introduced for the first time by Taylor, $D = \frac{R_{MAX} - R_{MIN}}{R_{MAX} + R_{MIN}}$, where R_{MAX} and R_{MIN} are the major and minor axes of the deformed ellipsoidal drop observed along the vorticity axis direction of the shear flow (side view experiment). It is well known that D depends linearly on Ca in the limit of small deformation, without walls confinement, $D = Ca \cdot \frac{19\lambda + 16}{16\lambda + 16}$, Taylor(1934).

In this section I investigated single Newtonian drop behaviour immersed into a Newtonian matrix, with drop to matrix viscosity ratio 1, submitted to a simple shear flow in the regime where drop diameter is comparable to gap width, $2R \approx d$. A new non dimensional parameter was considered, d/2R, namely non dimensional gap, to quantify the effect of the confinement on the drop deformation. Wall effects on drop shape were studied by performing a set of runs at reducing d/2R, starting from not confined regime.

We will focus on the drop deformation at steady state within the limit of small deformations, Capillary number lower than 0.2, as a function of d/2R, comparing for the first time experimental data with theoretical predictions of Shapira-Haber, Taylor and with the second order Newtonian theory. Drop dynamics at start-up will be briefly explored as function of non dimensional gap, d/2R. Drop shape at high Capillary

[55] Guido, S., Villone, M., "Three dimensional shape of a drop under simple scorrimento flow", Journal of Rheology, 42, 395-415, (1998).

[56] Rallison, J. M., "The deformation of small viscous drops and bubbles in shear flows", Annual Review of Fluid Mechanics, 16, 45-66, (1984).

[57] C. Chaffey, H. Brenner and S. G. Mason, Particle motions of sheared suspensione XVIII. Wall migration (Theoretical). Rheol. Acta 4, 64 (1965).

numbers will be finally illustrated.

6.2 Materials and methods

The fluids used in this work were two Newtonian polymers, polyisobutylene (PIB) as matrix phase and polydimethylsiloxane (PDMS) as drop phase. In all experiments drop to matrix viscosity ratio was 1. All the experiments were performed at room temperature, 23°C. For sake of brevity I don't show rheological data for the PIB and PDMS samples. For both matrix and drop phase, up to shear rates around 1 s^{-1} viscosity is essentially constant with the shear rate. The viscosity at 23°C is $83.3 Pa \cdot s$ for PIB and $83.1 Pa \cdot s$ for PDMS.

The shear device used in this work has been well described by Guido and Villone (1998) and illustrated in the material and methods section.

The experimental apparatus essentially consists of a couple of parallel glass plates mounted on motorized supports and of an optical microscope, Axioscop FS (Zeiss) equipped with an analogical CCD camera. Sheared drop was observed only along the vorticity axis direction of the shear flow (side view experiment). The two axes R_{MAX} and R_{MIN} of the ellipsoidal drop, major drop length L and the angle θ between the major axis R_{MAX} and the velocity direction (see the schematic drawing in the Materials and methods section) were calculated. L is equal to R_{MAX} within the limit of small deformations and without confinement effects, as well illustrated by Guido and Villone (1998).

After loading matrix phase between the glass parallel plates, a single drop of PDMS was injected in the sample by using a tiny glass capillary, fixed on an homemade micromanipulator. The parallelism accuracy was estimated to about 10 μm over the whole plate length. Gap width was gently reduced during the experiment to vary non dimensional gap d/2R, taking care of avoiding drop squeezing out of the parallel plates.

A sets of runs at different d/2R were carried out, from d/2R=9 up to d/2R=0.5.

The interfacial tension of the couple of fluids has been calculated from the slope of the linear fit of D at steady state versus the shear rate, within the limit of D<2, and d/2R>7 to be sure that wall effects were negligible, σ=2.4 mN/m.

6.3 Results

Images of the deformed drop at steady state (Ca=0.1) for different non dimensional gap values, d/2R, are reported in Figure 48. Deformation parameter D as a function of d/2R is also reported at Ca=0.1 and Ca=0.2. Experimental data are compared with the predictions of Shapira-Haber. It is clear, as predicted by Shapira-Haber and Kennedy et al, that within the limit of small deformations, drop shape and its orientation angle at steady state don't depend on the closeness of the walls up to d/2R=2. Below d/2R=2 drop steady shape, the orientation angle and its non dimensional major length change drastically. As predicted by Shapira-Haber the presence of the wall exacerbates the deformation of the drop. Theoretical prediction underestimates the increase of the deformation parameter D, because it doesn't predict the deviation of drop shape from the ellipsoidal one, when d/2R is close to 1. Major and minor axes, R_{MAX} and R_{MIN}, are reported in Figure 49 as a function of the non dimensional gap d/2R, at Ca=0.2. Shapira-Haber theoretical prediction is also reported. As previously discussed, drop major and minor length don't change up to non dimensional gap 2.

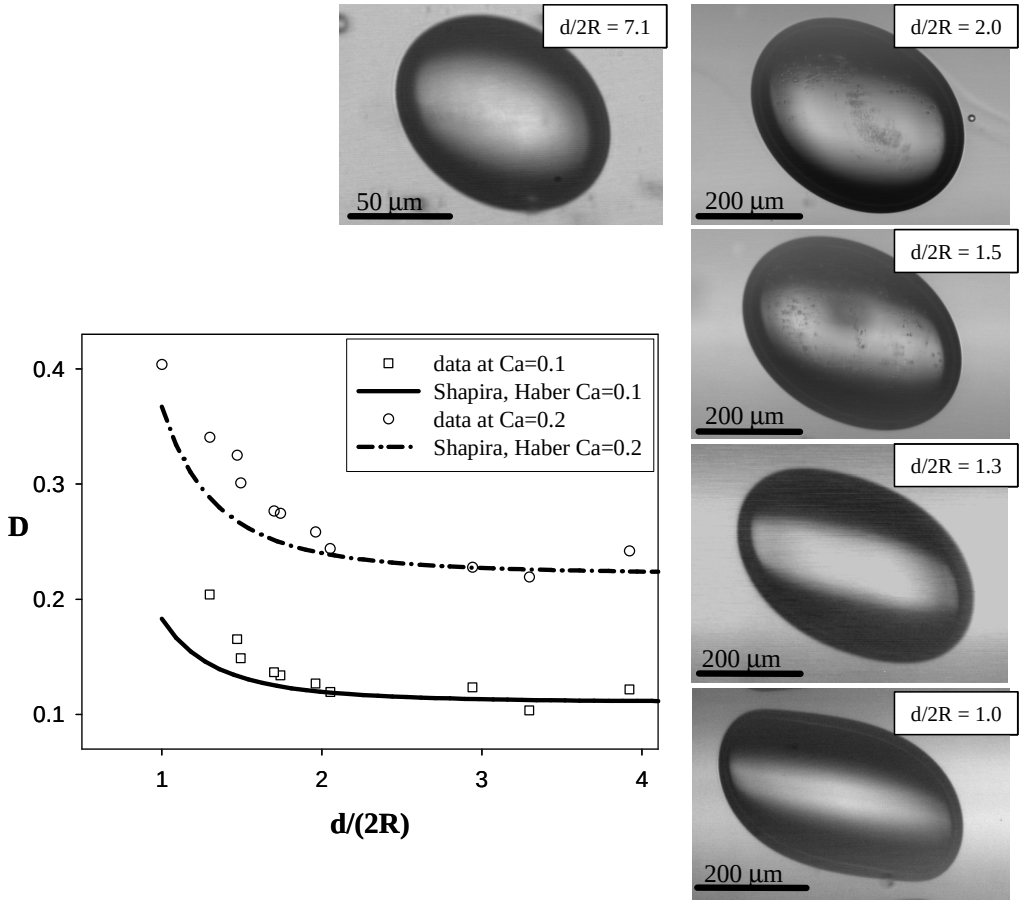

Figure 48: Images of the deformed drop at steady state as a function of d/2R, at Ca=0.1. Experimental data are compared with predictions of Shapira-Haber at Ca=0.1 and Ca=0.2.

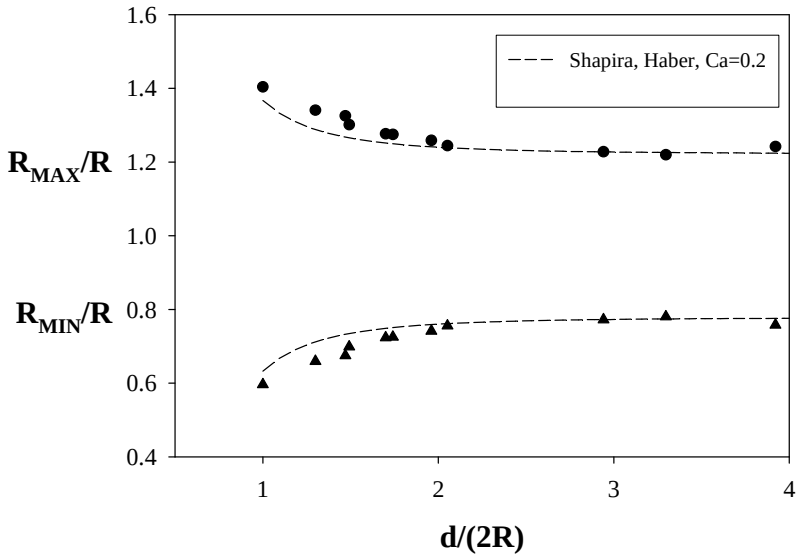

Figure 49: Major and minor axis at steady state as a function of d/2R, at Ca=0.2. Dashed lines are predictions of Shapira-Haber.

In Figure 50 the drop orientation angle θ versus d/2R is reported at Ca=0.1 and

Ca=0.2. The angle of orientation is also remarkably influenced by the reduction of the gap width. As consequence of the confinement drop progressively increases its alignment to the flow direction.

The Shapira-Haber theory is a first order analytical solution of the hydrodynamic interaction between the drop immersed in a shear flow and the containing walls. It predicts that the orientation angle is always 45°. Therefore in absence of an exact theoretical prediction of the orientation angle as a function of the confinement, a simple regression of the experimental data has been presented, using the equation, $\theta = \theta_{Taylor} \cdot \left[1 - a\left(\frac{2R}{d}\right)^3\right]$, where θ_{Taylor} is the experimental orientation angle at steady state for d/2R>>2 or in absence of confinement effects.

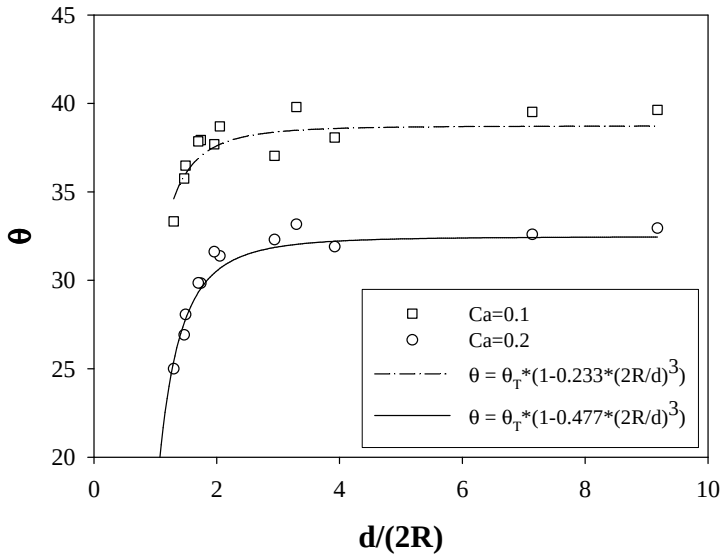

Figure 50: The drop orientation angle θ vs. d/2R, at Ca=0.1 and Ca=0.2. Lines were obtained by fitting the data using the equation $\theta = \theta_{Taylor} \cdot \left[1 - a\left(\frac{2R}{d}\right)^3\right]$.

In Figure 51 the deformation parameter D and major length of the drop at steady state are reported as a function of the Capillary number and for different values of d/2R. It is clear that the deformation of the drop increases as consequence of the decrease of

the non dimensional gap. However, D data don't exhibit any deviation from linearity within the explored range of Ca.

It's important to notice that drop shape at steady state seems not to be influenced by the closeness to the walls up to d/2R~2, as previously observed in Figure 48 and Figure 49. I would to underline that, for Ca=0.3 and d/2R=1, drop length is almost 40% higher with respect to not confined case, and drop shape is not more ellipsoidal (see micrographs of Figure 53).

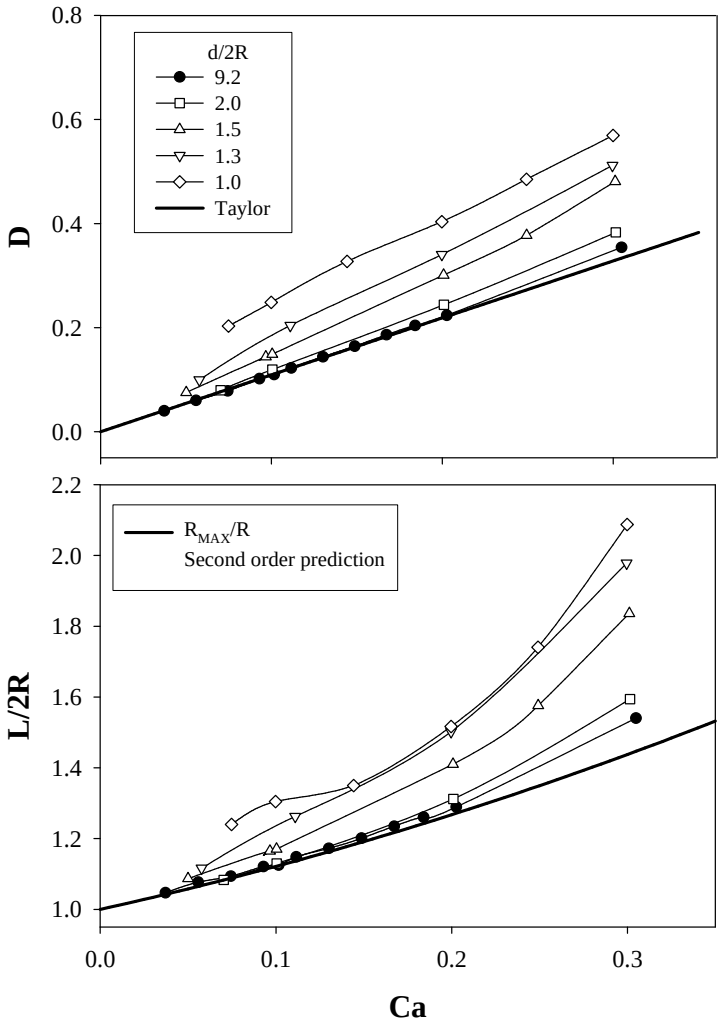

Figure 51: Deformation parameter D and non dimensional length L/2R vs. Ca, at various d/2R.

In Figure 52 the orientation angle is reported as a function of the Capillary number for different non dimensional gap values. As observed in Figure 50, as consequence of

the confinement, drop progressively enhances its alignment to the flow direction. Probably this is due to a pressure difference from the walls to the drop during the shear flow, caused by the crushing of the flow lines between drop and wall.

It is important to underline that drop pushed by the walls is closer to the velocity direction with respect to the Newtonian case without confinement, as a non Newtonian drop sheared into a Newtonian matrix (see previous section) or vice versa. In fact Guido et al. (2003) demonstrated that a Newtonian drop immersed into a non Newtonian matrix displays a stronger alignment in the flow direction respect with the fully Newtonian case. They explained that this behaviour was due to the first normal stresses difference, N_1,of the viscoelastic phase, which is a pressure difference. So we can argue that drop generally tends to align itself to the flow direction if a pressure difference is present.

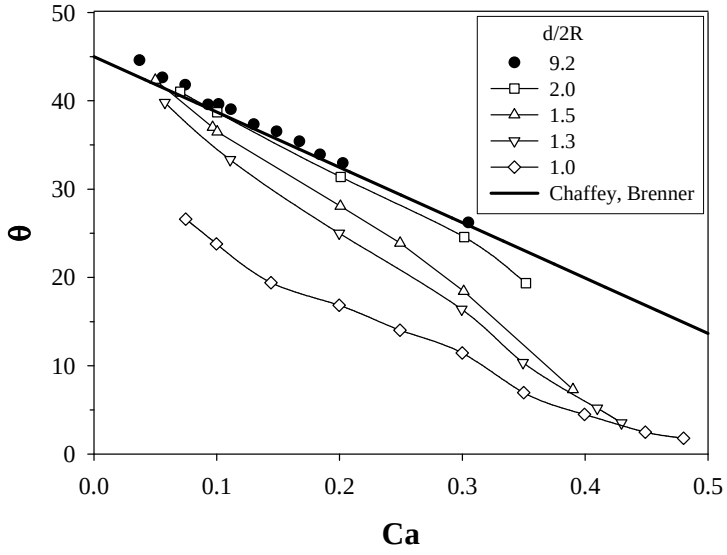

Figure 52: The drop orientation angle θ vs. Ca, at various non dimensional gap width d/2R.

Here images of the drop subjected to Ca=0.3 at steady state are presented for different non dimensional gap. All results previously illustrated are now confirmed at high capillary number. Drop shape and its orientation change drastically when d/2R is

lower than 2. In Figure 53 drop length time-evolution is also reported. It is clear that drop transient also change drastically when drop closeness to the walls becomes significant. It is important to underline that drop start-up at d/2R=1 is characterized by an overshoot. Probably this phenomenon is due to the drag of the drop, caused by the walls during the initial time of the flow, when drop is still in contact with them.

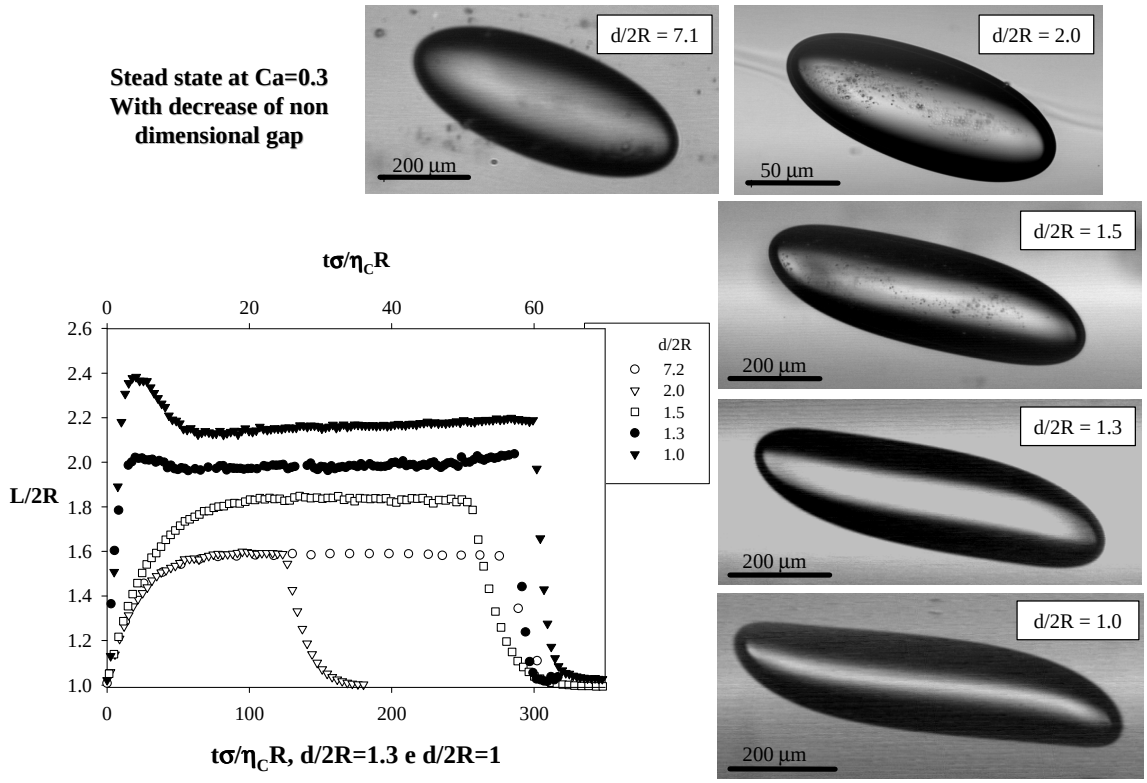

Figure 53: Images of the deformed drop under steady shear flow at Ca=0.3, for various non dimensional gap width d/2R. Drop length time-evolution is also reported.

Section References

1. C. Chaffey, H. Brenner and S. G. Mason, Particle motions of sheared suspension XVIII. Wall migration (Theoretical). Rheol. Acta 4, 64 (1965).
2. Grace H P.. “Dispersion phenomena in high viscosity immiscible fluid systems and application of static mixers as dispersion devices in such systems”. Chem. Eng. Commun., 14, (1982) 225-277.
3. Guido S, Simeone M and Greco F, “Deformation of a Newtonian drop in a viscoelastic matrix under steady shear flow. Experimental validation of slow flow theory”, J. Non-Newtonian Fluid Mech., 114 (2003) 65-82.
4. Guido, S. and Villone, M. (1998) Three dimensional shape of a drop under simple shear flow. Journal of Rheology, 42, 395-415.
5. M. R. Kennedy, C. Pozrikidis and R. Skalak, Motion and deformation of liquid drops and the rheology of dilute emulsions in simple shear flow. Computer Fluids Vol.23, No.2,pp.251-278, (1994).
6. Rallison, J. M., “The deformation of small viscous drops and bubbles in shear flows”, Annual Review of Fluid Mechanics, 16, 45-66, (1984).
7. M. Shapira and S. Haber, Lew Reynolds number motion of a droplet in shear flow includin wall effect. Int. J. Multiphase Flow 16, 305 (1990).
8. Taylor G I, (1934) The formation of emulsions in definable fields of flow. Proc. R. Soc. London A, 146, 501-523.
9. Youngoon Son, Nicos S. Martys, John G. Hagerdon, and Kalman B. Migler, “Suppression of Capillary instability of a polymeric thread via parallel plate confinement”, Macromolecules, 35, 5825-5833, (2003).